


8-2020

## Elevated cochlear adenosine causes hearing loss via ADORA2B signaling

Jeanne Manalo

Follow this and additional works at: [https://digitalcommons.library.tmc.edu/utgsbs\\_dissertations](https://digitalcommons.library.tmc.edu/utgsbs_dissertations)

 Part of the [Biochemistry Commons](#), [Molecular and Cellular Neuroscience Commons](#), [Molecular Biology Commons](#), [Other Neuroscience and Neurobiology Commons](#), and the [Systems Neuroscience Commons](#)

---

### Recommended Citation

Manalo, Jeanne, "Elevated cochlear adenosine causes hearing loss via ADORA2B signaling" (2020). *The University of Texas MD Anderson Cancer Center UTHealth Graduate School of Biomedical Sciences Dissertations and Theses (Open Access)*. 1033.

[https://digitalcommons.library.tmc.edu/utgsbs\\_dissertations/1033](https://digitalcommons.library.tmc.edu/utgsbs_dissertations/1033)

This Dissertation (PhD) is brought to you for free and open access by the The University of Texas MD Anderson Cancer Center UTHealth Graduate School of Biomedical Sciences at DigitalCommons@TMC. It has been accepted for inclusion in The University of Texas MD Anderson Cancer Center UTHealth Graduate School of Biomedical Sciences Dissertations and Theses (Open Access) by an authorized administrator of DigitalCommons@TMC. For more information, please contact [digitalcommons@library.tmc.edu](mailto:digitalcommons@library.tmc.edu).

**ELEVATED COCHLEAR ADENOSINE CAUSES HEARING LOSS VIA ADORA2B  
SIGNALING**


by

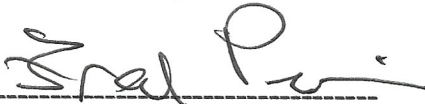
Jeanne Marie Dominique P. Manalo, B.S.


APPROVED:


  
-----  
Yang Xia, M.D., Ph.D.

  
-----  
Michael Beierlein, Ph.D.

  
-----  
John O'Brien, Ph.D.

  
-----  
Fred A. Pereira, Ph.D.

  
-----  
Qingchun Tong, Ph.D.

  
-----  
Neal Waxham, Ph.D.

APPROVED:

-----  
Dean, The University of Texas  
MD Anderson Cancer Center UHealth Graduate School of Biomedical Sciences

ELEVATED COCHLEAR ADENOSINE CAUSES HEARING LOSS VIA ADORA2B  
SIGNALING

A

DISSERTATION

Presented to the Faculty of

The University of Texas

MD Anderson Cancer Center UTHealth

Graduate School of Biomedical Sciences

in Partial Fulfillment

of the Requirements

for the Degree of

DOCTOR OF PHILOSOPHY

by

Jeanne Marie Dominique P. Manalo, B.S.

Houston, Texas

*August, 2020*

## **DEDICATION**

*This work is dedicated to my loving family and friends, husband, and Mango Pineapple.*



## ACKNOWLEDGEMENTS

There is an endless list of people to thank who have supported me in these past 4 years. These people are from inside and outside the lab that have inspired me to keep going whether they knew it or not. Firstly, I would like to thank the custodial staff that have kept my lab space clean and the vet techs who have kept my mice well-taken cared for. Namely, Luisa, who always practiced my Spanish with me and never failed to put a smile on my face. She always made sure to greet me with cheerfulness amidst her laborious tasks. I would also like to thank Josue and Erica from what was once The French Corner in MSB. They always served food with enthusiasm and conversations that were always filled with encouragement. These are the people that I would like to thank first because it is easy to forget those that we encounter on an ordinary basis.

I would like to thank my lab family. Yang has fostered an environment that inspires collaboration with the love for science and eating meals together. My first two years were very special because I met outstanding students: Hong, Kaiqi, and Morayo. Kaiqi has really showed me the ropes for skills applicable in lab and out in the real world. Morayo taught me to be strong and had my back when I felt like I could not handle difficulties. The rest of the years were heavily guided by Yujin and Anren. I'd like to express how much I appreciate Anren, our *shifu*. My Ph.D. experience would not be of much substance had he not been there to remind me of doing experiments excellently while upholding moral character. He fondly cooked and baked bread for all of us while maintaining good leadership. I'm not sure this kind of leadership exists elsewhere. I'd also like to give many thanks to the smartest and hardest working people I have ever met: Seisuke, for sharing your culture with me and for being a good friend; Rongrong, Xiudong, Ying, Tingting, Ping, Xiaoli, Changan, Qingfen, Shuai, and Yangxi. They all made late night experiments much more enjoyable and lightened a lot of the burden that came with research. I will never forget their kindness and hope to visit them around the world!

I would also like to thank the Neuroscience program, the BMB Department, and the GSBS community. Firstly, I'd like to share my deep gratitude to Dr. Blackburn, Dr. Mattox, and Bunny. They have been nothing but supportive throughout this journey through both triumphs and tribulations. Additionally, my time as a student council leader was a breeze because of all of Amanda's hard work, we really owe it to her. The Neuroscience program would not be the same without JJ, Sam, Melissa, Jing, Rachel, Xu, Kyla, Alexis, Cana, etc. I truly enjoyed their company and scientific discussions during classes and NJC. The BMB department was also one of the reasons why I chose my lab. A successful department led by Dr. Kellems with My, Vanessa, and the rest of the office ladies who were extremely supportive. I would also like to acknowledge my *titas* at GSBS. Mrs. Joy, Bunny, and Lily always brightened my day! I am so fortunate to have found caring and generous women who I could talk to and feel instantly better after. I really don't think I would have survived this journey without them.

I would like to thank my advisory committee: Dr. Beierlein, Dr. Waxham, Dr. Tong, Dr. O'Brien, and Dr. Pereira. I appreciated the scientific rigor that was expected of me to achieve. The hard questions kept me afloat and curious! I would like to especially thank Dr. Waxham for teaching me techniques that made me appreciate the art in biology even more. Additionally, I am grateful for Dr. Pereira's general guidance since my BCM's SMART program days. And last, but not the least, I would also like to thank Dr. Beierlein for being an excellent program director who never fails to listen and give advice whenever needed.

My degree would not be possible without my mentor, Yang. I am so grateful to have been mentored by a strong and passionate woman. She has taught me how to persevere in times of difficulty and allowed me to explore and intellectually grow independently. She has also given me many opportunities to learn how to adapt and be skillfully versatile in other fields that I have enjoyed writing and collaborating for. Yang has built a family full of intelligent and dedicated

scientists across the world that I am proud to be a part of. To belong in a world-class network as Yang's mentee will be always be unforgettable.

Although I was consumed by completing this degree, I could never forget to acknowledge friends who have helped me through this journey. I would like thank Iman, Ryan, and Alex who have been there for me through thick and thin. Ryan, for always being there to marvel at beautiful photographs of creatures and artworks with me and for simply being an awesome friend. Iman, the person I owe a lot of my sanity to, has been there through everything. She made every class, leadership commitment, and any other hardship outside of school, bearable. She is truly a gem of a friend and I'm forever grateful that graduate school brought us together. Alex, who is a constant inspiration in my life as a scientist, friend, and mother. I will truly miss walking to Starbucks every day at 9 am with her, but I know our friendship will remain outside of school. I'm also grateful for the rest of my friends who have been supportive of my education since I was in high school, even through some of my absence and busyness: Krystin, Keisha, Maria, Ammy, Christian, and Diego. I'm lucky to have consistent friends who are rooted in something special. And of course, I'm grateful for my best friend, Rachel, who never fails to talk me through my insecurities and remind me of my strengths.

Lastly, I'd like to thank my family—for being so compassionate, understanding, and encouraging when things are tough and for celebrating big and small accomplishments. Every week, my goal was to accomplish tasks I set my mind to so I have time to see them on the weekends. Spending time with my three older brothers, sisters-in-law, and their children remind me that there is a bigger world outside of the bench. I would also like to thank my my loving mother-in law, Georganne. She always reminds me to stay true to my myself no matter what my environment may bring. I'd like to thank my mom and dad for making the sacrifice of bringing us to America, but most of all, for loving me unconditionally. I am motivated by making them proud and reminding them that their sacrifices and hard work are not in vain. Last but not the

least, I'd like to thank my husband Daniel, for not only helping me proof-read through the years, but for being patient and supportive through everything. Thank you for constantly reminding me of my enthusiasm for science and discovery. *Thank you for giving me the adventure of a lifetime!*

# ELEVATED COCHLEAR ADENOSINE CAUSES HEARING LOSS VIA ADORA2B SIGNALING

Jeanne Marie Dominique P. Manalo, B.S.

Advisory Professor: Yang Xia, M.D., Ph.D.

Over 538 million people in the world have been diagnosed with hearing loss (HL). Current treatments for the most common type of HL, sensorineural HL, are limited to hearing aids and cochlear implants with no FDA-drugs available. The hearing process demands an abundance of ATP and HL is often attributed to a disruption in this metabolic energy currency. Patients who lack adenosine deaminase (ADA), the enzyme that irreversibly metabolizes adenosine, have high levels of adenosine that yield severe health problems, including HL; however, the pathogenic mechanisms behind HL and adenosine remain elusive. Our lab has found a HL phenotype in *Ada*-deficient mice (*Ada*<sup>-/-</sup>) that parallels ADA-deficient humans. We characterized shifts in both DPOAE and ABR thresholds in *Ada*<sup>-/-</sup> mice with high adenosine levels. Moreover, we found that these mice have an overall lowered firing capacity of both peripheral and cochlear nucleus and slow latency transmission between structures. We also observed nerve fiber density loss and aberrant myelin compaction. More importantly, we found that treatment of FDA-approved drug, polyethylene glycol-ADA (PEG-ADA), lowered cochlear adenosine levels and improved functional and structural phenotypes of *Ada*<sup>-/-</sup> mice. In addition to continuous treatment of PEG-ADA in *Ada*<sup>-/-</sup> mice, we also rescued these phenotypes in mice with HL after adenosine accumulation for two weeks. Together, these results

provide fundamental evidence that elevated cochlear adenosine causes hearing loss via perturbations of myelin structures.

Interestingly, out of all four adenosine receptors, adenosine a2b (ADORA2B) was found to have the highest mRNA expression in untreated *Ada*<sup>-/-</sup> cochlea. We observed that genetically and pharmacologically ablating ADORA2B in the *Ada*<sup>-/-</sup> mice attenuated hearing deficiencies and rescued nerve fiber density and myelin compaction of cochlear nerve. With these findings, we reveal that elevated adenosine-mediated hearing loss is dependent on ADORA2B signaling that leads to overall hearing sensitivity decline.

Extending from our *Ada*<sup>-/-</sup> mice, we used aged mice as an additional SNHL model. Aging organs have been associated with hypoxia and, consequently, increased adenosine levels. Indeed, we found that aged *Adora2b*<sup>-/-</sup> rescued hearing sensitivity. Moreover, we used a therapeutic approach for both models to further validate the role of ADORA2B by using a specific-ADORA2B antagonist, PSB1115. PSB1115-treated aging mice also have rescued hearing sensitivity. We also explored another disease model that our lab found to have elevated systemic adenosine with reported HL in the clinic: sickle-cell disease (SCD). We found that C57B6/J mice transplanted with SCD mice bone marrow (BM) have hearing loss; however, we found that *Adora2b*<sup>-/-</sup> mice with SCD BM have attenuated hearing loss. Overall, our study supports the clinical and existing research on the relationship between adenosine signaling and hearing loss. Understanding this purinergic signaling establishes a strong foundation for molecular-based therapy in a very common disability.

## TABLE OF CONTENTS

Approval Page .....	i
Title Page.....	ii
Dedication.....	iii
Acknowledgments .....	iv
Abstract.....	viii
Table of Contents .....	x
List of Contents .....	xv
Abbreviations .....	xviii
CHAPTER 1: Background and Significance .....	1
1.1 Introduction .....	2
1.2 Hearing Process .....	5
Function and Structure of the Auditory Pathway .....	5
1.3 Hearing Loss and Adenosine Signaling .....	6
Clinical Significance .....	6
Current Findings in Adenosine Signaling & Hearing .....	7
1.4 ADORA2B Signaling.....	9
ADORA1, ADORA2A, and ADORA3 in Hearing Loss .....	9
ADORA2B signaling may play a role in hearing.....	10
CHAPTER 2: Elevated Cochlear Adenosine and Hearing Loss .....	12

2.1 Introduction .....	13
2.3 Materials & Methods .....	13
Ada <sup>-/-</sup> Mice .....	13
PEG-ADA generation and regimen .....	13
Hair Cell Loss and Cochleograms .....	14
Cochlea EM .....	14
Cochlea isolation, immunohistochemistry, imaging, and analysis .....	15
Auditory brainstem response recording .....	15
ABR waveform detection and calculation .....	16
Distortion product otoacoustic emission measurements .....	17
2.3 Results .....	17
Elevated Cochlear Adenosine and Hearing Loss .....	17
Adenosine and Distortion Product Otoacoustic Emissions .....	20
Adenosine and SGN→CN Amplitude Peaks & Latency .....	21
Elevated Adenosine and Hair cell Structures .....	23
Elevated Adenosine and Axon Structures .....	25
Adenosine and Myelin Structures .....	26
ADA Enzyme Therapy Resumption Rescue .....	28
2.4 Discussion .....	32
Elevated cochlear adenosine perturbs spiral ganglion neuron myelination .....	33
Adenosine levels play a role in MPZ function and expression .....	34
CHAPTER 3: Hearing Loss via ADORA2B Signaling .....	36
3.1 Introduction .....	37



3.3 Materials & Methods .....	37
Ada <sup>-/-</sup> Mice and PSB1115 prevention regimen.....	37
Ada <sup>-/-</sup> /Adora2b <sup>-/-</sup> mice.....	37
RT-PCR .....	37
Cochlea isolation, immunohistochemistry, imaging, and analysis.....	38
Auditory brainstem response recording.....	39
ABR waveform detection and calculation.....	39
Distortion product otoacoustic emission measurements .....	40
3.3 Results .....	41
Cochlear Adora2b expression.....	41
PSB1115-treated Ada <sup>-/-</sup> Auditory Brainstem Response and Distortion Product Otoacoustic Emissions Analyses .....	42
SGN→CN Amplitude Peaks & Latency in PSB1115-treated Ada <sup>-/-</sup> .....	42
ADORA2B-inhibition in Elevated Cochlear Adenosine and Axon Structures.....	44
Ada <sup>-/-</sup> /Adora 2b <sup>-/-</sup> Auditory Brainstem Response and Distortion Product Otoacoustic Emissions Analyses .....	45
SGN→CN Amplitude Peaks & Latency in Ada <sup>-/-</sup> /Adora2b <sup>-/-</sup> .....	47
3.4 Discussion.....	49
ADORA2B as a common pathogenic factor underlies hypomyelination in both Ada <sup>-/-</sup> mice and aging-dependent SNHL .....	49
ADORA2B impairs MPZ integration to myelin sheaths in peripheral nervous system.....	51
Novelty and Therapeutics for SNHL.....	52
CHAPTER 4: Other HL Models and Future Directions .....	53
4.1 Introduction .....	54

4.2 Materials and Methods .....	54
Adora2b-deficient Aging Mice.....	54
PSB1115-therapy of Aging Mice .....	54
Sickle-Cell Disease Mice .....	55
Cochlea isolation, immunohistochemistry, imaging, and analysis.....	55
Auditory brainstem response recording.....	56
ABR waveform detection and calculation.....	57
Distortion product otoacoustic emission measurements .....	57
4.2 Results .....	58
Adora2b-deficient Aging Mice and Hearing Loss .....	58
Distortion Product Otoacoustic Emissions of Aging Mouse Models.....	59
SGN→ CN Amplitude Peaks & Latency in Aging Mouse Models .....	59
PSB1115 therapy on Aging WT Mice.....	61
Structural and potential molecular mechanisms in Aging Models.....	63
Possible Molecular Pathogenesis in SNHL Associated with Elevated Adenosine .....	65
Other Disease Models: Sickle-Cell Disease and Hearing Loss.....	69
4.4 Future Directions .....	73
1) What is the cellular and metabolic basis underlying the natural progression of elevated adenosine-induced HL in <i>Ada</i> <sup>-/-</sup> mice? .....	73
2) What is ADORA2B’s role in the cellular and metabolic disturbance in HL in <i>Ada</i> <sup>-/-</sup> mice?.....	77
Bibliography .....	80
Vita .....	98



## LIST OF ILLUSTRATIONS

Figure 1. Overview of the Hearing Process

Figure 2. PEG-ADA therapy in *Ada*<sup>-/-</sup> mice

Figure 3. Elevated adenosine contributes to hearing loss sensitivity

Figure 4. Elevated adenosine causes outer hair cell dysfunction at low frequencies

Figure 5. Elevated cochlear adenosine decreases amplitudes of peripheral nerve and cochlear nucleus

Figure 6. Elevated cochlear adenosine changes peripheral nerve and cochlear nucleus neuronal response latency

Figure 7. Cochleogram of PEG-ADA treated and untreated *Ada*<sup>-/-</sup> and schematic diagram of tonotopic frequency mapping in inner ear

Figure 8. Cochleogram analysis comparing hair cell loss of PEG-ADA treated and untreated *Ada*<sup>-/-</sup> mice

Figure 9. Nerve structure in *Ada*<sup>-/-</sup> mice cochlea with and without PEG-ADA therapy

Figure 10. Labeling of nerve fiber and MPZ protein on cochlear nerve

Figure 11. ABR thresholds post PEG-ADA treatment during STOP treatment regimen

Figure 12. PEG-ADA rescue therapy on STOP treatment *Ada*<sup>-/-</sup> mice

Figure 13. ABR analysis on *Ada*<sup>-/-</sup> after PEG-ADA rescue therapy

Figure 14. Peak I and II analysis on *Ada*<sup>-/-</sup> mice after PEG-ADA rescue therapy

Figure 15. Peak I-II latency analysis on *Ada*<sup>-/-</sup> mice after PEG-ADA rescue therapy

Figure 16. Nerve fiber and MPZ protein immunofluorescent staining on *Ada*<sup>-/-</sup> mice cochlear nerve

Figure 17. Adenosine receptors mRNA expression in *Ada*<sup>-/-</sup> whole cochlea

Figure 18. PSB1115 therapy on *Ada*<sup>-/-</sup> mice

Figure 19. Auditory brainstem response and distortion product otoacoustic emission analysis on *Ada*<sup>-/-</sup> mice with PSB1115

Figure 20. Peak I and II analysis on *Ada*<sup>-/-</sup> mice after PSB1115 therapy

Figure 21. Peak I-II latency analysis on *Ada*<sup>-/-</sup> mice after PSB1115 therapy

Figure 22. Nerve fiber and MPZ protein immunofluorescent staining on *Ada*<sup>-/-</sup> mice with PSB1115 therapy cochlear nerve

Figure 23. *Ada*<sup>-/-</sup>/*Adora2b*<sup>-/-</sup> mouse model

Figure 24. Auditory brainstem response and distortion product otoacoustic emission analysis on *Ada*<sup>-/-</sup>/*Adora2b*<sup>-/-</sup> mice

Figure 25. Peak I and II analysis on *Ada*<sup>-/-</sup>/*Adora2b*<sup>-/-</sup> mice compared to STOP treatment *Ada*<sup>-/-</sup> mice

Figure 26. Peak I-II latency analysis on *Ada*<sup>-/-</sup>/*Adora2b*<sup>-/-</sup> mice compared with STOP-treatment *Ada*<sup>-/-</sup> mice

Figure 27. ABR analysis of aged WT mice and aged *Adora2b*<sup>-/-</sup> mice

Figure 28. Peak I and II analysis of aged *Adora2b*<sup>-/-</sup> mice compared to aged WT

Figure 29. Peak I-II latency analysis of aged *Adora2b*<sup>-/-</sup> mice compared to aged WT

Figure 30. PSB1115 therapy on 6-month-old C57B6J mice

Figure 31. ABR analyses on PSB1115-treated 6-month-old C57B6J mice

Figure 32. DPOAE analysis on PSB1115-treated 6-month-old C57B6J mice

Figure 33. Nerve fiber and MPZ protein immunofluorescent staining on aged *Adora2b*<sup>-/-</sup> cochlear nerve compared to aged WT

Figure 34. Mitochondrial fatty acid metabolism pathways and related metabolomics profile of PEG-ADA treated and untreated *Ada*<sup>-/-</sup> mice

Figure 35. Working Model

Figure 36. ABR analysis of sickle-cell transplanted -WT, *CD73*<sup>-/-</sup>, and *Adora2b*<sup>-/-</sup>

Figure 37. DPOAE analysis of sickle-cell transplanted -WT, *CD73*<sup>-/-</sup>, and *Adora2b*<sup>-/-</sup>

Figure 38. Peak I and II analysis of sickle-cell transplanted -WT, *CD73*<sup>-/-</sup>, and *Adora2b*<sup>-/-</sup>

## ABBREVIATIONS

ABR	auditory brainstem response
ADA	Adenosine deaminase
ADORA1	Adenosine A1 receptor
ADORA2A	Adenosine A2A receptor
ADORA2B	Adenosine A2B receptor
ADORA3	Adenosine A3 receptor
CMT	Charcot Marie Tooth Disease
CN	cochlear nucleus
CPT1	carnitine-palmitoyl transferase 1
CPT2	carnitine-palmitoyl transferase 2
DPOAE	distortion product otoacoustic emission
ENTs	equilibrative nucleotide transporters
HL	hearing loss
IHC	inner hair cell
LCA	long-chain acylcarnitines
MPZ	myelin protein zero
NF	nerve fiber
OHC	outer hair cell
PEG-ADA	polyethylene glycol-ADA
PNS	peripheral nervous system
SCD	sickle-cell disease
SGN	spiral ganglion neuron
SNHL	sensorineural hearing loss

VOC vaso-occlusive crisis



## **CHAPTER 1: Background and Significance**

## *1.1 Introduction*

Hearing loss (HL) affects millions of people worldwide resulting in an annual global cost of over \$700 billion (1). HL impacts effective communication with others, loss of cognitive function, and can lead to depression (2). Current treatments for the most common type of HL, sensorineural HL (SNHL), are limited to hearing aids and cochlear implants, with no FDA-approved drugs available. Multiple conditions are known to cause HL including genetic, drug, aging and noise. It is commonly accepted that the hearing process demands an abundance of ATP and that HL is often attributed to a disturbance in this metabolic energy currency (3–9). Thus, it is imperative to investigate the metabolic and molecular basis underlying HL, a leading public health concern, and establish novel approaches to treat and prevent its progression.

Adenosine functions as a signaling nucleoside that orchestrates a physiological and pathological response to energy deficiency or cell injury by the activation of one or more of the four adenosine receptors (10). Under hypoxia, energy insufficiency, and cellular damage, ATP is released from cells, which can then be hydrolyzed into AMP and further into adenosine by two ectonucleotidases, CD39 and CD73. Extracellular adenosine is eliminated by the uptake into cells by of equilibrative nucleotide transporters (ENTs). Intracellular adenosine is irreversibly degraded by adenosine deaminase (ADA), leading to increased uptake of extracellular adenosine by ENT2. However, extracellular adenosine concentrations can reach as high as 100  $\mu$ M under stress (9). Adenosine signaling activates four adenosine receptors (ADORA-1, -2A, -2B, and -3.) that are found present in rodent cochlea (11). These receptors fulfill different roles due to their variable distribution of expression in different cell types and according to the level of adenosine present (9).

Presbycusis, age-related hearing loss, is the most common type of SNHL. Age-related cochlear pathogenesis has been posited to be due to increased levels of ROS, perturbed blood

flow, and persistent noise-exposure (12–14). Previous studies have shown that acoustic-overstimulation result in increased ATP release in the cochlear partition (3,15,16). Although the effects of sustained levels of cochlear adenosine have yet to be determined, studies have shown that various organs have elevated adenosine during the aging process, especially the auditory cortex (17–24). Early studies showed that adenosine signaling is involved in multiple animal models of HL. For example, ADORA-1 and -3 have a protective role in noise-induced and cisplatin-induced models of HL by regulating antioxidant production and presynaptic glutamate release among other functions (9). ADORA2A, on the other hand, is mainly expressed in the organ of Corti, spiral ganglion neurons (SGN), and cochlear vasculature and may play a detrimental role in HL by persistent vasodilation (9,25). Among four adenosine receptors, ADORA2B has the least affinity for adenosine and is, therefore, only activated by chronically elevated levels of adenosine. Early studies showed that excess adenosine signaling via ADORA2B leads to multiple cellular damage, dysfunction and disease progression including chronic kidney disease, sickle cell disease, priapism and preeclampsia (26–32). However, the functional role of ADORA2B signaling in SNHL remains unknown.

Patients with ADA-deficiency have chronically elevated levels of circulating adenosine that result in severe health problems including immunodeficiency (7). Unexpectedly, ADA-deficient patients developed bilateral SNHL (7,33,34). Deafness and SNHL in ADA-deficient patients were not ascribed to any genetic-, structural-, drug-, or infection-affiliated cause, implicating a metabolic disturbance related to elevated adenosine (7). Consistently, recent studies validated that ADA-deficient mice (*Ada*<sup>-/-</sup>) mimicking ADA-deficient humans display the phenotype of HL and that polyethylene glycol-ADA (PEG-ADA) treated 7-day post-partum *Ada*<sup>-/-</sup> mice have improved hearing and immune abnormalities (35). Thus, elevated cochlear adenosine is likely a common metabolic signaling molecule involved in SNHL in ADA-deficiency and other conditions such as aging, noise and drugs. To define the pathogenic mechanism of elevated

cochlear adenosine in SNHL, we took advantage of adult *Ada*<sup>-/-</sup> mice *and aged* wild type (WT) mice, two distinct animal models with SNHL, to probe cellular, molecular and metabolic basis underlying elevated cochlear adenosine in SNHL with a goal to develop innovative therapies.

Here we report that ADORA2B-mediated impairment of myelination of SGN is a common pathogenic mechanism underlying SNHL in both *Ada*<sup>-/-</sup> mice and aged WT mice, establishing a strong foundation for adenosine-based therapy in SNHL, a very common disability.

## 1.2 Hearing Process

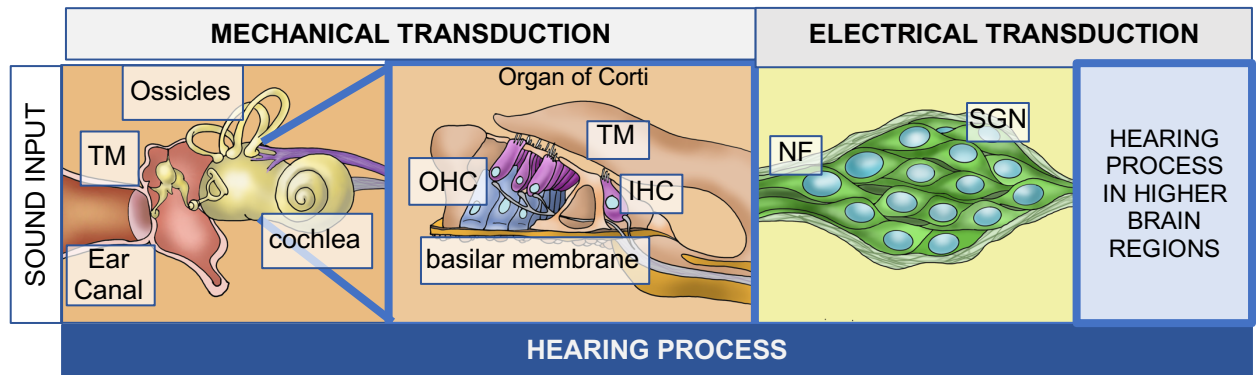


Figure 1. Overview of the Hearing Process

Schematic diagram of the hearing process starting from the sound input into the external ear that vibrates the middle ear ossicles, followed by stimulation of the inner ear sensory cells found in the cochlea. Hair cell movement of outer and inner hair cells (OHC, IHC) releases neurotransmitters onto the bipolar spiral ganglion neurons (SGN) that communicate with higher brain regions.

### Function and Structure of the Auditory Pathway

The hearing process requires a sophisticated orchestration of multiple structures and cell types. This involves the external ear, middle ear, and inner ear that produce consecutive mechanical and electrical transduction upon sound stimulation. Sound is a wave from a vibrating object that propagates pressure variation through air (36). Thus, when sound waves reach the ear, it creates a vibration that sets hearing into motion through the ear drums.

The external ear is responsible for capturing sound from surroundings through the pinna. Sound travels through the ear canal, which begins the transfer of sound waves from air into a denser medium, the tympanic membrane (Figure 1). This is the beginning of the mechanical transduction of the hearing process.

The tympanic membrane, then, transmits this vibration into the ossicles in the middle ear. This causes the oval window of the inner ear to also vibrate, leading to the motion of inner ear fluid. The inner ear is comprised of the vestibular system and the cochlea, responsible for sensing balance and equilibrium, as well as hearing, respectively.

The cochlea contains fluid compartments: perilymph that is found in scala tympani, and scala vestibuli and endolymph found in the scala media. Vibrations in the scala media are the impetus of electrical stimulation in the hearing process. The mechano-electrical transition occurs in the Organ of Corti, which includes the inner and outer hair cells sitting on the basilar membrane that spans from the base to the apex of the cochlea. These hair cells have hair bundles, composed of stereocilia, on its apical surface that are “sheared” by the tectorial membrane (TM) upon vibration of Organ of Corti and basilar membrane (Figure 1).

The mechanical shearing of hair cells causes depolarization, consequently releasing neurotransmitters to stimulate cochlear nerve fibers. Depolarization of hair cells sends signals to bipolar first order neurons (spiral ganglion cells) that synapse to the cochlear nucleus. Activation of cochlear nucleus is processed into the higher regions of the central auditory pathways.

### *1.3 Hearing Loss and Adenosine Signaling*

#### *Clinical Significance*

According to the World Health Organization (WHO), hearing loss affects around 466 million people worldwide. WHO also predicts that this number will rise to almost a billion by

2050 (1). HL impacts effective communication with others, loss of cognitive function, and can lead to depression (2). There are several types of HL, however, the most commonly reported is sensorineural HL (SNHL). Patients with SNHL have damaged cochlea and auditory nerve where the hair cells and spiral ganglion neurons (SGN) are non-regenerative. Currently, SNHL patients are limited to hearing aids and cochlear implants with no pharmacological therapeutic options (37).

Noise exposure and age-related hearing loss, or presbycusis, are the most common causes of SNHL in adults. Noise exposure can damage hair cells that are more sensitive to high frequency at the base of the cochlea. Patients with presbycusis, on the other hand, may still be sensitive to low-frequency sounds, but have difficulty distinguishing high-frequency sounds that can affect spoken communication. This loss of sensitivity to high-frequency sounds usually has nerve cell and stria vascularis damage and can progressively worsen to deterioration of low and middle-frequency hearing over time.

#### *Current Findings in Adenosine Signaling & Hearing*

Elevated extracellular adenosine is an important signaling molecule involved in pathological conditions. Cells under stress release high levels of ATP extracellularly which are consequently hydrolyzed into ADP and adenosine by ectonucleotidases. Adenosine is then irreversibly metabolized into inosine by adenosine deaminase (ADA), or is uptake by nucleoside transporters intracellularly for further breakdown into inosine or AMP by ADA and adenosine kinase (ADK), respectively. As many studies have shown, tissues under stress can induce a persistent release of ATP and accumulation of adenosine that result in a deleterious pathogenic cycle.

Age-related hearing loss (ARHL), presbycusis, is a type of SNHL that has been attributed to a variety of causes. ARHL occurs with more frequency with people increasing in age, such as

other age-related disease like atherosclerosis, cancer, cardiovascular disease, and so on (38). Aging is the naturally occurring gradual decline of organ function orchestrated by damaging biological processes overtime; however, the exact molecular mechanisms that underlie ARHL remain to be elucidated. Persistent noise trauma can accelerate presbycusis and studies have shown that acoustic-overstimulation can result in increased ATP in cochlear fluid (3,15,16). Additionally, age-related diseases like atherosclerosis and diabetes can perturb blood flow and supply in the cochlea, respectively (39). One study showed that pharmacological inhibition of ADK prevented ARHL in mice and postulated that increased cochlear endogenous adenosine levels preserves sensorineural functions in low-frequency, apical region (40). Overall, preserving cells in aging cochlea; however, this study did not evaluate how the direct changes in adenosine levels affect hearing. The manipulation of cochlear adenosine levels during the aging process has never been investigated. However, previous studies have shown an increase in adenosine levels in aging organs (17,18,20–24). Particularly, the thalamus and auditory cortex where adenosine has been shown to play a role in auditory plasticity in the CNS (19). This study points out how adenosine levels play an important role in hearing.

SNHL was reported in humans lacking adenosine deaminase (ADA), an enzyme that irreversibly metabolizes adenosine into inosine (7,33,34). HL in these patients was not attributed to genetic, drug, infection, or treatment-related causes; therefore HL in these patients is implicated to be a metabolic disturbance due to elevated systemic adenosine levels (7). In 2019, a study showed for the first time how ADA-deficient mice (*Ada*<sup>-/-</sup>) parallel ADA-deficient humans by having bilateral HL (35). They also showed how enzyme replacement therapy with polyethylene glycol-ADA (PEG-ADA) can improve hearing and immune pathologies in young developing mice (35). However, the exact pathogenic mechanisms of elevated adenosine levels in HL still remain elusive.



Future objectives in hearing loss research should determine the molecular basis of how elevated adenosine results in HL to develop effective treatment and preventative therapeutic options. Fulfilling these objectives will not only broaden our understanding of adenosine signaling in inner ear physiology and help treat a very common disability. The impact of the proposed research alleviates both patient suffering and overall economic burden of billions of dollars dedicated to HL health sectors and educational support systems (41).

#### *1.4 ADORA2B Signaling*

##### *ADORA1, ADORA2A, and ADORA3 in Hearing Loss*

Adenosine receptors are G-protein coupled-receptors that induce a variety of intracellular signaling pathways, depending on whether they stimulate or inhibit adenylyl cyclase. Adenosine receptor 1 (ADORA1) and adenosine receptor 3 (ADORA3) both inhibit adenylyl cyclase by coupling to  $G_{i/o}$  proteins. Adenosine 2a and adenosine 2b receptors, on the other hand, stimulate adenylyl cyclase via  $(9)G_s$  or  $G_{olf}$  proteins. Several studies in the hearing field have investigated the roles of ADORA1, -2A, and 3, exemplifying their different roles through activating various downstream pathways with evidence dependent on varying adenosine levels.

All four adenosine receptors have different affinities for adenosine, with ADORA1 having the highest. ADORA1 stimulation has been found to generally be protective in noise- and drug-induced HL (4,42–44). ADORA1 is posited to have a cytoprotective role under cochlear stress through inhibiting glutamate excitotoxicity by inhibiting glutamate release, a known ADORA1 function in the central nervous system (4). Another hypothesis is the idea that ADORA1 may be reducing oxidative stress and reduce apoptotic effects during cochlear acoustic trauma, overall protecting hair cells (8).

ADORA2A has the highest affinity for adenosine next to ADORA1. ADORA2A has been the major adenosine receptor for modulating inflammation. In hearing research, however,

previous studies show that whole genetic deletion of ADORA2A in mouse exposed to noise preserved outer hair cells ribbon synapses, and spiral ganglion neurons, which may indicate while both ADORA2A and ADORA1 play a role in apoptosis, they may have differing regulatory functions (45).

ADORA3 stimulation has varying effects in the cochlea that are dependent on agonist dosage. Previous studies have shown that lower dosages of ADORA3 agonists may induce pathways that promote tissue survival, but may promote apoptosis at higher dosages (9,46,47). Overall, little is known about ADORA3 functionality in the hearing field and needs to be investigated further.

All three high-affinity adenosine receptors have been investigated in the hearing field. While these receptors have been studied in rodents, a molecular function gleaned from these studies remain a mystery. Additionally, identifying each receptor's role and how they orchestrate downstream pathways in response to different levels of extracellular adenosine remains to be investigated.

#### *ADORA2B signaling may play a role in hearing*

While all four receptors are found to be expressed in rodent cochlea, ADORA2B is the remaining receptor yet to be investigated in the hearing field. ADORA2B receptor has the least affinity among the four adenosine receptors. ADORA2B's activation is dependent on excessive and chronic extracellular adenosine presence and is known to induce downstream pathological pathways, such as sickle cell disease, chronic kidney disease, and priapism and preeclampsia (26–32). Although ADORA2B has not been studied in the hearing process, it has been posited that

activation of this receptor can activate JNK, where inhibition of JNK has been found to protect acoustic trauma and cytotoxic antibiotics through hair cell survival (48,49).

## **CHAPTER 2: Elevated Cochlear Adenosine and Hearing Loss**

## *2.1 Introduction*

As previously mentioned in Chapter 1, the exact molecular mechanism of how elevated adenosine causes hearing loss remains to be studied. To address this, we used *Ada*<sup>-/-</sup> deficient mice and PEG-ADA enzyme replacement therapy to study how manipulations in systemic adenosine levels can affect hearing. In this chapter, we show how cochlear elevated adenosine affects hearing sensitivity and sensory cells in the cochlear. More importantly, we also show whether resumption of PEG-ADA in *Ada*<sup>-/-</sup> mice with hearing loss caused by elevated adenosine can rescue pathological phenotypes.

## *2.3 Materials & Methods*

### *Ada*<sup>-/-</sup> Mice

*Ada*<sup>-/-</sup> mice were generated and genotyped as previously reported (50). Mice homozygous for the null *Ada* allele were labeled *Ada*<sup>-/-</sup>, while mice genotyped with the *Ada* allele were labeled as *Ada*<sup>wt</sup>. All mice were congenic on a C57BL/6 background, and all phenotypic comparisons were performed among littermates.

### *PEG-ADA generation and regimen*

Polyethylene glycol-modified-ADA (PEG-ADA) was produced from purified bovine ADA with activated PEG previously described (51–53). *Ada* mice were injected 15 ul intramuscularly from birth to postpartum day 18 every 4 days. Mice older than postpartum day 18 were injected once a week with 100 ul of diluted PEG-ADA (1:5 with 1x sterile DPBS) intraperitoneal injections until they reach 8 weeks of age. PEG-ADA treated group were given this treatment continuously from 8-10 weeks of age, while STOP-treatment group were deprived of drug within these two weeks. RESCUE group had PEG-ADA withdrawn for two weeks at 8

weeks followed by PEG-ADA resumption of intraperitoneal injections every other day for one week.

#### Hair Cell Loss and Cochleograms

Cochleae were prepared and evaluated as previously described (54,55). The anesthetized mice were decapitated and their bullae was quickly removed and opened to expose the inner ear. Afterward, the cochleae were immersed in 10% formalin fixative and shipped to University of Buffalo for analysis. Cochleae were stained with Ehrlich's hematoxylin solution, the organ of Corti carefully microdissected out into two or three segments and mounted as a flat surface preparation in glycerin on glass slides (54). Surface preparations were examined with a light microscope (Zeiss Standard, 400X magnification). Surface preparations were photographed with a digital camera (SPOT Insight, Diagnostic Instruments Inc), processed with imaging software (SPOT Software, version 4.6) and images assembled with Adobe Photoshop 5.5. Inner hair cells (IHC) and outer hair cells (OHC) were counted along successive 0.12-0.24 mm intervals of the organ of Corti beginning at the apex. Hair cells were counted as present if the cell body and cuticular plate were intact. Cochleograms showing percent hair cells missing as a function of percent total distance from the apex were constructed for each animal. Percent hair cell losses were based on laboratory norms for young CBA mice (54).

#### Cochlea EM

Cochlea was fixed in 2% buffered glutaraldehyde, followed by decalcification with a formic acid/formalin solution (1M formaldehyde, 2.5M formic acid, pH 2.0). Fixed cochlea was dehydrated and was embedded in plastic via an automated tissue processor for electron microscopic specimens. Embedded tissues were sectioned at 0.6 micrometers. The tissue sections were stained with uranyl acetate and lead citrate. The tissue was examined using a transmission

electron microscope and digital images were obtained. G-Ratio analyses was adapted from Gratio ImageJ plug-in (<http://gratio.efil.de/download/>).

#### Cochlea isolation, immunohistochemistry, imaging, and analysis

Temporal bones were dissected in PBS, incubated in 4% paraformaldehyde (PFA) in PBS overnight at 4°C, decalcified in 0.2 M EDTA for 5–7 d. Fixed tissue was embedded in OCT compound, cryosectioned at 10  $\mu$ m, followed by standard immunohistochemistry procedure. The tissue sections were washed with 1x phosphate-buffered saline (PBS), followed by a 1 hr incubation in 5% BSA with 1% Triton X-100 in 1xPBS. These sections were then incubated in primary antibodies overnight at 4°C. The primary antibodies used for this study were: nerve fiber filament (mouse anti-NF-200, Sigma, 1:200), neuron cell bodies (rabbit anti-NeuN, Abcam, 1:500), and myelin protein zero (rabbit anti-MPZ, Abcam 1:200). Tissues were then incubated with incubated with appropriate Alexa-Fluor conjugated secondary antibodies (Invitrogen, 1:500), followed by DAPI mountant (ProLong Gold Antifade, Thermo Fisher Scientific).

Confocal z-stacks of each cochlea were taken using Zeiss LSM T-PMT microscope equipped with 63x (2x digital zoom) oil immersion lens. MPZ- and NF-200 areas were quantified using ImageJ by selecting via consistent color threshold for each antibody used across all experiment groups (n=3 each) and normalizing each sample by total area of the axon. These MPZ+/total axon area and NF200+/total axon quantifications were collectively compared across all experiments via a Mann-Whitney nonparametric two-tailed t-test. All statistical analyses were performed via Prism 8.

#### Auditory brainstem response recording

Mice were intraperitoneally injected with ketamine-xylazine (100 mg/kg: 10mg/kg). Testing was performed in a soundproof faraday cage booth while mice were placed on heating

pad to maintain normal body temperature throughout the procedure. Pure tone bursts (0.1 ms rise/fall, 2 ms duration, 21 presentations/s) from 4 to 48 kHz were generated using System 3 digital signal processing hardware and software (Tucker Davis Technologies). The intensity of the tone stimuli was calibrated using a type 4938 one-quarter inch pressure-field calibration microphone (Bruel & Kjaer). EC1 ultrasonic, low-distortion electrostatic speakers were coupled to the ear canal to deliver stimuli within 3 mm of the tympanic membrane. Response signals were recorded with subcutaneous needle electrodes inserted at the vertex of the scalp (channel 1), the postauricular bulla region (reference), and the back leg (ground), and averaged over 500 presentations of the tone bursts (56). Electrode-recorded activity was filtered (high pass, 300 Hz; low pass, 3kHz; notch, 60Hz) before averaging to minimize background noise. Auditory thresholds were determined by decreasing the sound intensity of each stimulus to 10 dB from 90 dB in 5 dB steps until the lowest sound intensity with reproducible and recognizable waveforms was detected. Thresholds were determined to within 5 dB for each frequency by two raters to ensure reliability. SD (dB SPL) were plotted as a function of stimulus frequency (kilohertz) and analyzed for group differences by a two-way ANOVA, followed by a multiple-comparison test, to reveal overall trends. Prism 8 was used for all statistical analyses.

#### *ABR waveform detection and calculation*

Peak amplitudes (I and II) were visually determined from ABR waves detected from each stimulus from 90 to 10 dB in 5 dB increments at each frequency. Peak amplitudes were measured by subtracting the peak voltage from the trough voltage at every dB presentation, averaged per experimental group. All averaged peak amplitudes for each peak from each group were statistically compared using two-way ANOVA, followed by a multiple comparison test.



Peak latencies from peak I and II were calculated by subtracting Peak I's peak amplitude temporal onset (in ms) from Peak II's peak amplitude temporal time onset (in ms). Time measurements were averaged per experimental group. Averaged latencies per group were compared via two-way ANOVA, followed by a multiple comparison test.

All statistical analyses were performed through Prism 8.

### *Distortion product otoacoustic emission measurements*

DPOAEs were measured from a probe tip microphone placed in the external canal of the mouse ear that were elicited by two 1-second sine-wave tones of varying frequencies ( $F_2=1.2 \cdot F_1$ ).  $F_2$  had a varied range of frequencies from 4 to 90 kHz. These two tones were presented in identical intensities that ranged from 15 to 75 dB Sound Pressure Level (SPL) in 15 dB increments. The magnitude of the  $2 \cdot F_1 - F_2$  DP was determined by FFT. DPOAE thresholds ( $> -5$  dB SPL and greater than two std. dev above noise floor) were analyzed off-line via BioSigRZ program. If no DPOAE was detected, we defined the threshold to be at 75 dB, as our equipment is limited to 80 dB SPL. DPOAE thresholds were averaged per experimental group and compared via one-way ANOVA, followed by a multiple comparisons test. All statistical analyses were done through Prism 8.

## *2.3 Results*

### *Elevated Cochlear Adenosine and Hearing Loss*

To determine the pathogenic mechanisms of HL mediated by chronically elevated adenosine as seen in ADA-deficient humans, we took advantage of using *Ada*<sup>-/-</sup> mice, which manifest most of the phenotypes observed in ADA-deficient humans including HL (26,27,31,52,57). Although ADA-deficiency is a lethal condition for humans and mice, ADA-

deficient humans and mice can survive indefinitely by enzyme replacement therapy that involves weekly injection of polyethylene glycol-ADA (PEG-ADA), an FDA-approved drug to reduce excessive levels of adenosine in ADA-deficient humans and mice(50). Furthermore, the experimental ease with which adenosine levels can be regulated by administration of PEG-ADA represents a powerful investigative strategy (50). Thus, we used PEG-ADA enzyme therapy as a powerful experimental approach to determine how elevated adenosine contributes to HL in *Ada*<sup>-/-</sup> mice. Specifically, *Ada*<sup>-/-</sup> mice were maintained on a high dose regimen of PEG-ADA treatment (5U/wk) from birth to 8wks of age to allow normal neuro-physiological development, including the auditory system. At 8-weeks of age a control group of *Ada*<sup>-/-</sup> mice continued to be treated with PEG-ADA (PEG-ADA treated *Ada*<sup>-/-</sup>). A second group was deprived of PEG-ADA therapy for 2 weeks to allow adenosine to accumulate, named STOP treatment *Ada*<sup>-/-</sup> (Figure 2).

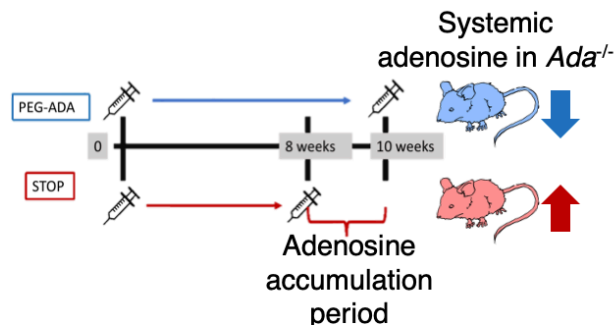


Figure 2. PEG-ADA therapy in *Ada*<sup>-/-</sup> mice. *Ada*<sup>-/-</sup> mice are treated with PEG-ADA from birth to 8 weeks for normal development. For two weeks, PEG-ADA-treated mice are continually treated with the drug, while STOP-treatment mice are withdrawn from the drug.

We used HPLC to validate that the *Ada*<sup>-/-</sup> mice following 2 week-withdrawal of the PEG-ADA treatment contained significantly elevated cochlear adenosine levels compared to *Ada*<sup>-/-</sup> mice with continuous PEG-ADA treatment (Figure 3, left). However, continuous treatment of

*ADA*<sup>-/-</sup> mice with PEG-ADA did not completely eliminate elevated cochlear adenosine levels to that observed in WT mice (Figure 3, left).

Next, we tested auditory function in these mice by measuring the auditory brainstem response (ABR). Consistent to elevated adenosine in *Ada*<sup>-/-</sup> mice subjected to PEG-ADA withdrawn for 2 weeks, these mice displayed significant HL across a wide frequency range (4kHz to 32kHz) (Figure 3, right), corresponding to a mild to severe HL on a clinical scale that is consistent with HL reported in ADA-deficient patients(33,34). Significantly, continuous treatment with PEG-ADA substantially prevented HL in *Ada*<sup>-/-</sup> mice (Figure 3, right). Supporting our observation that *Ada*<sup>-/-</sup> mice maintained on continuous PEG-ADA treatment regimen mice contained slightly higher cochlear adenosine levels than those of WT mice (Figure.3, left), these mice displayed very mild sensorineural HL (SNHL) compared to the WT mice (Figure 3, right). Altogether, using *Ada*<sup>-/-</sup> mice as a genetic tool coupled with PEG-ADA enzyme therapy to control cochlear adenosine levels, we provide solid genetic evidence that increased cochlear adenosine promoted HL in *Ada*<sup>-/-</sup> mice and that PEG-ADA treatment lowered adenosine and prevented HL in these mice.

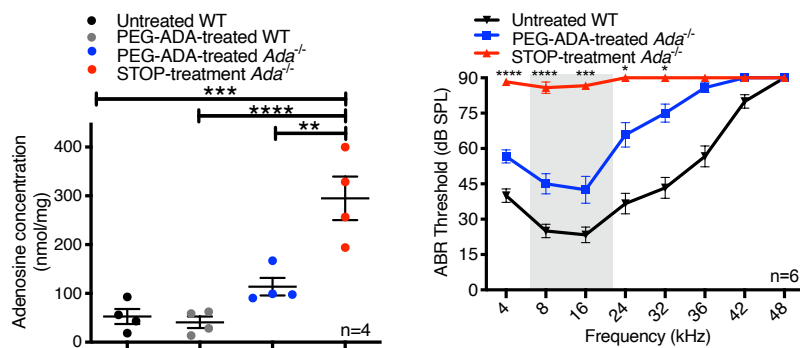


Figure 3. Elevated adenosine contributes to hearing loss sensitivity. (left) (mean ± SEM)

Adenosine levels are elevated in STOP-treatment mice compared to all other cohorts (p-value of

STOP-treatment and PEG-ADA, 0.0017) (n=4 for each condition). (right) (mean  $\pm$  SEM) After two-week PEG-ADA withdrawal, auditory brainstem response (ABR) thresholds at different frequencies demonstrate hearing loss in STOP-treatment mice (p-value of STOP-treatment and PEG-ADA at 8 and 16 kHz, <0.0001 and 0.0009, respectively) (n=6 for each cohort).

#### Adenosine and Distortion Product Otoacoustic Emissions

Upon onset of sound stimulation, normal hearing requires a proper mechanical transduction reflecting the function of overall cochlear amplifier and stimulation of the outer hair cells (OHC) and electrical transduction reflecting the number of spiral ganglion neurons (SGN) firing and the speed of transmission from hair cells, spiral ganglion neurons (SGNs) and cochlear nucleus (CN) in the auditory pathway leading to the brainstem (Figure 1). Thus, to define the specific impairment from mechanical to electrical transduction underlying HL in *Ada*<sup>-/-</sup> mice, we assessed mechanical transduction measured by the frequency-specific distortion product otoacoustic emission (DPOAE) analysis (Figure 4) and electrical transduction by measuring I and II peak amplitude (Figure 5) and inter-peak latency (Figure 6), respectively, in the auditory pathway leading to the brainstem.

Because hearing for mice is most sensitive at 8 and 16 kHz, we analyzed at these frequencies. STOP-treatment *Ada*<sup>-/-</sup> displayed an increase of DPOAE threshold compared to PEG-ADA treated *Ada*<sup>-/-</sup> mice at 8 kHz (Figure 4, left). A slight increase was also seen at 16 kHz, but the increase did not achieve significance (Figure 4, right). Overall these results indicate that elevated cochlear adenosine causes a mild defect in mechanical transduction from sound stimulation to firing of hair cells.

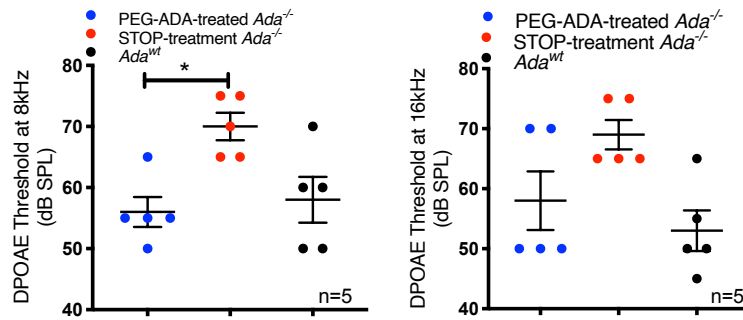


Figure 4. Elevated adenosine causes outer hair cell dysfunction at low frequencies. (mean  $\pm$  SEM)

Distortion-product otoacoustic emissions (DPOAEs) measured at 8 and 16 kHz demonstrate mild cochlear dysfunction in STOP treatment mice (p-value for 8 and 16 kHz, 0.0150 and 0.1334, respectively) (n=6 for each cohort).

#### Adenosine and SGN $\rightarrow$ CN Amplitude Peaks & Latency

In contrast to the mild decreased in DPOAE, averaged peak amplitudes of STOP-treatment  $Ada^{-/-}$  was significantly lower compared to PEG-ADA treated  $Ada^{-/-}$  at 8 and 16 kHz. (Figure 5). Additionally, extracted SGN  $\rightarrow$  CN peak I to peak II latency was significantly longer in STOP-treatment  $Ada^{-/-}$  mice compared to  $Ada^{-/-}$  mice with continuous PEG-ADA therapy (Figure 6). Thus, elevated cochlear adenosine contributes to NSHL in  $Ada^{-/-}$  mice via dual mechanisms: 1) a mild defect in mechanical transduction in the cochlear amplifier and outer hair cells; 2) a much more severe impairment of electrical transduction featured with the decreased firing of SGNs and transduction from SGNs to the CN.

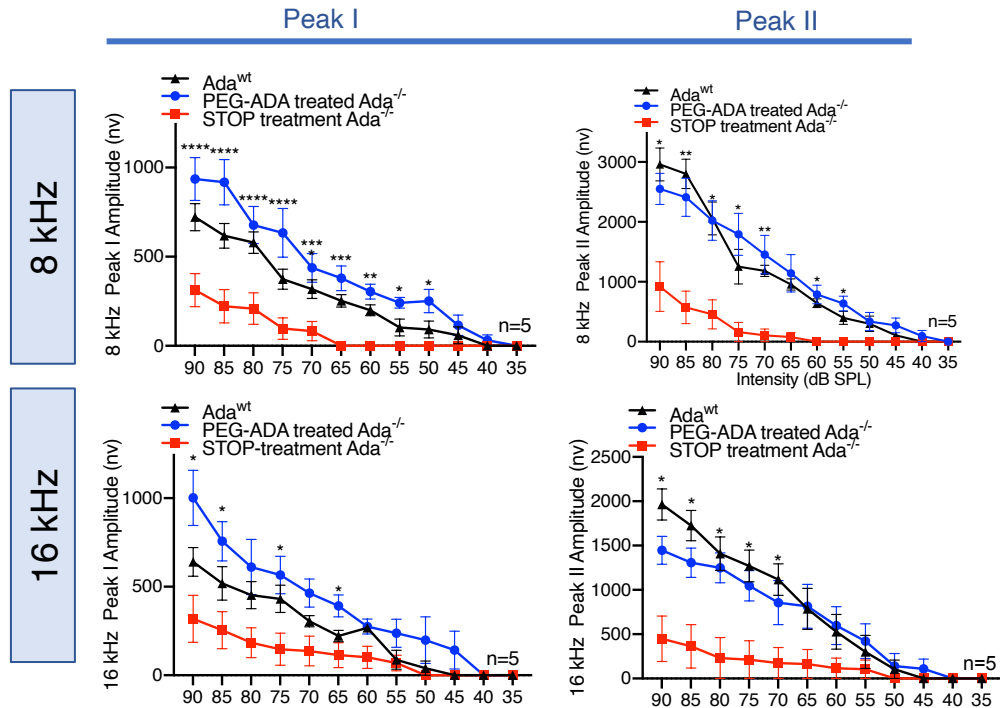


Figure 5. Elevated cochlear adenosine decreases amplitudes of peripheral nerve and cochlear nucleus. Auditory brainstem response traces were analyzed, where Peak 1 (peripheral nerve) amplitudes were elevated in PEG-ADA treated mice compared to STOP-treatment mice. Peak II pertains to cochlear nucleus, showing the same elevation as Peak I, indicating higher capacity of neurons to fire effectively with lowered adenosine. (p-value for 8 kHz for peak I for 90-75 dB, <0.0001) (p-value for 8 kHz for peak II 90-75 dB, 0.03096, 0.00623, 0.01439, 0.01468 respectively) (p-value for 8 kHz for peak I and II for 90-75 dB, 0.02534, 0.02643, 0.11141, 0.04031, respectively) (p-value for 16 kHz for peak I and II for 90-75 dB, 0.0323, 0.0352, 0.0207, 0.0396, respectively) (n=6 for each group)

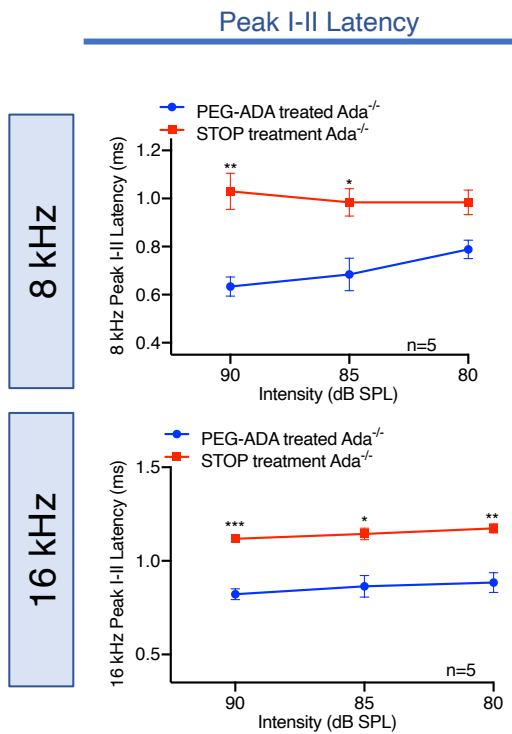


Figure 6. Elevated cochlear adenosine changes peripheral nerve and cochlear nucleus neuronal response latency. Peak I-II latency measures the efficiency of firing of peripheral nerves to cochlear nucleus in time (ms), showing faster conductance between two structures when adenosine is lower (p-value for 8kHz 90-80 dB, 0.0098 0.0296 0.0502, respectively) (p-value for 16kHz 90-80 dB, 0.0003 0.0152 0.0093 , respectively). Data are shown as mean  $\pm$  SEM.

### Elevated Adenosine and Hair cell Structures

Extending from functional understanding of pathogenic mechanism of SNHL in *Ada*<sup>-/-</sup> mice, we probed the specific cellular changes in *Ada*<sup>-/-</sup> mice through diverse histological and microscopic analyses. First, to determined how the spatial organization of hair cells from the base to the apex pertain to regions of sensitivity to resonant frequency, we prepared surface preparation of the entire organ of Corti (Figure 7, left) of PEG-ADA treated and STOP treatment mice and used them to prepare cochleogram showing the percent OHC and IHC loss as function of percent distance from the cochlea. Based on the nature of traveling waves moving through the basilar membrane, outer hair cells, depending on their distance from the apex of the cochlea, are more sensitive to certain hearing frequencies (Figure 7, right) (58). In STOP-treatment *Ada*<sup>-/-</sup> mice, the OHC (OHC row 1,2,3) losses declined from 100% at the extreme base to less than 10% loss at the 70% location, indicative of a hair cell functional loss around 48 kHz. OHC losses in PEG-

treated mice were similar, but were restricted to slightly more basal regions. However, we did not observe any ABR differences between the two groups at 48 kHz. However, we did not observe any ABR difference at 48 kHz. Thus, a 30% hair cell loss at the base of the cochlea did not cause functional defect in ABR (Figure 3, right) (59). We also observed 10% loss closer to the apex where it is sensitive to the lower frequencies, reflecting our DPOAE analysis showing a mild increase of auditory threshold at 8kHz (Figure 4, left)

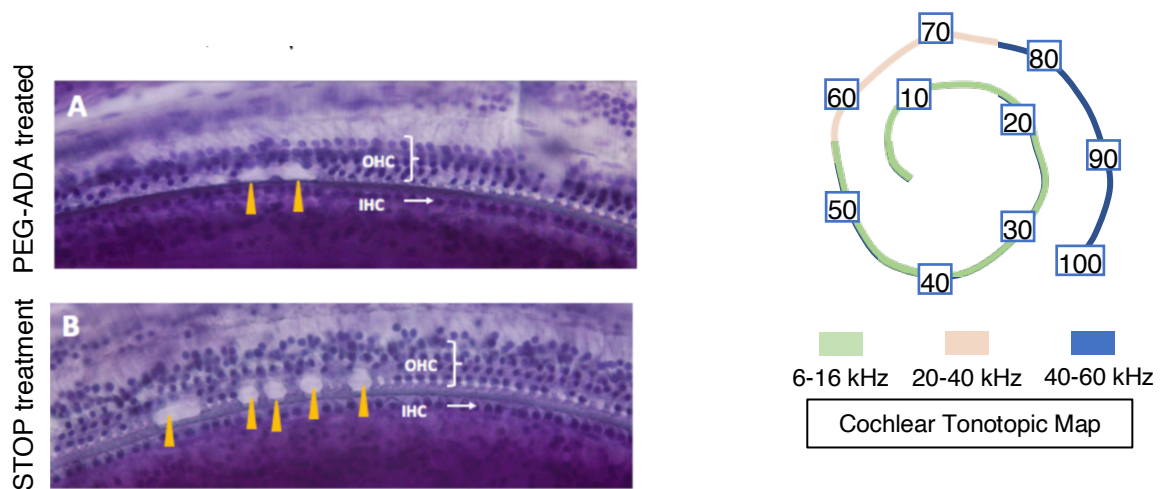


Figure 7. Cochleogram of PEG-ADA treated and untreated *Ada*<sup>-/-</sup> and schematic diagram of tonotopic frequency mapping in inner ear. (left) Representative pictomicrograph of uncoiled cochlea of B) *Ada*<sup>-/-</sup> STOP-treatment mice and A) PEG-ADA treated mice. STOP-treatment mice demonstrate more outer hair cell loss. (right) Schematic illustration representing the tonotopic mapping of frequency sensitivities with percent distance plotted from the apex of cochlea.



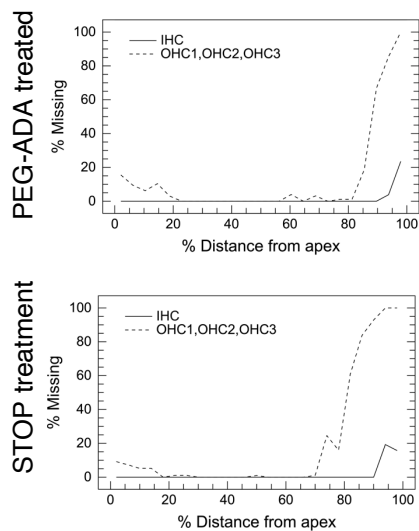


Figure 8. Cochleogram analysis comparing hair cell loss of PEG-ADA treated and untreated *Ada*<sup>-/-</sup> mice. Cochleogram from *Ada*<sup>-/-</sup> STOP-treatment mice and PEG-ADA treated mice. Note ~30% loss at cochlear basal turn in STOP-treatment mice compared to treated mice. This location corresponds to >48 kHz in mice. Data are shown as mean ± SEM

### Elevated Adenosine and Axon Structures

Our ABR assays showed the robust decrease in hearing sensitivity thresholds, wave peak I and II amplitudes, and prolonged inter-peak latencies in STOP-treatment *Ada*<sup>-/-</sup> compared to PEG-ADA treated *Ada*<sup>-/-</sup>, implicating the potential cellular impairment of SGN. To define the cellular changes of SGNs, we conducted Hematoxylin Eosin (H&E) histological studies to investigate the cellular changes in SGN. SGNs are grouped bipolar neuron cell bodies with synaptic dendrites that receive glutamate neurotransmitters released from the base of hair cells. We found significant cochlear nerve density loss via H&E staining in STOP-treatment *Ada*<sup>-/-</sup> compared to PEG-ADA treated *Ada*<sup>-/-</sup> (Figure. 9D, left panel). Changes in cochlear nerve density motivated us to closely examine the axonal structures by electron microscopy (EM). Supporting the finding in H&E, we found a significant increase in unmyelinated axons in STOP-treatment mice, as well as features of non-compact myelin (Figure. 9, middle and top right). Additionally, we found a significant increase in G-ratio, which is the ratio of the inner axonal diameter to the total axonal diameter, indicating the thinning of myelin sheaths in STOP-treatment *Ada*<sup>-/-</sup> mice (Figure. 9, bottom right). Both H&E and EM findings support our conclusion that elevated

cochlea adenosine impaired myelination of nerve fiber of SGNs without obvious changes of cell body of SGN.

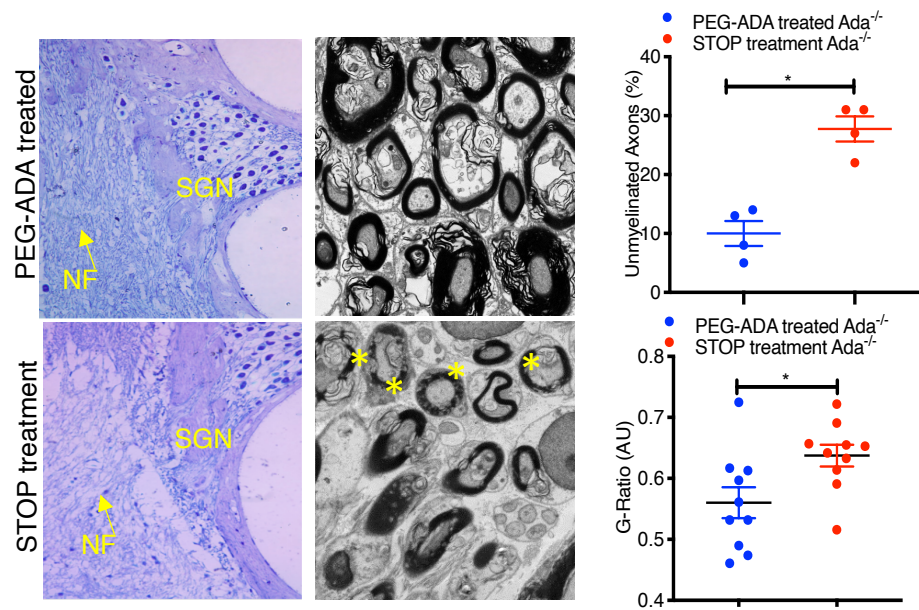


Figure 9. Nerve structure in *Ada*<sup>-/-</sup> mice cochlea with and without PEG-ADA therapy. (left) High power magnification of the spiral ganglion (SG) cell bodies in Rosenthal's canal and myelinated nerve fibers (NF) in the modiolus. Note dark blue staining of the myelin on the NF in PEG-ADA treated mice and absence of NF staining and loss of NF in ADA mice where treatment was discontinued. There seem to be many vacuoles and open spaces in the STOP-treatment group. (middle) Representative image of electron microscopy of transverse nerve fibers. Yellow stars indicate loosely compacted myelin (middle) (mean  $\pm$  SEM) Quantification of unmyelinated fibers between STOP-treatment and PEG-ADA mice (p-value, 0.0286) (right) (mean  $\pm$  SEM) Quantification of G-ratio from EM images, indicating the decrease in thickness in myelin sheaths in STOP treatment mice (p-value, 0.0229).

### Adenosine and Myelin Structures

Myelination in cochlear nerves is responsible for efficient transmission of sound-evoked spike responses. Therefore, we verified whether the nerve fibers that contact the hair cells directly

had changes in pro-myelinating protein responsible for myelin compaction, myelin protein zero (MPZ) (60–62). MPZ gene dosage is regulated and over expression of MPZ leads to inappropriate trafficking of the protein between the Schwann cell membranes, leading to a lack of myelin compaction (63,64). Surprisingly, we observed that STOP treatment *Ada*<sup>-/-</sup> mice have significantly elevated MPZ expression levels without the normal tubular expression found in PEG-ADA treated *Ada*<sup>-/-</sup> mice in compared to treated *Ada*<sup>-/-</sup> mice (Figure 10). Consistent to the H&E findings, nerve fiber stained by NF-200 was significantly reduced (Figure 10). Overall, using H&E, EM and IF multidisciplinary microscopic approaches, we demonstrated that elevated cochlear adenosine causes SNHL largely due to the impaired myelination of nerve fiber of SGN, particularly the myelin sheaths mediated by MPZ integration, and loss of nerve fiber.

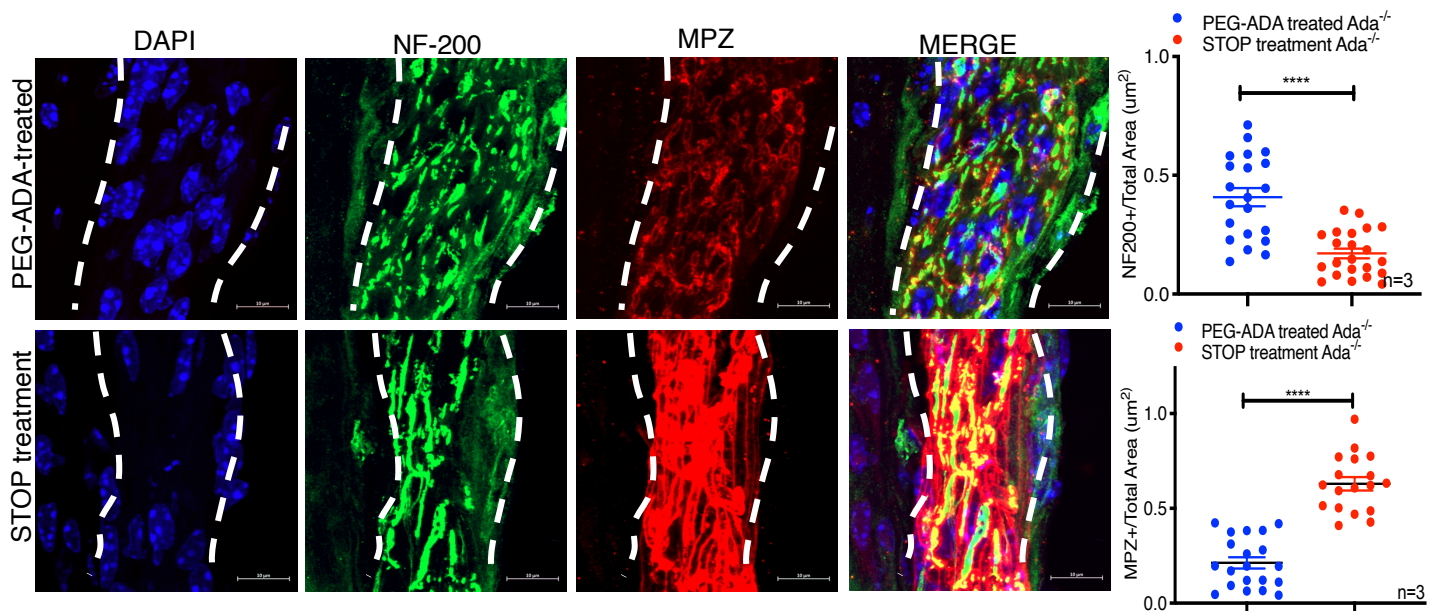


Figure 10. Labeling of nerve fiber and MPZ protein on cochlear nerve. Immunofluorescent staining of nerve fibers with myelin protein zero (MPZ) where STOP-treatment group have a more intense expression (p-value <0.0001). Data are shown as mean ± SEM.

### ADA Enzyme Therapy Resumption Rescue

Following withdrawal of PEG-ADA therapy for 2 weeks, *Ada*<sup>-/-</sup> mice develop the profound demyelination of nerve fiber of SGN with impaired integration of MPZ to myelin sheath. These findings prompted us to assess an important therapeutic possibility whether the elevated adenosine-induced SNHL is reversible. If so, we questioned how quickly and to what extent hearing thresholds recover, and if cellular disturbances in SGN would be corrected with PEG-ADA treatment. To address these questions, we first to determine when the SNHL developed within the period of PEG-ADA withdrawal over 2-weeks. PEG-ADA's half-life is 4 days upon PEG-ADA withdrawal and elevated plasma adenosine reached the peak around day 8 (31). Thus, within 2-weeks withdrawal of PEG-ADA, we found that the ABR threshold began to increase around day 4, peaked on day 7 and maintained its peak threshold up to day 14 (Figure 11). Based on this finding, we chose to resume treatment with 5U/week of PEG-ADA at the end of 2-week withdrawal of PEG-ADA for one-week treatment (Figure 12). Following resumption of PEG-ADA therapy, auditory function was monitored using ABR and DPOAE every 4 days until no further changes are observed (Figure 13).

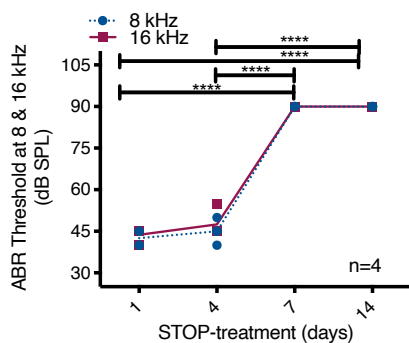


Figure 11. ABR thresholds post PEG-ADA treatment during STOP treatment regimen. STOP-treatment mice hearing capacity after PEG-ADA withdrawal decreases overtime, namely after 7 days and beyond (all comparisons beside day 1 vs 4 and 7 vs 14 have p-value of <0.0001) (C) After one week of PEG-ADA reintroduction to *Ada*<sup>-/-</sup> mice auditory brainstem

response (ABR) thresholds at different frequencies demonstrate a rescued hearing phenotype (p-value for STOP treatment vs PEG-ADA at 4, 8, 16 kHz, <0.0001) (n=5 for each cohort).

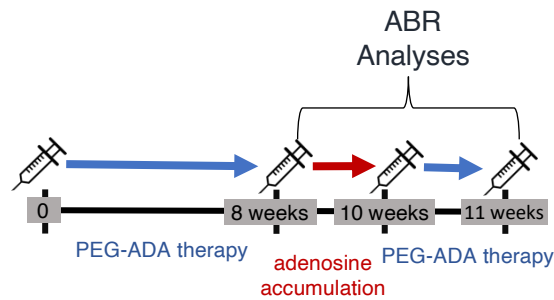


Figure 12. PEG-ADA rescue therapy on STOP treatment *Ada*<sup>-/-</sup> mice. *Ada*<sup>-/-</sup> mice are treated with PEG-ADA from birth to 8 weeks for normal development. For two weeks, STOP-treatment mice are withdrawn from the drug and RESCUE

mice are given PEG-ADA shortly after for one week.

Intriguingly, we found that resumption of PEG-ADA treatment for two weeks significantly lowered ABR threshold (Figure 13) but no significant effects on DPOAE thresholds comparing to STOP-treatment *Ada*<sup>-/-</sup> mice (data not shown). This improvement of hearing sensitivity by resumption of PEG-ADA therapy was accompanied by a mild increase in Peak I amplitude at 8kHz (Figure 14) and a consistent decrease of latency at 8 and 16 kHz at higher decibels (Figure 15). Thus, PEG-ADA treatment successfully rescue the SNHL in *Ada*<sup>-/-</sup> mice with withdrawal of PEG-ADA therapy for 2 weeks largely by restoring the firing ability of SGN and inter-peak transduction from SGN to CN but no obvious improvement in cochlear amplifier and outer hair cell function.

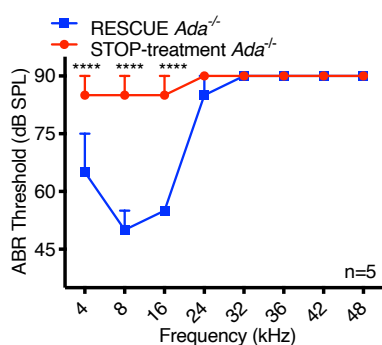


Figure 13. ABR analysis on *Ada*<sup>-/-</sup> after PEG-ADA rescue therapy. After one week of PEG-ADA reintroduction to *Ada*<sup>-/-</sup> mice auditory brainstem response (ABR) thresholds at different frequencies demonstrate a rescued hearing phenotype (p-value for STOP treatment vs PEG-ADA at 4, 8, 16 kHz, <0.0001) (n=5

for each cohort).

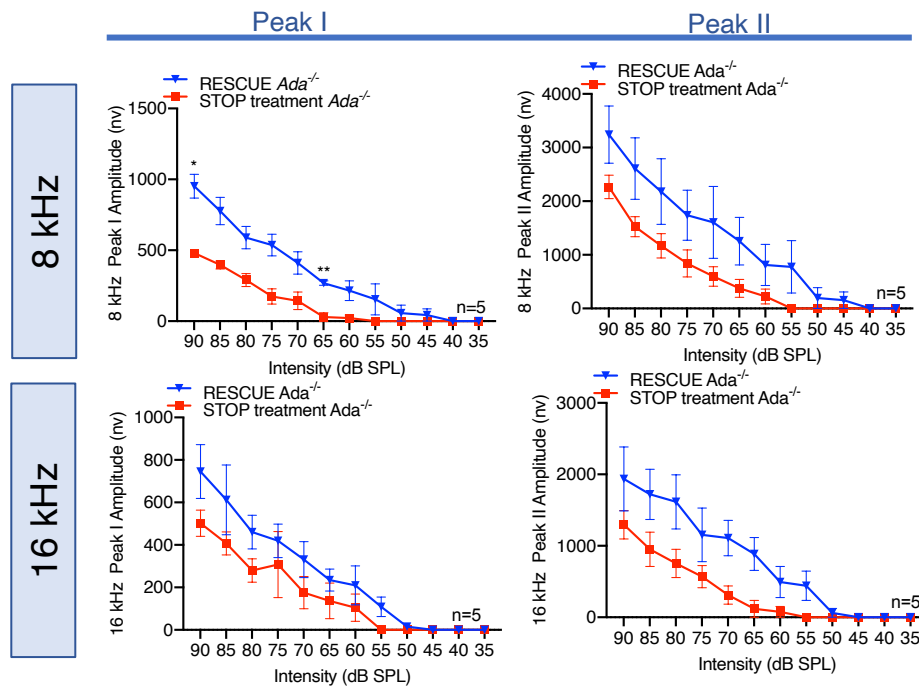


Figure 14. Peak I and II analysis on *Ada*<sup>-/-</sup> mice after PEG-ADA rescue therapy. (mean ± SEM) Auditory brainstem response traces were analyzed, where Peak 1 amplitudes were elevated in Rescue cohort compared to STOP-treatment mice. Peak II is similar to Peak I, indicating higher capacity of neurons to fire effectively with lowered adenosine after onset of hearing loss at two-weeks PEG-ADA withdrawal (p-value, 8kHz peak I p-value for 90-80, 0.0436, 0.1708, 0.1813, respectively) (p-value, 8kHz peak II p-value for 90-80, 0.6663, 0.6529, 0.6663, respectively) (p-value, 16kHz peak I p-value for 90-80, 0.59643, 0.79332, 0.56095, respectively) (p-value, 16kHz peak II p-value for 90-80, 0.9643, 0.7634, 0.6783, respectively) (n=5 for each group)

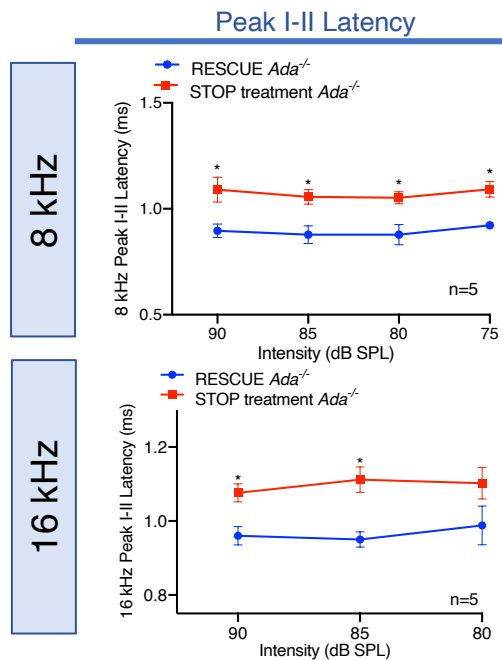


Figure 15. Peak I-II latency analysis on *Ada*<sup>-/-</sup> mice after PEG-ADA rescue therapy. Peak I-II latency measures the efficiency of firing of peripheral nerves to cochlear nucleus in time (ms), showing faster peak amplitudes between two structures when adenosine is lower. (p-value for 8 kHz at 90-75 dB, 0.01951, 0.01096, 0.01399, 0.00250, respectively) (p-value for 16 kHz at 90-80 dB, 0.01065, 0.00384, 0.12941, respectively). Data are shown as mean ± SEM

Next, we conducted IF to determine whether PEG-ADA therapy is capable of restoring the impaired myelination and prevent the fiber loss of SGN in *Ada*<sup>-/-</sup> mice with withdrawal of PEG-ADA therapy for 2 weeks. Strikingly, we found that that PEG-ADA therapy induced improved integration of MPZ to the myelin sheaths and restored nerve fibers (Figure 16). Taken together, we demonstrated that PEG-ADA therapy restores the integration of MPZ to myelin sheaths, reverses the loss of nerve fiber of SGN, and rescues SNHL in *Ada*<sup>-/-</sup> mice.



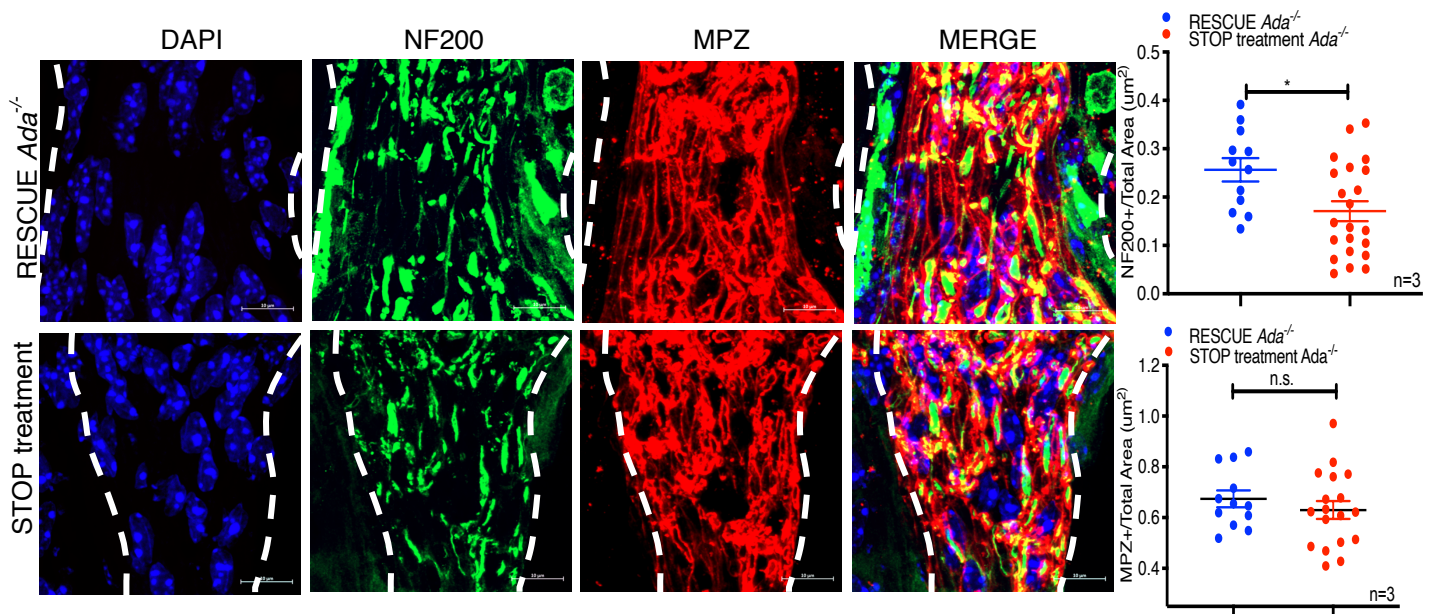


Figure 16. Nerve fiber and MPZ protein immunofluorescent staining on *Ada*<sup>-/-</sup> mice cochlear nerve. MPZ staining of peripheral nerve fiber of SGN, showing no significance between the two except for organization of structures. (G) (mean ± SEM) Quantification of total expression of NF200 and MPZ over total axon area (p-value for NF200 and MPZ, 0.0134 and 0.397343, respectively) (n=3 for each group) Data are shown as mean ± SEM

## 2.4 Discussion

Extracellular adenosine is a signaling metabolite that orchestrates a physiological and pathological response to energy deficiency or cell injury by functioning via one or more of the four adenosine receptors. The pathogenic role of elevated adenosine in SNHL associated with ADA-deficiency (33,34) in humans is confirmed and validated in *Ada*<sup>-/-</sup> mice (35). Defining the pathogenic mechanism of SNHL in ADA-deficient humans is difficult for ethical and experimental reasons. Although ADA deficiency is a lethal condition in humans and mice, PEG-ADA enzyme therapy, a treatment that substantially reduces (but does not eliminate) the accumulation of adenosine, successfully prolongs life indefinitely. Thus, we took full advantage



of our genetic model of adenosine-induced SNHL in *Ada*<sup>-/-</sup> mice and our ability to experimentally regulate cochlear adenosine levels by administration of PEG-ADA to determine the natural progression and molecular basis underlying SNHL in *Ada*<sup>-/-</sup> mice, which is impossible to study in *Ada*<sup>-/-</sup> patients. First, we found that *Ada*<sup>-/-</sup> mice begin to develop bilateral SNHL after 7 days and up to 14 days after stopping PEG-ADA treatment. Second, continuous ADA enzyme therapy normalizes the cochlear adenosine levels and prevents SNHL in *Ada*<sup>-/-</sup> mice. Third, *Ada*<sup>-/-</sup> mice display a minor loss of OHCs, severe unmyelinated myelin sheaths with impaired MPZ integration and thus SNHL. Fourth, we provide a clear window of therapeutic opportunity for PEG-ADA treatment for SNHL by revealing that PEG-ADA therapy reverses impaired MPZ integration to myelin sheaths, restores myelinated nerve fiber of SGNs and rescues SNHL of *Ada*<sup>-/-</sup> mice following a two-week STOP-treatment with PEG-ADA. Thus, our findings add a significant new insight that elevated cochlear adenosine as a signaling metabolite rapidly promotes SNHL within 7 days, while PEG-ADA enzyme therapy can effectively prevent and quickly reverse SNHL by improving myelination of nerve fibers of SGNs in *Ada*<sup>-/-</sup> mice. Overall, our finding, not only provide substantial new insight regarding the cellular and metabolic basis underlying natural progression of prolonged elevated adenosine-induced SNHL in *Ada*<sup>-/-</sup> mice, but also provide a clear window of therapeutic opportunity for PEG-ADA treatment for SNHL in these mice.

#### *Elevated cochlear adenosine perturbs spiral ganglion neuron myelination*

Here, we have characterized how elevated cochlear adenosine affects the hearing process, from a physiological to a cellular perspective. We conclude that elevated cochlear adenosine causes hearing loss mainly through perturbing proper myelination in the inner ear. We know this because of the mild hair cell losses we find in untreated *Ada*<sup>-/-</sup> mice and the rescue capabilities of

reintroducing PEG-ADA therapy after two weeks of withdrawal when we observe the hearing loss.

To our knowledge, there are no current studies that show the direct role of adenosine in peripheral myelination. Given our one-week resumption of PEG-ADA in our rescue experiment, we hypothesize that, during this period, normalizing adenosine levels were enhancing axonal structure and myelin organization. Without proper nerve fiber structures, auditory processing from mechanical transduction of the middle ear ossicles and hair cells will simply not transmit to higher brain regions. In this study, we focused on the cochlear VII nerve and cochlear nucleus amplitude and latency where we saw blatant changes when adenosine is high or lowered with PEG-ADA. While many cellular drivers could be responsible for this phenomenon we narrowed it to two: a change in SGN number or perturbation in how the auditory information is transmitted. When we found that SGN cell body count did not change with adenosine levels, we then looked at the axons.

#### *Adenosine levels play a role in MPZ function and expression*

Axons play an important role in transmitting electrical impulses and most axon function and structure are maintained through myelin escheatment. Many studies have shown the important role of adenosine in myelination in the CNS (65), however, adenosine-regulated maintenance of axonal structure remains to be determined. We found differences in NF-200 and MPZ expression when adenosine levels were manipulated through PEG-ADA therapy. In elevated cochlear adenosine, MPZ levels were elevated while nerve fiber structures were decreased. MPZ is the most abundant peripheral myelin protein expressed and integrated in Schwann cell plasma membranes that primarily keeps myelin properly coiled via in trans homophilic adhesion in its extracellular domain (63,66–68). Clinical studies have shown the that MPZ dosage is important for its proper function, where increased overexpression in peripheral nerves show

hypomyelination neuropathy and axon-sorting defects and heterozygous and complete MPZ knockouts in mice both present neuropathic phenotypes of progressive demyelination or dysmyelination (69–72). Studies have also posited the possibility of detecting levels of MPZ in cerebrospinal fluid (CSF) to determine the degree of demyelination in neuropathies (73). Taken together, it would not be surprising to find increasing expression of MPZ in stress-induced cochlear environment matched with increasing levels of adenosine.

As previously mentioned, environmental stress, such as acoustic trauma, can induce elevated levels of adenosine. Studies in other tissues have found that elevated adenosine also stimulates increased levels of ectonucleotidase CD73; thus, metabolizing more ATP and increasing adenosine level. In our mouse model, extracellular adenosine metabolism is inhibited, exacerbating the extracellular environment with the accumulation of adenosine levels that may induce downstream pathogenic signaling. The exact downstream mechanism as to how sustained elevated adenosine can prompt demyelination remains unknown and will be further discussed in the next chapter.

## **CHAPTER 3: Hearing Loss via ADORA2B Signaling**

### 3.1 Introduction

The previous chapters highlighted the characterization of how elevated adenosine affects sensorineural hearing on a cellular level and a therapeutic perspective. This chapter will discuss how adenosine a2b receptor is a potential downstream signaling pathway that leads to hearing loss. In this study, we used a specific ADORA2B receptor inhibitor, PSB1115, and a total knock-out *Adora2b* in the *Ada* mouse model. We found that ADORA2B ablation improved overall hearing sensitivity and myelination in these models.

### 3.3 Materials & Methods

#### *Ada*<sup>-/-</sup> Mice and PSB1115 prevention regimen

*Ada*<sup>-/-</sup> mice were generated and genotyped as previously reported (50). Mice homozygous for the null *Ada* allele were labeled *Ada*<sup>-/-</sup>, while mice genotyped with the *Ada* allele were labeled as *Ada*<sup>wt</sup>. All mice were congenic on a C57BL/6 background, and all phenotypic comparisons were performed among littermates. PSB1115 was generated from water-soluble, HPLC grade, powder from Tocris Bioscience diluted with sterile 1x DPBS (200 ug/per day). *Ada*<sup>-/-</sup> mice were raised with PEG-ADA as described above from birth to 8 weeks. PSB1115 was injected intraperitoneally every other day for two weeks.

#### *Ada*<sup>-/-</sup>/*Adora2b*<sup>-/-</sup> mice

*Ada*<sup>-/-</sup>/*Adora2b*<sup>-/-</sup> mice were generated by mating *Ada*<sup>-/-</sup> mice with *Adora2b*<sup>-/-</sup>. *Ada*<sup>-/-</sup>/*Adora2b*<sup>-/-</sup> mice were raised with PEG-ADA as described above from birth to 8 weeks. All mice were congenic on a C57BL/6 background, and all phenotypic comparisons were performed among littermates.

#### RT-PCR

Total RNA was isolated from mouse whole DRG or DRG culture for 48h by using TRIzol reagent (Invitrogen, Carlsbad, CA, USA). RNase-free DNase (Invitrogen) was used to eliminate

genomic DNA contamination. Transcript levels were quantified using SYBR green reporter dye. Primer sequences for ADORA1, ADORA2A, ADORA2B, and ADORA3 expression analysis were referenced from previous work (27,28,74). GAPDH was used as endogenous control for normalization.

#### *Cochlea isolation, immunohistochemistry, imaging, and analysis*

Temporal bones were dissected in PBS, incubated in 4% paraformaldehyde (PFA) in PBS overnight at 4°C, decalcified in 0.2 M EDTA for 5–7 d. Fixed tissue were embedded in OCT compound, cryosectioned at 10  $\mu$ m, followed by standard immunohistochemistry procedure. The tissue sections were washed with 1x phosphate-buffered saline (PBS), followed by a 1 hr incubation in 5% BSA with 1% Triton X-100 in 1xPBS. These sections were then incubated in primary antibodies overnight at 4°C. The primary antibodies used for this study were: nerve fiber filament (mouse anti-NF-200, Sigma, 1:200), neuron cell bodies (rabbit anti-NeuN, Abcam, 1:500), and myelin protein zero (rabbit anti-MPZ, Abcam 1:200). Tissues were then incubated with appropriate Alexa-Fluor conjugated secondary antibodies (Invitrogen, 1:500), followed by DAPI mountant (ProLong Gold Antifade, Thermo Fisher Scientific).

Confocal z-stacks of each cochlea were taken using Zeiss LSM T-PMT microscope equipped with 63x (2x digital zoom) oil immersion lens. MPZ- and NF-200 areas were quantified using ImageJ by selecting via consistent color threshold for each antibody used across all experiment groups (n=3 each) and normalizing each sample by total area of the axon. These MPZ+/total axon area and NF200+/total axon quantifications were collectively compared across all experiments via a Mann-Whitney nonparametric two-tailed t-test. All statistical analyses were performed via Prism 8.

### Auditory brainstem response recording

Mice were intraperitoneally injected with ketamine-xylazine (100 mg/kg; 10mg/kg). Testing was performed in a soundproof faraday cage booth while mice were placed on heating pad to maintain normal body temperature throughout the procedure. Pure tone bursts (0.1 ms rise/fall, 2 ms duration, 21 presentations/s) from 4 to 48 kHz were generated using System 3 digital signal processing hardware and software (Tucker Davis Technologies). The intensity of the tone stimuli was calibrated using a type 4938 one-quarter inch pressure-field calibration microphone (Bruël & Kjær). EC1 ultrasonic, low-distortion electrostatic speakers were coupled to the ear canal to deliver stimuli within 3 mm of the tympanic membrane. Response signals were recorded with subcutaneous needle electrodes inserted at the vertex of the scalp (channel 1), the postauricular bulla region (reference), and the back leg (ground), and averaged over 500 presentations of the tone bursts (56). Electrode-recorded activity was filtered (high pass, 300 Hz; low pass, 3kHz; notch, 60Hz) before averaging to minimize background noise. Auditory thresholds were determined by decreasing the sound intensity of each stimulus to 10 dB from 90 dB in 5 dB steps until the lowest sound intensity with reproducible and recognizable waveforms was detected. Thresholds were determined to within 5 dB for each frequency by two raters to ensure reliability. SD (dB SPL) were plotted as a function of stimulus frequency (kilohertz) and analyzed for group differences by a two-way ANOVA, followed by a multiple-comparison test, to reveal overall trends. Prism 8 was used for all statistical analyses.

### ABR waveform detection and calculation

Peak amplitudes (I and II) were visually determined from ABR waves detected from each stimulus from 90 to 10 dB in 5 dB increments at each frequency. Peak amplitudes were measured by subtracting the peak voltage from the trough voltage at every dB presentation, averaged per

experimental group. All averaged peak amplitudes for each peak from each group were statistically compared using two-way ANOVA, followed by a multiple comparison test.

Peak latencies from peak I and II were calculated by subtracting Peak I's peak amplitude temporal onset (in ms) from Peak II's peak amplitude temporal time onset (in ms). Time measurements were averaged per experimental group. Averaged latencies per group were compared via two-way ANOVA, followed by a multiple comparison test.

All statistical analyses were performed through Prism 8.

#### *Distortion product otoacoustic emission measurements*

DPOAEs were measured from a probe tip microphone placed in the external canal of the mouse ear that were elicited by two 1-second sine-wave tones of varying frequencies ( $F2=1.2 \cdot F1$ ). F2 had a varied range of frequencies from 4 to 90 kHz. These two tones were presented in identical intensities that ranged from 15 to 75 dB SPL in 15 dB increments. The magnitude of the  $2 \cdot F1 - F2$  DP was determined by FFT. DPOAE thresholds ( $> -5$  dB SPL and greater than two std. dev above noise floor) were analyzed off-line via BioSigRZ program. If no DPOAE was detected, we defined the threshold to be at 75 dB, as our equipment is limited to 80 dB SPL. DPOAE thresholds were averaged per experimental group and compared via one-way ANOVA, followed by a multiple comparisons test. All statistical analyses were done through Prism 8.



### 3.3 Results

#### Cochlear *Adora2b* expression

To determine which adenosine receptor is responsible for the decrease in wave peak amplitudes and axonal structure changes in elevated cochlear adenosine-induced hearing loss, we performed an RT-PCR analysis for four adenosine receptors in STOP- and PEG-ADA-treated mice. We found that *Adora2b* mRNA was preferentially and significantly induced compared with PEG-ADA treated *Adora*<sup>-/-</sup> and WT (C57B6-J) mice (Figure 17). Given the fact that ADORA2B has the lowest affinity to adenosine and it is frequently activated under pathological conditions with an excess level of adenosine (31,75), we immediately hypothesized that elevated ADORA2B in the cochlea functions as a malicious cycle to promote elevated cochlear adenosine-induced SNHL in *Adora*<sup>-/-</sup> mice. To test this possibility, we conducted preclinical studies to see whether inhibition of ADORA2B activation by its specific inhibitor, PSB1115, can serve as a potential therapy (Figure 18).

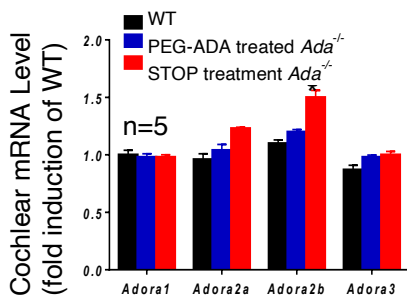


Figure 17. Adenosine receptors mRNA expression in *Adora*<sup>-/-</sup> whole cochlea. RT-PCR of *Adora2b* gene with highest expression in STOP-treatment mice compared to other groups (n=10).

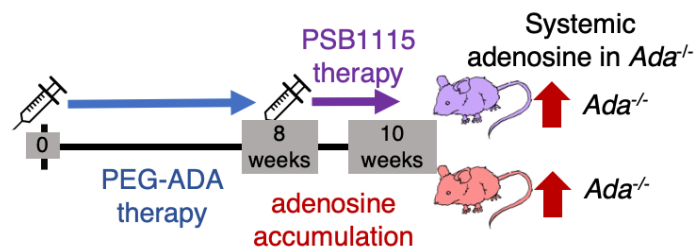


Figure 18. PSB1115 therapy on *Adora*<sup>-/-</sup> mice. Schematic diagram of PSB1115 therapy where STOP-treatment mice are compared with mice treated with PSB1115 treatment.

## PSB1115-treated *Ada*<sup>-/-</sup> Auditory Brainstem Response and Distortion Product Otoacoustic

### Emissions Analyses

Indeed, we found significant improvements in ABR thresholds (Figure 19, left) and mild improvements in DPOAE thresholds (Figure 19, middle and right).

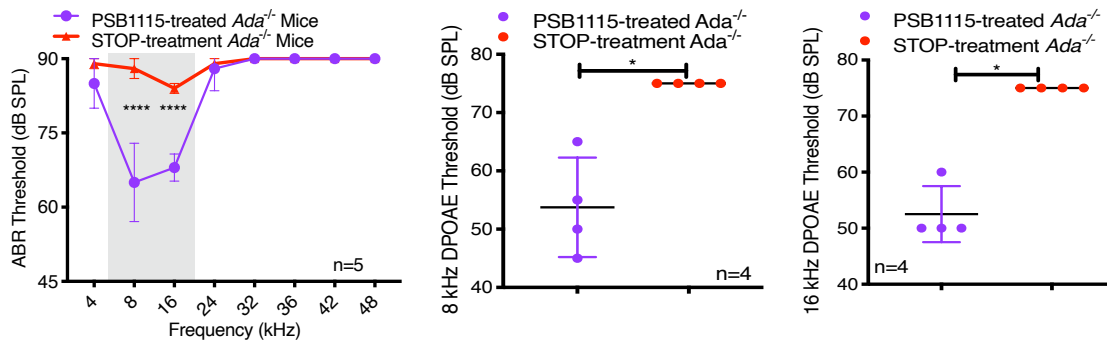


Figure 19. Auditory brainstem response and distortion product otoacoustic emission analysis on *Ada*<sup>-/-</sup> mice with PSB1115. (left) After one week of PSB1115 therapy in *Ada*<sup>-/-</sup> mice auditory brainstem response (ABR) thresholds at different frequencies demonstrate a rescued hearing phenotype (p-value for 4-16 kHz, 0.2960, <0.0001, <0.0001, respectively) (n=5 for each cohort). (middle and right) (mean ± SEM) Distortion-product otoacoustic emissions (DPOAEs) measured at 8 and 16 kHz demonstrate improved outer hair cell and cochlear amplifier function in PSB1115-treated mice compared to STOP treatment mice (p-value, 0.0286) (n=4 for each cohort).

### SGN → CN Amplitude Peaks & Latency in PSB1115-treated *Ada*<sup>-/-</sup>

Moreover, at 8 and 16 kHz, peak 1 and 2 ABR amplitudes and latencies improved substantially (Figure 20-21). Similar to PEG-ADA therapy, we found that PSB1115 treatment significantly improved integration of MPZ to myelin sheaths and prevented nerve fiber loss of SGN (Figure. 4G). Overall, these data support our hypothesis that ADORA2B activation mediated by elevated cochlear adenosine plays an essential role in nerve fiber deterioration, which in turn, affects hearing sensitivity in *Ada*<sup>-/-</sup> mice.

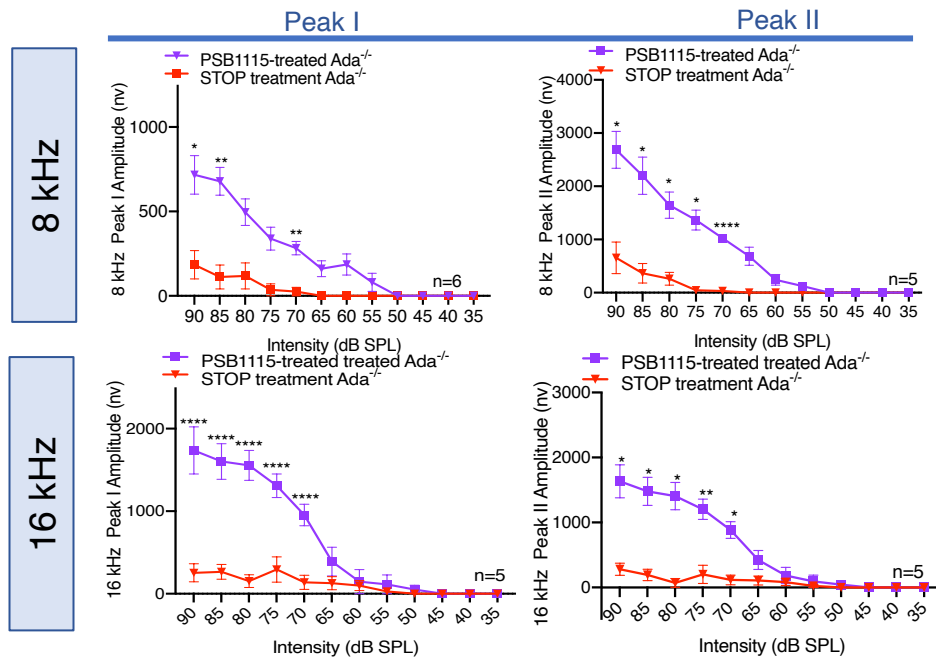


Figure 20. Peak I and II analysis on *Ada*<sup>-/-</sup> mice after PSB1115 therapy. (mean ± SEM) Auditory brainstem response traces were analyzed, where Peak 1 amplitudes were elevated in PSB1115-treated cohort compared to STOP-treatment mice. Peak II is similar to Peak I, indicating higher capacity of neurons to fire effectively inhibition of ADORA2B despite high adenosine levels (p-value for 8kHz peak I, 90-80dB, 0.04973, 0.00486, 0.07595, respectively) (p-value for 8kHz peak II, 90-80dB, 0.0265 0.0400 0.0316, respectively) (p-value for 16kHz peak I, 90-80dB, <0.0001 ) (p-value for 16kHz peak II, 90-80dB, 0.02547, 0.01265, 0.01077 , respectively) (n=5 per group)

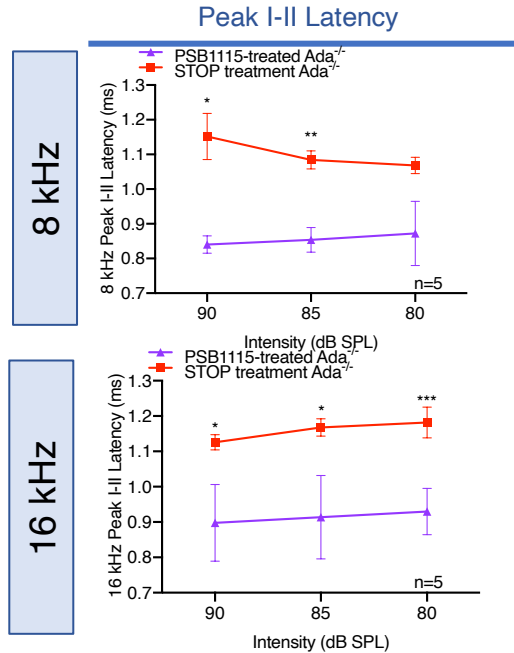


Figure 21. Peak I-II latency analysis on *Ada*<sup>-/-</sup> mice after PSB1115 therapy. Peak I-II latency measures the efficiency of firing of peripheral nerves to cochlear nucleus in time (ms), showing faster peak amplitudes between two structures when ADORA2B is blocked in high adenosine levels. (p-value for 8 kHz at 90-80 dB, 0.004801, 0.002448, 0.074985 , respectively) (p-value for 16 kHz at 90-80 dB, 0.003111, 0.003111,0.000301, respectively) (n=5. per group) Data are shown as mean ± SEM.

### *ADORA2B-inhibition in Elevated Cochlear Adenosine and Axon Structures*

Similar to PEG-ADA therapy, we found that PSB1115 treatment significantly improved integration of MPZ to myelin sheaths and prevented nerve fiber loss of SGN (Figure 22). Overall, these data support our hypothesis that ADORA2B activation mediated by elevated cochlear adenosine plays an essential role in nerve fiber deterioration, which in turn, affects hearing sensitivity in *Ada*<sup>-/-</sup> mice.

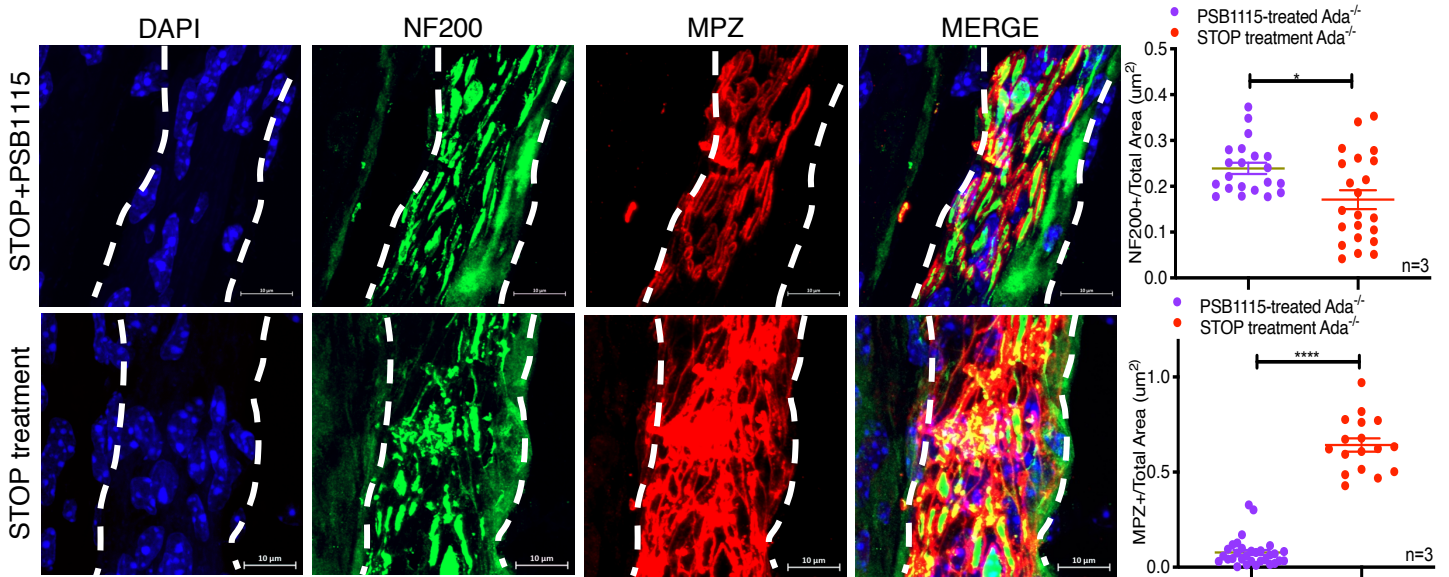


Figure 22. Nerve fiber and MPZ protein immunofluorescent staining on *Ada*<sup>-/-</sup> mice with PSB1115 therapy cochlear nerve. MPZ and NF200 staining is less and improved in organizational pattern in PSB1115 treated mice with elevated adenosine compared to STOP-treatment mice with elevated adenosine (p-value, left panel, 0.1732, middle panel, 0.0192, right panel, <0.0001)(n=3 per group) Data are shown as mean ± SEM.

### *Ada*<sup>-/-</sup>/*Adora 2b*<sup>-/-</sup> Auditory Brainstem Response and Distortion Product Otoacoustic Emissions

#### Analyses

Similar to our PEG-ADA and PSB1115-treated *Ada*<sup>-/-</sup> mice, genetic deletion of *Adora2b* in *Ada*<sup>-/-</sup> mice have improved hearing thresholds through ABR analyses (Figure 24). These double-deficient mice were raised similar to *Ada*<sup>-/-</sup> mice with a PEG-ADA therapy from birth for normal development (Figure 23). Despite adenosine increase upon PEG-ADA withdrawal, hearing sensitivity was conserved. Although these decrease in threshold shifts are not as robust as PSB1115 therapy on *Ada*<sup>-/-</sup> mice, these results further demonstrate ADORA2B's role in hearing loss pathogenesis through both ABR and DPOAE analyses (Figure 24).

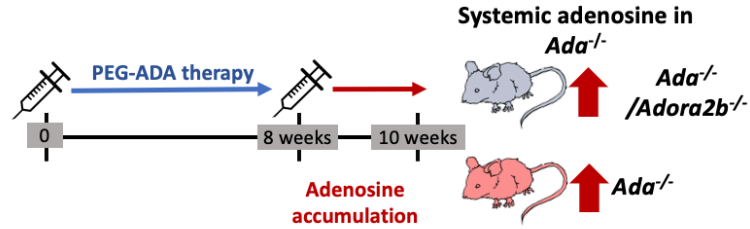


Figure 23. *Ada*<sup>-/-</sup>/*Adora2b*<sup>-/-</sup> mouse model. These double-deficient mice undergo normal development through the same PEG-ADA therapy regimen that was given to *Ada*<sup>-/-</sup> mice. However, after 8 weeks, PEG-ADA is withdrawn to allow the natural accumulation of adenosine for two weeks.

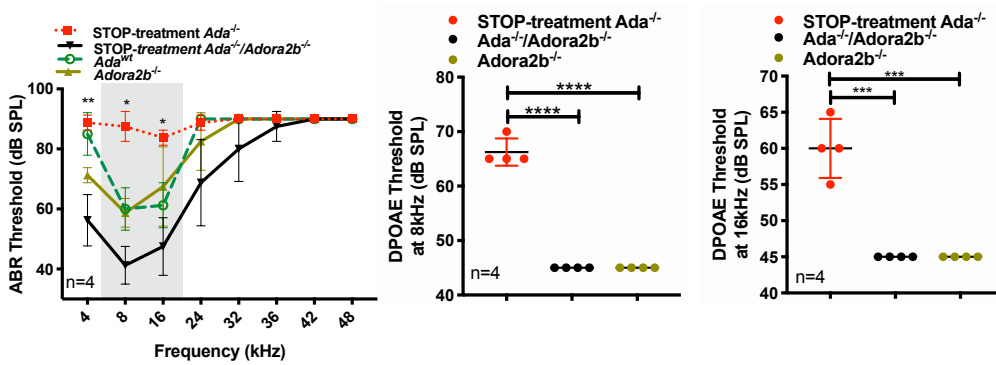


Figure 24. Auditory brainstem response and distortion product otoacoustic emission analysis on *Ada*<sup>-/-</sup>/*Adora2b*<sup>-/-</sup> mice. (left) After two weeks of PEG-ADA withdrawal in *Ada*<sup>-/-</sup>/*Adora2b*<sup>-/-</sup> mice auditory brainstem response (ABR) thresholds at lower frequencies demonstrate an improved hearing phenotype compared with STOP-treatment *Ada*<sup>-/-</sup> mice (p-value for 4-16 kHz, 0.0063, 0.0109, 0.0218, respectively) (n=4 for each cohort). (middle and right) (mean ± SEM) Distortion-product otoacoustic emissions (DPOAEs) measured at 8 and 16 kHz demonstrate improved outer hair cell and cochlear amplifier function in PSB1115-treated mice compared to STOP treatment mice (p-value for 8 and 16 kHz, <0.0001 and >0.0003, respectively) (n=4 for each cohort).

SGN → CN Amplitude Peaks & Latency in *Ada*<sup>-/-</sup>/*Adora2b*<sup>-/-</sup>

As we looked closely at the ABR traces, we found that at 8 and 16 kHz, peak 1 and 2 ABR amplitudes and latencies improved substantially in *Ada*<sup>-/-</sup>/*Adora2b*<sup>-/-</sup> mice compared to STOP-treatment mice (Figure 25). Additionally, *Ada*<sup>-/-</sup>/*Adora2b*<sup>-/-</sup> mice were observed to have a faster latency than STOP-treatment mice (Figure 26). Overall, these physiological ABR and DPOAE data further support our hypothesis that ADORA2B activation mediated by elevated cochlear adenosine plays an essential role in hearing loss pathogenesis.

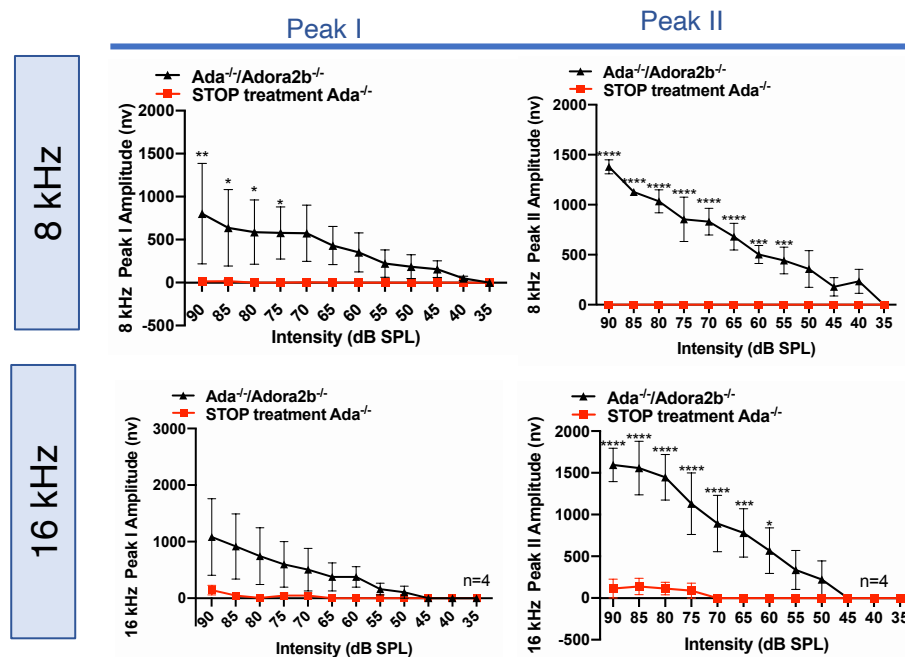
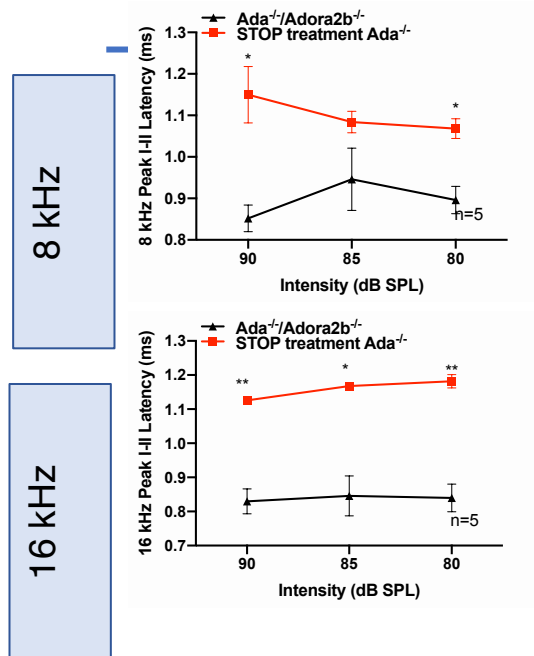


Figure 25. Peak I and II analysis on *Ada*<sup>-/-</sup>/*Adora2b*<sup>-/-</sup> mice compared to STOP treatment *Ada*<sup>-/-</sup> mice. (mean ± SEM) Auditory brainstem response traces were analyzed, where Peak I and II amplitudes at 8 kHz were elevated in *Ada*<sup>-/-</sup>/*Adora2b*<sup>-/-</sup> cohort compared to STOP-treatment mice despite elevated systemic adenosine in both groups. At 16 kHz, however, only Peak II had a significant increase in *Ada*<sup>-/-</sup>/*Adora2b*<sup>-/-</sup> cohort compared to STOP-treatment mice (p-value for 8kHz peak I, 90-80dB, 0.0030, 0.0283, 0.0438, respectively) (p-value for 8 kHz peak II, 90-80dB

is  $>0.0001$ ) (p-value for 16 kHz peak I, 90-80dB,  $<0.0001$ ) (p-value for 16 kHz peak II, 90-80dB is  $>0.0001$ ) (n=4 per group)



mean ± SEM.

Figure 26. Peak I-II latency analysis on *Ada*<sup>-/-</sup>/*Adora2b*<sup>-/-</sup> mice compared with STOP-treatment *Ada*<sup>-/-</sup> mice. Peak I-II latency measures the efficiency of firing of peripheral nerves to cochlear nucleus in time (ms), showing faster peak amplitudes at higher dBs between two structures when *Adora2b* is deleted in high adenosine levels (p-value for 8 kHz at 90 and 80 dB, 0.0249 and 0.0106 respectively) (p-value for 16 kHz at 90-80 dB, 0.0025, 0.0141, 0.0010, respectively) (n=5. per group) Data are shown as



### 3.4 Discussion

Although an unexpected bilateral SNHL was reported in humans with ADA-deficiency, the molecular basis underlying SNHL in ADA-deficient humans remains undefined. Here, we demonstrate that *Ada*<sup>-/-</sup> mice mimicking ADA-deficient humans display bilateral SNHL with severe hypomyelination of SGNs. Intriguingly, PEG-ADA therapy reverses the hypomyelination of SGNs and rescues SNHL in *Ada*<sup>-/-</sup> mice. Mechanistically, elevated cochlear adenosine preferentially induces *Adora2b* gene expression and that enhanced ADORA2B signaling functioning as a malicious cycle to further exacerbate SNHL in *Ada*<sup>-/-</sup> mice. Preclinically, blocking ADORA2B activation improves myelination and hearing sensitivity in *Ada*<sup>-/-</sup> mice. This is also validated by our *Ada*<sup>-/-</sup>/*Adora2b*<sup>-/-</sup> model that showed the same physiological improvements. Significantly, ADORA2B is a detrimental purinergic signaling component underlying hypomyelination of SGN and promoting aging-dependent SNHL, one of the common causes of SNHL. Overall, our studies revealed that ADORA2B is a common pathogenic factor impairing myelination in two independent models of SNHL and immediately highlights novel adenosine-based therapies for SNHL.

#### *ADORA2B as a common pathogenic factor underlies hypomyelination in both *Ada*<sup>-/-</sup> mice and aging-dependent SNHL*

Adenosine is perhaps best known for its role as a major signal transducer in response to hypoxia or tissue injury (76). Adenosine is a signaling nucleoside that elicits its effect on target cells by engaging four specific G-protein coupled receptors ADORA1 and ADORA3 receptors are coupled to adenylyl cyclase by the inhibitory G-protein (G $\alpha$ i) and hence serve to lower intracellular levels of the second messenger cAMP. The ADORA2A and ADORA2B receptors are commonly coupled to adenylyl cyclase by the stimulatory G-protein (G $\alpha$ s) and serve to

increase intracellular cAMP. Adenosine signaling plays important roles in regulating homeostasis in a number of physiological and pathological systems including the cardiovascular, nervous, renal and immune systems. On one hand, acute and transient elevation of adenosine protects tissues from hypoxia-ischemic-mediated damage by promoting vasodilation, O<sub>2</sub> delivery and anti-inflammation (75). On another hand, persistent accumulation of adenosine signaling via ADORA2B functions to promote or exacerbate tissue injury and disease progression including priapism, preeclampsia, chronic kidney disease, hypertension, pulmonary fibrosis, chronic pain, and sickle cell disease (26–32). However, functional role of ADORA2B in SNHL is unrecognized prior to our study presented here. Previous histological studies have shown the specific cellular expression in the cochlea of all adenosine receptors but one, ADORA2B (9,46), which it is not surprise since ADORA2B antibody is not well accepted in the field for either immunostaining or even Western blot analysis. Consistent with early studies that *Adora2b* expression is induced in chronic disease states, particularly in sustained adenosine levels (26–32), we found that *Adora2b* mRNA is increased with elevated adenosine levels after PEG-ADA withdrawal for 2 weeks in *Ada*<sup>-/-</sup> mice. Pharmacologically inhibiting ADORA2B improves cochlear nerve fiber by increasing MPZ integrating to myelin sheaths and thus attenuates SNHL in *Ada*<sup>-/-</sup> mice. Prompted by the detrimental role of ADORA2B signaling-mediated impaired myelination in *Ada*<sup>-/-</sup> mice, we further demonstrated that genetic deletion of ADORA2B promotes integration of MPZ to myelin sheaths, protects nerve fiber and thus slows down the progression of SNHL induced by elevated adenosine. Thus, both preclinical and genetic studies point to the detrimental role of ADORA2B in another chronic disease condition, SNHL, and pave a way for receptor-based specific therapies for the disease.

### *ADORA2B impairs MPZ integration to myelin sheaths in peripheral nervous system*

Schwann cells are the only cell type that express MPZ, a major promyelinating protein driving remyelination and responsible for myelin compaction in the peripheral nervous system (PNS). Previous studies have shown importance of MPZ in several neuropathies, such as Charcot Marie Tooth Disease (CMT) (61). CMT patients have disrupted Schwann cell and peripheral nerve axons, as well as bilateral “hidden” HL similar to ADA-deficient patients (77). If MPZ is not properly integrated into myelin sheaths, it may be secreted from Schwann cells as a soluble molecule. Thus, the soluble MPZ level in cerebral spinal fluid is used to determine the severity of a neuropathy in the clinic (61). Additionally, previous studies point to the aberrant effects of elevated MPZ expression, indicating the importance of myelin compaction in axonal integrity (63,78). It is important to note that MPZ requires a critical dosage for proper myelin function, otherwise, it leads to hypomyelination (63,68). How MPZ expression is finely regulated and properly assembled to myelin sheaths remains poorly understood. To our surprise, we found that MPZ is elevated and disorganized expression throughout the whole nerve bundle of SGN in *Ada*<sup>-/-</sup> mice. However, pharmacologically interfering ADORA2B attenuates elevated MPZ expression, restoring MPZ integrating to myelin sheaths and maintain myelination of nerve fibers of SGN in these mice. Similarly, genetic deletion of ADORA2B improves MPZ assembling to myelin sheaths. Thus, our findings revealed that ADORA2B is a common pathogenic receptor impairing integration of MPZ to myelin sheaths, inducing hypomyelinated nerve fibers of SGNs and thus promoting SNHL. Notably, early studies showed that acute exposure of adenosine promotes myelination by inducing oligodendrocyte progenitor cells differentiation to myelinated oligodendrocytes in the central nervous system (CNS) (65). Thus, it is very important to define how persistently elevated adenosine signals via ADORA2B and regulates myelination mediated by oligodendrocyte in CNS.

### *Novelty and Therapeutics for SNHL*

In conclusion, SNHL is a challenging condition. However, specific means to prevent or treat SNHL are limited due to a lack of understanding of the underlying mechanisms. Our discovery about elevated adenosine signaling via ADORA2B-mediated demyelination of peripheral SGNs in *Ada*<sup>-/-</sup> mice has provided molecular insight to SNHL in ADA-deficient patients. Extending from *Ada*<sup>-/-</sup> mice, the discovery of pathogenic role of ADORA2B in aging-induced SNHL is also highly innovative. Overall, our studies revealed that ADORA2B is a common pathogenic factor impairing myelination in two independent models of SNHL and immediately highlights novel adenosine-based therapies for SNHL. In this way our findings reveal important novel opportunities to treat and prevent SNHL by targeting adenosine signaling and ADORA2B-mediated effects. Moreover, our findings immediately suggest that reducing adenosine-ADORA2B-mediated demyelination of SGNs are likely innovative therapeutic possibilities to treat and prevent progression of SNHL by improving myelination in SGNs. Altogether, our findings provide us better understanding of the molecular basis underlying SNHL and highlight multiple therapeutic strategies to treat SNHL and to prevent the progression to becoming debilitating.

## **CHAPTER 4: Other HL Models and Future Directions**

#### *4.1 Introduction*

Sensorineural hearing loss is a very broad and common disability that does not have a definitive known cause; however, we believe that exploring another model apart from *Ada*<sup>-/-</sup> will give us a better understanding on what drives this irreversible sensory damage. We decided to look at the most common type of sensorineural hearing loss, presbycusis, or age-related hearing loss. This chapter will discuss how ADORA2B-mediated adenosine signaling plays a role in aging mice on a functional and cellular level. Indeed, we found that hair cell dysfunction and demyelination can be prevented by *Adora2b* deletion in aging mice. In addition to our aging model, we explored how ADORA2B might play a role in sickle-cell disease, a disease with elevated systemic adenosine and hearing-loss incidence. Finally, this chapter will highlight potential therapies and discuss future directions for studying elevated cochlear adenosine in sensorineural hearing loss.

#### *4.2 Materials and Methods*

##### *Adora2b-deficient Aging Mice*

For aging studies, we compared *Adora2b*<sup>-/-</sup> mice that are 1.5 years old with age-matched C57BL/6. *Adora2b*<sup>-/-</sup> mice were generated in our laboratory that were initially transferred from Dr. Michael Blackburn's laboratory. 6-month old C57B6J mice were generously provided by Dr. Louise McCullough and Dr. Claudio Soto's labs. All studies were reviewed and approved by the University of Texas Health Science Center at Houston Animal Welfare Committee.

##### *PSB1115-therapy of Aging Mice*

PSB1115 was generated from water-soluble, HPLC grade, powder from Tocris Bioscience diluted with sterile 1x DPBS (200 ug/per day). We treated 6-month old C57BL/6 mice with PSB1115 and measured ABR days after.

### Sickle-Cell Disease Mice

Berkeley SCD transgenic mice were purchased from The Jackson Laboratory. Bone marrow transplantation (BMT) was achieved in *Adora2b*<sup>-/-</sup> mice by collecting and purifying bone marrow from SCD transgenic mice donor and transplanted into irradiated and previously fed 0.2 % neomycin for one day *Adora2b*<sup>-/-</sup> mice retro-orbitally under isoflurane anesthesia. SCD-A2B mice were fed with 0.2% neomycine sulfate water for two weeks after transplantation and are monitored for two weeks.

### Cochlea isolation, immunohistochemistry, imaging, and analysis

Temporal bones were dissected in PBS, incubated in 4% paraformaldehyde (PFA) in PBS overnight at 4°C, decalcified in 0.2 M EDTA for 5–7 d. Fixed tissue was embedded in OCT compound, cryosectioned at 10 µm, followed by standard immunohistochemistry procedure. The tissue sections were washed with 1x phosphate-buffered saline (PBS), followed by a 1 hr incubation in 5% BSA with 1% Triton X-100 in 1xPBS. These sections were then incubated in primary antibodies overnight at 4°C. The primary antibodies used for this study were: nerve fiber filament (mouse anti-NF-200, Sigma, 1:200), neuron cell bodies (rabbit anti-NeuN, Abcam, 1:500), and myelin protein zero (rabbit anti-MPZ, Abcam 1:200). Tissues were incubated with appropriate Alexa-Fluor conjugated secondary antibodies (Invitrogen, 1:500), followed by DAPI mountant (ProLong Gold Antifade, Thermo Fisher Scientific).

Confocal z-stacks of each cochlea were taken using Zeiss LSM T-PMT microscope equipped with 63x (2x digital zoom) oil immersion lens. MPZ- and NF-200 areas were quantified using ImageJ by selecting via consistent color threshold for each antibody used across all experiment groups (n=3 each) and normalizing each sample by total area of the axon. These MPZ+/total axon area and NF200+/total axon quantifications were collectively compared across

all experiments via a Mann-Whitney nonparametric two-tailed t-test. All statistical analyses were performed via Prism 8.

#### *Auditory brainstem response recording*

Mice were intraperitoneally injected with ketamine-xylazine (100 mg/kg: 10mg/kg). Testing was performed in a soundproof faraday cage booth while mice were placed on heating pad to maintain normal body temperature throughout the procedure. Pure tone bursts (0.1 ms rise/fall, 2 ms duration, 21 presentations/s) from 4 to 48 kHz were generated using System 3 digital signal processing hardware and software (Tucker Davis Technologies). The intensity of the tone stimuli was calibrated using a type 4938 one-quarter inch pressure-field calibration microphone (Bruel & Kjaer). EC1 ultrasonic, low-distortion electrostatic speakers were coupled to the ear canal to deliver stimuli within 3 mm of the tympanic membrane. Response signals were recorded with subcutaneous needle electrodes inserted at the vertex of the scalp (channel 1), the postauricular bulla region (reference), and the back leg (ground), and averaged over 500 presentations of the tone bursts (56). Electrode-recorded activity was filtered (high pass, 300 Hz; low pass, 3kHz; notch, 60Hz) before averaging to minimize background noise. Auditory thresholds were determined by decreasing sound intensity of each stimulus to 10 dB from 90 dB in 5 dB steps until the lowest sound intensity with reproducible and recognizable waveforms was detected. Thresholds were determined to within 5 dB for each frequency by two raters to ensure reliability. SD (dB SPL) were plotted as a function of stimulus frequency (kilohertz) and analyzed for group differences by a two-way ANOVA, followed by a multiple-comparison test, to reveal overall trends. Prism 8 was used for all statistical analyses.



### ABR waveform detection and calculation

Peak amplitudes (I and II) were visually determined from ABR waves detected from each stimulus from 90 to 10 dB in 5 dB increments at each frequency. Peak amplitudes were measured by subtracting the peak voltage from the trough voltage at every dB presentation, averaged per experimental group. All averaged peak amplitudes for each peak from each group were statistically compared using two-way ANOVA, followed by a multiple comparison test.

Peak latencies from peak I and II were calculated by subtracting Peak I's peak amplitude temporal onset (in ms) from Peak II's peak amplitude temporal time onset (in ms). Time measurements were averaged per experimental group. Averaged latencies per group were compared via two-way ANOVA, followed by a multiple comparison test.

All statistical analyses were performed through Prism 8.

### Distortion product otoacoustic emission measurements

DPOAEs were measured from a probe tip microphone placed in the external canal of the mouse ear that were elicited by two 1-second sine-wave tones of varying frequencies ( $F_2=1.2 \cdot F_1$ ).  $F_2$  had a varied range of frequencies from 4 to 90 kHz. These two tones were presented in identical intensities that ranged from 15 to 75 dB SPL in 15 dB increments. The magnitude of the  $2 \cdot F_1 - F_2$  DP was determined by FFT. DPOAE thresholds ( $> -5$  dB SPL and greater than two std. dev above noise floor) were analyzed off-line via BioSigRZ program. If no DPOAE was detected, we defined the threshold to be at 75 dB, as our equipment is limited to 80 dB SPL. DPOAE thresholds were averaged per experimental group and compared via one-way ANOVA, followed by a multiple comparisons test. All statistical analyses were done through Prism 8.

## 4.2 Results

### Adora2b-deficient Aging Mice and Hearing Loss

Previous studies have shown that presbycusis in aging mice is associated with increased thresholds, latencies and decreased amplitudes in early waves (Peak I of cochlear nerve and lower brainstem nuclei) (79), which is similar to the phenotype of SNHL seen in *Ada*<sup>-/-</sup> mice. Thus, we extended from our *Ada*<sup>-/-</sup> mice to determine if ADORA2B signaling plays a role in age-dependent-SNHL. It is known that C57B6J mice (WT) begin to decrease hearing sensitivity after 6 months of age and progress to SNHL at 1 year old (79–81). Thus, we tested if ADORA2B ablation would also improve hearing sensitivity in aging mice. We compared hearing sensitivity by measuring ABR thresholds of *Adora2b*<sup>-/-</sup> mice and WT mice at 6 months (young) and at 1 year (aged), respectively.

Similar to *Ada*<sup>-/-</sup> mice treated with ADORA2B inhibitor (Figure 19), we found that aged *Adora2b*<sup>-/-</sup> mice conserved lower ABR thresholds compared to aged WT, while no difference of ABR thresholds between *Adora2b*<sup>-/-</sup> mice and WT mice at 6-month old young age (Figure 27).

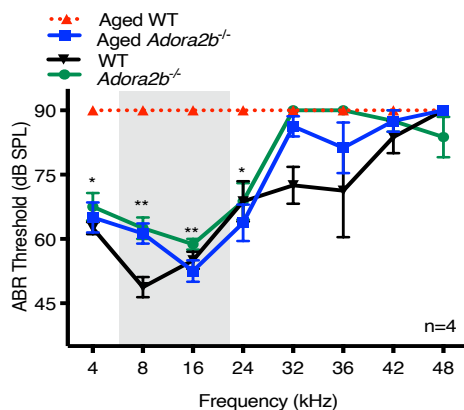


Figure 27. ABR analysis of aged WT mice and aged *Adora2b*<sup>-/-</sup> mice. (mean ± SEM) ABR show aged WT at 90 dB hearing threshold compared to aged and young *Adora2b*<sup>-/-</sup>, and young WT demonstrating conserved hearing sensitivity via *Adora2b* ablation in aging for lower frequencies (p-value between aged WT and *Adora2b*<sup>-/-</sup> for 4-16 kHz, 0.0175, 0.0038, 0.0020, respectively) (n=4 for each cohort).

### *Distortion Product Otoacoustic Emissions of Aging Mouse Models*

As expected, aged mice did not have functional mechanical transduction. DPOAE analysis between aged WT and aged *Adora2b*<sup>-/-</sup> mice revealed that both groups had 75 dB as thresholds for both 8 and 16 kHz (data not shown). Previous studies have shown that C57B6J mice have progressive increase of auditory thresholds due to hair cell and spiral ganglion cell degeneration (82). Age-related hearing loss is posited to be largely due to OHC loss beginning as early as 2 months of age in these mice (82). Interestingly, hearing sensitivity can be preserved despite loss of OHC electromotile properties. Hair cell loss during aging, especially in C57B6 mice, has been posited to be independent of SGN loss during the aging process(83). The exact mechanisms for this matter remain to be studied.

### *SGN → CN Amplitude Peaks & Latency in Aging Mouse Models*

The lack of DPOAE signals indicate age-related changes in OHC function; however, we still found differences in ABR thresholds between WT and *Adora2b*<sup>-/-</sup> aged mice. ABR thresholds only indicate hearing sensitivity on neuronal transduction levels in regions after SGN stimulation. We wanted to delineate further how ADORA2B may play a role in the hearing process. Indeed, we found that ABR peak I and II amplitudes and latencies in 8 and 16 kHz of *Adora2b*<sup>-/-</sup> aged mice were also significantly higher than WT, indicating preserved SGN firing capacity (Figure 28) and no neuronal transduction delay (Figure 29). Thus, we provide genetic evidence that ADORA2B is a pathogenic receptor for aging-induced SNHL.

Figure 28. Peak I and II analysis of aged *Adora2b*<sup>-/-</sup> mice compared to aged WT. (mean ± SEM) Auditory brainstem response traces were analyzed, where Peak 1 amplitudes were elevated in aged *Adora2b*<sup>-/-</sup> cohort compared aged WT mice. Peak II is similar to Peak I, indicating higher capacity of neurons to fire effectively ablation of ADORA2B in aging mice (p-value for 8kHz and 16kHz peak I and II from 90-80dB is <0.0001) (n=5 per group)

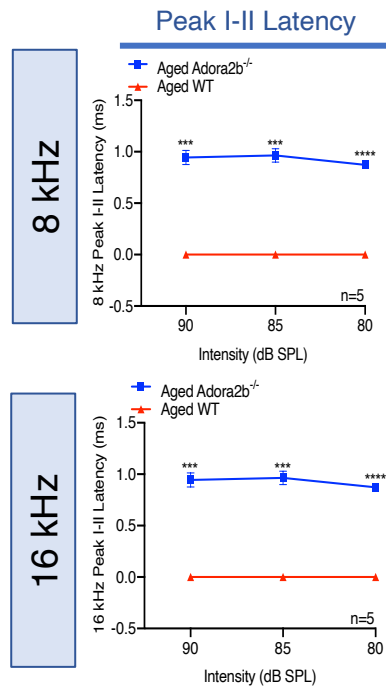
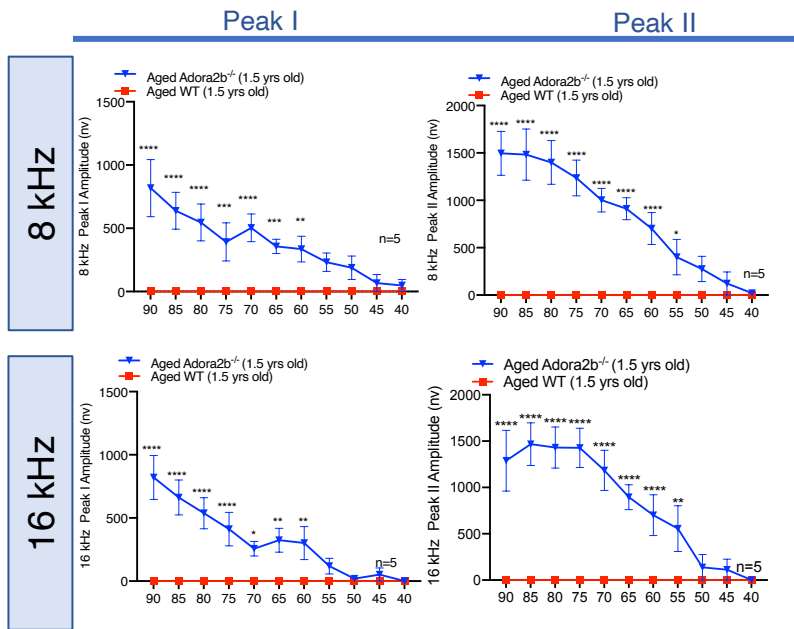


Figure 29. Peak I-II latency analysis of aged *Adora2b*<sup>-/-</sup> mice compared to aged WT. Peak I-II latency measures the efficiency of firing of peripheral nerves to cochlear nucleus in time (ms), showing faster peak amplitudes between two structures when ADORA2B is ablated in high aged mice. (p-value for 8 kHz at 90-80 dB, 0.00046, 0.00038, 0.00006, respectively) (p-value for 16 kHz at 90-80 dB, 0.00046, 0.00038, 0.00006, respectively) (n=5. per group).

### PSB1115 therapy on Aging WT Mice

We have shown that ADORA2B is a receptor that could play a role in age-related hearing loss pathogenesis genetically; however, whole knock-out deletions in mice has their limitations. Therefore, we tested if the effects of ADORA2B inhibitor, PSB1115, will present the same attenuating effects on aging mice. C57B6J are known to have severe hearing loss by 9-month old and threshold shifts after 6 therefore, we wanted to test whether these mice will have improved hearing sensitivity before they have complete hearing loss at >1-year-old if we blocked ADORA2B pharmacologically at 6-months of age (79–81) (Figure 30). Indeed, we found that PSB1115-treated WT mice at 6 months have improved ABR after one day of treatment (Figure 31, left). Additionally, we observed a steady day-by-day increase of ABR thresholds after PSB1115 treatment on these 6-month old WT mice(Figure 31, right). DPOAE thresholds were also improved but limited to 16 kHz (Figure 32). However, no overt differences were observed in ABR peaks 1 & 2 at 8 and 16 kHz (data not shown). ABR thresholds are often an indication of summated auditory response starting at higher dB; however, when peak amplitudes do not reflect ABR threshold shifts, differences in firing capacity may not be as robustly different at higher dBs despite the decreased firing capacity differences at lower dBs where the thresholds are determined. These data are in parallel with the rescued hearing phenotypes of aging mice with the genetic ablation of *Adora2b* and suggest that this receptor plays a role in aging associated with adenosine.

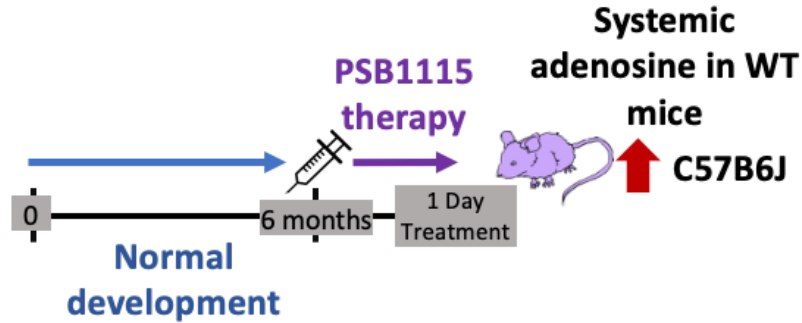


Figure 30. PSB1115 therapy on 6-month-old C57B6J mice. 6-month-old C57B6J mice are treated with PSB1115 to see how an ADORA2B inhibitor will affect normal hearing in younger mice with mostly healthy auditory system.

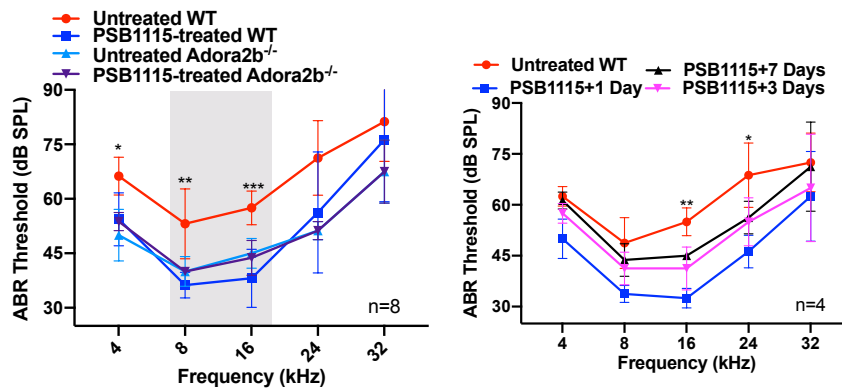


Figure 31. ABR analyses on PSB1115-treated 6-month-old C57B6J mice. (mean  $\pm$  SEM) (left) ABR analysis on 6-month-old WT mice after one day of PSB1115 therapy. (right) Consecutive ABR analyses of 6-month-old WT mice after 1, 3, and 7 days of PSB1115 therapy (p-value between PSB111-treated WT and untreated WT for 4-16 kHz, 0.0125 , 0.0062, 0.0005 , respectively) (n=8).

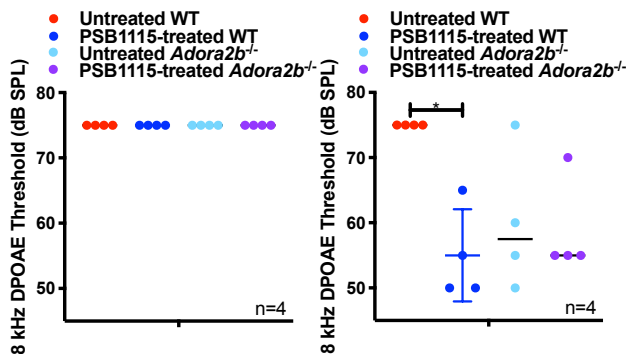


Figure 32. DPOAE analysis on PSB1115-treated 6-month-old C57B6J mice. (mean  $\pm$  SEM) DPOAE analysis at 8 and 16 kHz on 6-month-old WT mice after one day of

PSB1115 therapy (p-value between PSB111-treated WT and untreated WT for 8 kHz is 0.0342) (n=4).

Structural and potential molecular mechanisms in Aging Models

Aging in mice inevitably loosens and unravels myelin sheaths with eventual demyelination(84). This often leads to the lack of protection of nerve fiber filaments, which we observed in our aged WT mice (Figure 27). In view of the detrimental role of ADORA2B in the demyelination of SGN in *Adora2b*<sup>-/-</sup> mice (Figure 10) and given the similar improvement of hearing sensitivity in aged *Adora2b*<sup>-/-</sup> mice and ADORA2B inhibitor treated *Adora2b*<sup>-/-</sup> mice, we hypothesize that ADORA2B is a previously unrecognized molecule responsible for demyelination seen in aging-induced SNHL. Similar to PSB1115 treated *Adora2b*<sup>-/-</sup> mice (Figure 22), we found that aged *Adora2b*<sup>-/-</sup> mice conserved nerve fiber (Figure 33). These findings provide genetic evidence that ADORA2B is detrimental to cause demyelination in aging-induced SNHL.

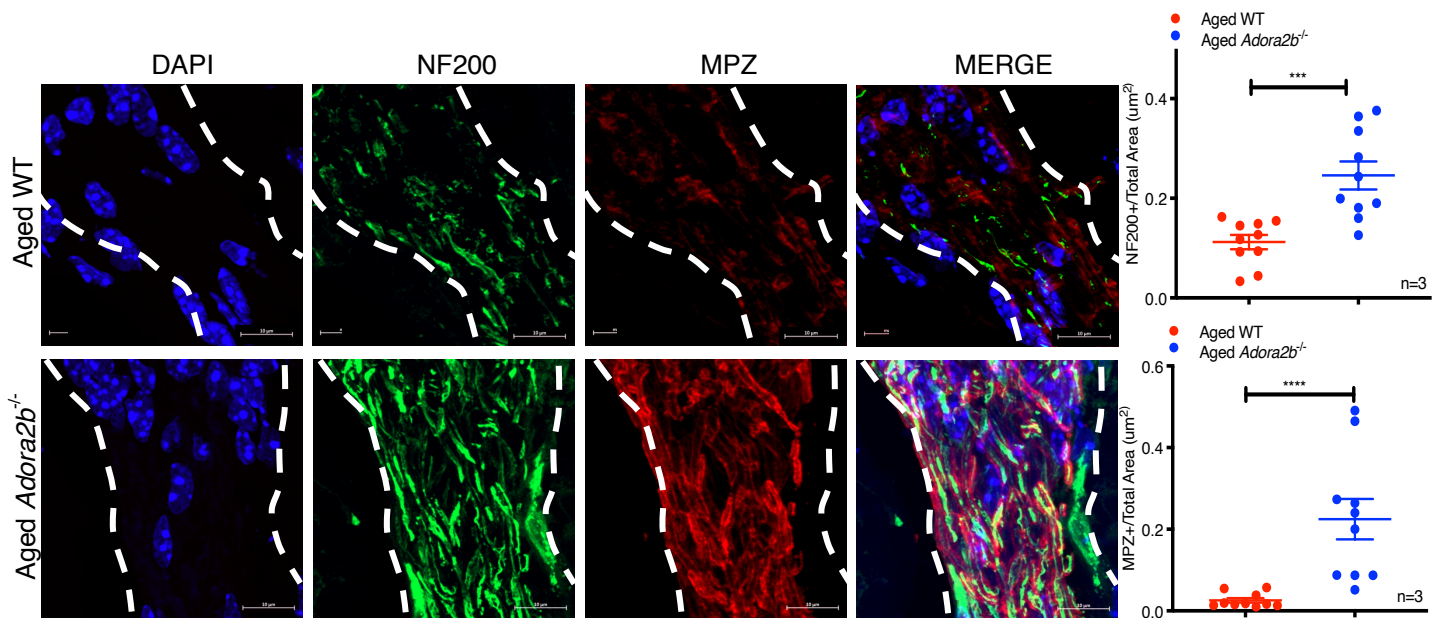


Figure 33. Nerve fiber and MPZ protein immunofluorescent staining on aged *Adora2b*<sup>-/-</sup> cochlear nerve compared to aged WT. Spiral ganglion neurons stained with dapi. MPZ and NF200 staining is increased and improved in organizational pattern in *Adora2b*<sup>-/-</sup> aged mice compared to WT aged

mice (p-value, left panel, 0.0003, right panel, <0.0001) (n=3 per group) Data are shown as mean  $\pm$  SEM.

Aging in mice also affects morphologic and functional elements of the myelin sheaths of peripheral nervous system (PNS) with the decrease of MPZ expression(85–87). Decreased MPZ expression in aging contributes to loosening and unraveling of myelin sheaths as it is an integral membrane protein that maintains the multilamellar structure of myelin sheaths (64). Given the discovery of ADORA2B in impaired compact of MPZ to myelin sheaths in *Ada*<sup>-/-</sup> mice, we tested the possible role of ADORA2B in MPZ compaction in myelin sheaths in aging-induced SNHL. Similar to PSB1115 treated *Ada*<sup>-/-</sup> mice, *Adora2b*<sup>-/-</sup> mice showed a significant improvement of MPZ expression in myelin sheaths compared to aged WT mice (Figure 33), suggesting detrimental role of *Adora2b* in myelin sheath organization in aging-induced SNHL and in ADA-deficiency-induced SNHL. Taken together, we conclude that genetic deletion of ADORA2B markedly attenuates impairment of MPZ integrating to myelin sheaths and demyelination of cochlear nerve fibers and thus improves sensory hearing ability during aging.

On a pharmacological level, 6-month-old WT mice ABR thresholds improved after 1-day treatment of ADORA2B antagonist, PSB1115. This is a remarkably fast response; therefore, we posit that ADORA2B-specific inhibition is producing a response on a metabolic level. One possibility is ADORA2B's role in the regulation of metabolites in the Organ of Corti. Within the Organ of Corti, ATP is periodically released from supporting cells that lead to eventual potassium release (88). This culmination of potassium then leads to depolarization of inner hair cells that lead to glutamate release that will activate SGNs (88). The hearing process requires a balance in glutamate release, otherwise it will be excitotoxic. ADORA2B could play a role in any of these fast-acting responses, such as the vesicular release of glutamate. Cochlear excitotoxic mechanisms are still unknown; however, it is known that glutamate is concentrated in synaptic vesicular transporter, vesicular glutamate transporter type 3 (Vglut3) (89). To date, the role of



ADORA2B in VGLUT3's function is unknown. Overall, we can only conclude that ADORA2B inhibition via PSB1115 has a fast-acting response to threshold shifts. This is useful information for future studies, especially in a therapeutic setting. Whether PSB1115 can be used as a treatment to temporary hearing loss or prevent age-related hearing loss remains to be elucidated.

#### *Possible Molecular Pathogenesis in SNHL Associated with Elevated Adenosine*

It is no surprise that purinergic signaling is a pathway explored in earlier works of SNHL. The hearing process demands an abundance of ATP and HL is often attributed to a disruption in this metabolic energy currency. While we do not provide evidence of an intricate molecular pathway for the pathogenesis of SNHL, we have narrowed down a potential signaling pathway that can be targeted therapeutically.

Our research is built on substantial data generated from *Ada*-deficient mice that display bilateral sensorineural HL mimicking ADA-deficient humans. Additionally, we use the same FDA-drug (PEG-ADA) ADA-deficient patients use to lower systemic adenosine and monitor how adenosine progression contributes to HL. This pharmacological approach revealed a correlation between adenosine progression and gradual HL, as we have shown with the steady increase of ABR threshold. More importantly, we found that this pathogenesis to be reversible within a specific time-frame of adenosine accumulation. Further studies are required to understand how elevated adenosine signaling play a role in myelination in the inner ear. Given that myelin has high lipid content, any disruption of Schwann cell mitochondria where purinergic signaling is perturbed can lead to dysfunction in fatty acid metabolism.

Our metabolomics profiling revealed that these untreated mice have abnormally high levels of long-chain acylcarnitines (LCA) and succinate (Figure 34), metabolites involved in mitochondrial functions, such as the carnitine-shuttle system and the TCA cycle. ATP is generated

via transport of activated long-chain fatty acids from the cytoplasm to the mitochondria through carnitine-shuttle system (90,91). On the outer mitochondrial membrane, carnitine palmitoyltransferase I (CPT1) transesterifies CoA moiety for carnitine which yields in LCAs (90,91). LCAs are transported through the mitochondrial matrix where they are metabolized back into free-carnitine and acyl-CoA by carnitine palmitoyltransferase II (CPT2) in the inner mitochondrial membrane(90). Acyl-CoA subsequently undergoes beta-oxidation to provide energy for high-ATP demand tissues (90,92). Studies have shown that CPT2-deficiency leads to mitochondria-generated oxidative stress that lead to energy-deficiency and cell death (93,94). CPT2's relationship with adenosine and HL, however, is unknown. Our preliminary data suggests that chronic elevation of adenosine results in detrimental accumulation of LCAs.

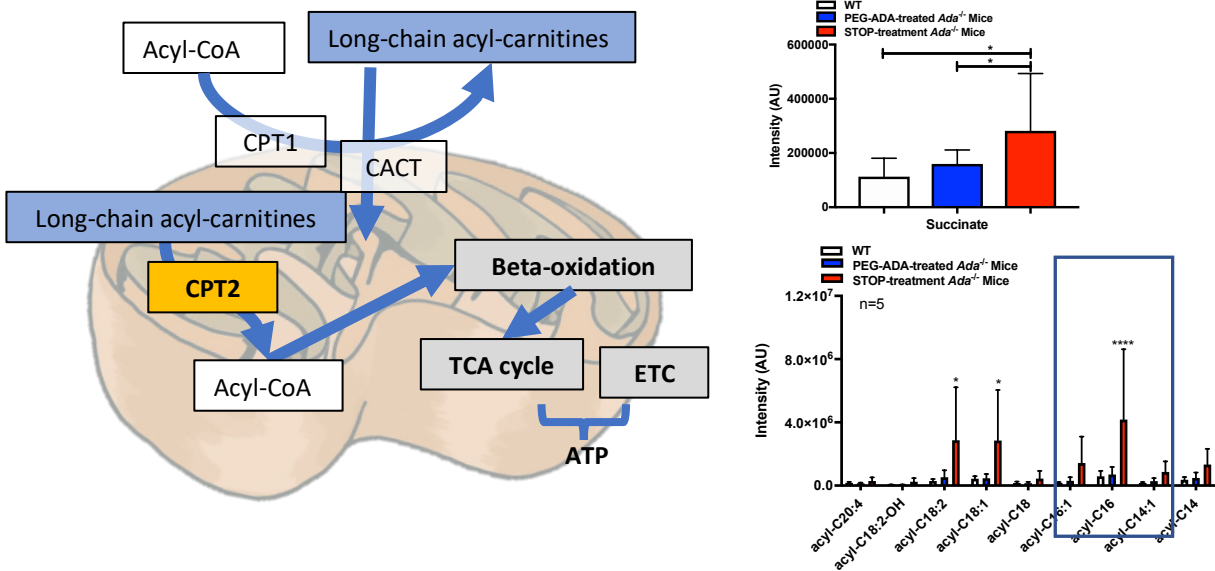


Figure 34. Mitochondrial fatty acid metabolism pathways and related metabolomics profile of PEG-ADA treated and untreated *Ada*<sup>-/-</sup> mice. (left) Schematic diagram of carnitine-shuttling system, a process required for long-chain fatty acids to enter the mitochondria for metabolism and overall energy production. (right) PEG-ADA withdrawal results in elevated cochlear long-chain acylcarnitines and succinate in *Ada*<sup>-/-</sup> mice. Metabolomics profiling reveal cochlear long-chain

acylcarnitines and succinate levels were significantly increased in *Ada*<sup>-/-</sup> mice following withdrawal of PEG-ADA therapy (n=6). Data are shown as mean ± SEM.

Myelin sheaths contain 70% of lipid and 30% of proteins, where the most abundant protein is MPZ that holds the sheaths together in PNS (61). Previous studies have shown that aberrant Schwann cell lipid metabolism is linked to mitochondrial dysfunction that lead to axon degeneration and neuropathy (95). In this study, they showed elevated palmitoylcarnitines that correlated with elevated axon degeneration, which parallels our metabolomic study and decreased expression of NF-200 in elevated cochlear adenosine (95). Our cochlear metabolomics profile reveals the highest significant accumulation of palmitoylcarnitine, in particular. Palmitoylcarnitines facilitate transfer of long-chain fatty acids through the mitochondrial membranes for beta-oxidation to generate ATP. The continuous release of ATP to be hydrolyzed into adenosine presents a cyclic pathology and elevated levels of long-chain acyl-carnitines can alter membrane fluidity through hydrophobic bonds with lipids and membrane proteins. Alternatively, previous studies have shown that hypoxia can induce elevated levels of long-chain acyl-carnitines, and from our lab's previous work, we know that hypoxia is associated with sustained levels of adenosine (96–99). Moreover, multiple early studies have shown elevated adenosine plays a role in lipid metabolism (100–102). However, whether and how ADORA2B disturbs lipid metabolism, leading to decreased lipid integrity, releasing soluble MPZ, hypomyelination or axon degeneration and progression of SNHL remain elusive.

To our knowledge, there are no studies that link ADORA2B signaling with acylcarnitine accumulation, however, one possible pathway could be due to ADORA2B's capability to induce PKA signaling. Our lab has previously found that elevated adenosine levels activate ADORA2B that induces PKA phosphorylation, followed by proteasomal degradation of a protein necessary

for cellular homeostasis(103). ADORA2B-mediated proteasomal degradation may play a role in decreasing CPT2 levels, resulting in long-chain acylcarnitine accumulation. Palmitoylcarnitines, in particular, have been found to inhibit PKC, an important protein for MPZ phosphorylation that allows it to be adhesive for myelin compaction (104,105). Overall, we posit that ADORA2B disturbs lipid integrity in myelin compaction, leading to demyelination, axonal damage, and decreased hearing sensitivity (Figure 35).

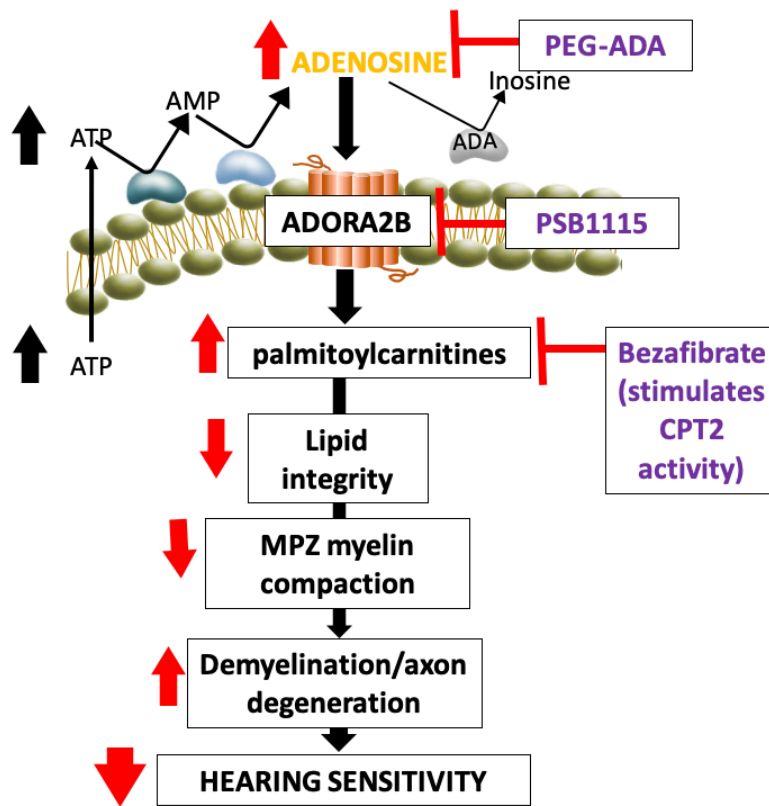


Figure 35. Working Model. Chronically elevated cochlear adenosine causes hearing loss via preferentially amplified ADORA2B signaling, increasing levels of palmitoylcarnitines that disrupt myelin compaction via disruption of membrane fluidity and MPZ function, leading to demyelination and axon degeneration, and overall leading to sensorineural hearing loss (SNHL) in *Ada*<sup>-/-</sup> mice. Lowering adenosine (PEG-ADA) or inhibiting (PSB1115) ADORA2B improves and

prevents SNHL by attenuating nerve fiber and MPZ structure that are otherwise damaged in *Ada*<sup>-/-</sup> mice. Genetic deletion of ADORA2B improves MPZ integrating to myelin sheaths, attenuates demyelination and slows down the progression of SNHL in aging. Thus, ADORA2B is a common pathogenic factor underlying SNHL in both *Ada*<sup>-/-</sup> mice and aged WT mice and an innovative therapeutic target. Downstream targets like CPT2 with bezafibrate could be a potential therapeutic regimen for hearing loss to decrease palmitoylcarnitines that inhibit PKC activity for MPZ phosphorylation that retain their adhesion properties, overall composing the myelin integrity.

### Other Disease Models: Sickle-Cell Disease and Hearing Loss

Bilateral hearing loss is the most common hearing loss complication in sickle-cell disease (SCD) patients, however, little is known of its pathophysiology. Interestingly, SCD patients and rodent models have elevated systemic adenosine (31,101,106–111). Our lab has found that SCD patients and mouse models have elevated circulating adenosine that lead to various multi-organ damages, such as pain and priapism (31,111)(101). Pain and priapism pathophysiology studies in SCD transgenic mice were attributed to ADORA2B-mediated signaling from sustained systemic adenosine levels(26,31). With prior knowledge of purinergic signaling playing a role in hearing loss, it was reasonable to test hearing capacities in SCD transgenic mice.

The Berkeley SCD transgenic mouse is a widely accepted SCD model that expresses the human sickle hemoglobin exclusively, and we found that WT mice with bone marrow transplants (BMT) from SCD mice phenocopy hearing loss from SCD patients. SCD-WT mice nearly have complete hearing loss at higher dBs; however, when SCD BMT was conducted in either *CD73*<sup>-/-</sup> or *Adora2b*<sup>-/-</sup> mice (SCD-*CD73*<sup>-/-</sup> & SCD-*Adora2b*<sup>-/-</sup>, respectively), this hearing loss is improved (Figure 36). At 8 and 16 kHz, SCD-*CD73*<sup>-/-</sup> mice have significantly lowered ABR thresholds compared to SCD-WT, while SCD-*Adora2b*<sup>-/-</sup> was only significantly lower at 8kHz. As previously mentioned in Chapter 1, CD73 is an ectonucleosidase that metabolizes AMP into adenosine, therefore, SCD-*CD73*<sup>-/-</sup> theoretically lowers adenosine systemically while SCD-*Adora2b*<sup>-/-</sup> have high adenosine levels without global ADORA2B signaling stimulation. Here, we concluded that, similar to PEG-ADA and ADORA2B ablation, lowering adenosine or inhibiting ADORA2B activation improves or prevents hearing loss.

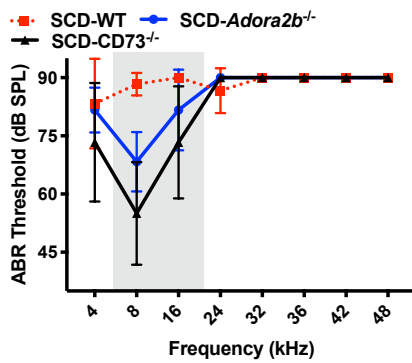


Figure 36. ABR analysis of sickle-cell transplanted -WT, *CD73<sup>-/-</sup>*, and *Adora2b<sup>-/-</sup>*. Berkeley SCD bone marrow transplanted in *CD73<sup>-/-</sup>* and *Adora2b<sup>-/-</sup>* mice show decreased ABR thresholds compared to SCD bone marrow transplanted C57B6J mice, indicating *CD73* and *Adora2b* ablation improves hearing in SCD.

Interestingly, OHC functionality in SCD-*CD73<sup>-/-</sup>* and SCD-*Adora2b<sup>-/-</sup>* only had lowered thresholds in 16 kHz compared to SCD-WT, while thresholds at 8 kHz in all three groups were similarly low (Figure 37). This may be an indication that SCD-WT may have outer hair cell damage at the apex of the cochlea, where stimulation at 16 kHz is more sensitive. Sickle-cell anemia can cause vaso-occlusive crisis (VOCs), leading to ischemia in the labyrinthine artery in the inner ear(112). Hypoxia in the inner ear can lead to outer hair cell death, an irreversible damage; however, lacking *CD73* or *ADORA2B* seem to prevent this possible hearing loss onset in SCD mouse models.

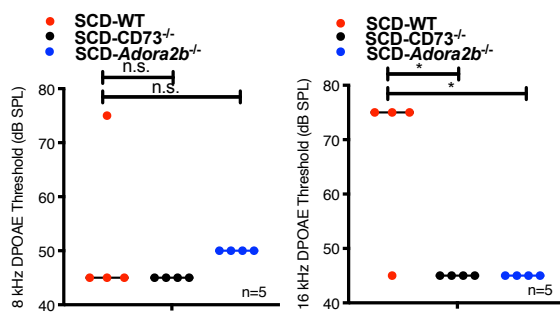


Figure 37. DPOAE analysis of sickle-cell transplanted -WT, *CD73<sup>-/-</sup>*, and *Adora2b<sup>-/-</sup>*. Berkeley SCD bone marrow transplanted in *CD73<sup>-/-</sup>* and *Adora2b<sup>-/-</sup>* mice show decreased DPOAE thresholds compared to SCD bone marrow transplanted C57B6J mice, indicating *CD73* and *Adora2b* ablation improves outer hair cell functionality at 16 kHz in SCD. DPOAE thresholds at 8 kHz show no difference between three groups. (at 16 kHz, p-value between SCD-WT and SCD-*CD73<sup>-/-</sup>* is 0.0128 and p-value between SCD-WT and SCD-*Adora2b<sup>-/-</sup>* is 0.0128 ) (n=5).

As we looked closer in our SCD mice ABR traces, we found the same trend that only 16 kHz frequency revealed statistically significant differences between 3 groups. While peaks I and II (cochlear VIII nerve and cochlear nucleus, respectively) amplitudes at 8 kHz did not reveal significant changes in all three groups (data not shown), both revealed the same trend of having lowered amplitude at higher dBs in SCD-WT compared with transplanted *CD73*<sup>-/-</sup> or *Adora2b*<sup>-/-</sup>, suggesting a lower capacity for hearing and sending electrical transduction to higher brain regions. 16 kHz, on the other hand, revealed that ablation of *CD73* or *Adora2b* can improve this process (Figure 38). Whether outer hair cells that respond to 16 kHz frequency is directly correlated with this process remains to be determined; however, we do know that SGN type II synapse with basal OHC and only account for 5% of the ganglion cells, while type I SGNs synapse with IHCs, and both types directly innervate to the cochlear nuclei. Latency analyses of peak I to II reveal that both frequencies do not have any statistically significant changes in temporal neuronal activity transmission (data not shown).

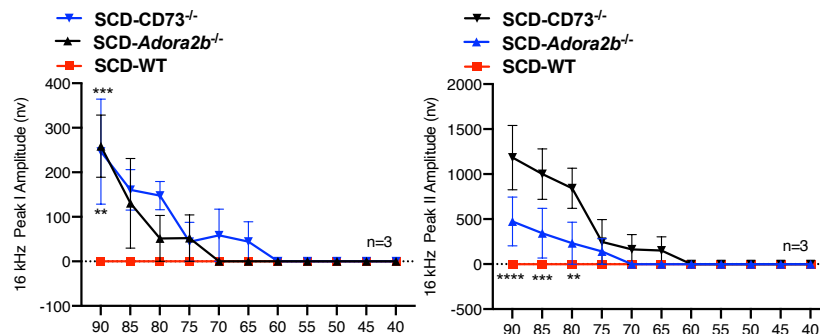


Figure 38. Peak I and II analysis of sickle-cell transplanted -WT, *CD73*<sup>-/-</sup>, and *Adora2b*<sup>-/-</sup>. (mean ± SEM) Auditory brainstem response traces were analyzed, where Peak 1 amplitudes were elevated in Berkeley SCD bone marrow transplanted in *CD73*<sup>-/-</sup> and *Adora2b*<sup>-/-</sup> mice compared to SCD bone marrow transplanted C57B6J mice in 16 kHz Peak I at higher dB (cochlear VII nerve). While only transplanted *CD73*<sup>-/-</sup> cohort have elevated peak II amplitudes (cochlear nucleus)

compared to transplanted WT mice. (Peak I SCD-WT vs SCD-*CD73*<sup>-/-</sup> p-value for 90 dB is 0.0014. While SCD-WT vs SCD-*Adora2b*<sup>-/-</sup> p-value is 0.0007. Peak I SCD-WT vs SCD-*CD73*<sup>-/-</sup> p-value for 90, 85, and 80 dB is <0.0001, 0.4507, and 0.0211, respectively) (n=3 per group)

Overall, we show that the SCD mouse model parallels SCD patient hearing loss phenotypes. To our knowledge, these findings have yet to be published in literature. While several studies have published incidences of hearing loss in SCD patients across the world, deeper molecular studies in patients or animal models have yet to be investigated. Previous studies have shown higher frequency hearing loss in SCD patients and suggest that this may be due to the nature of the cochlea having terminal arteries(108,109). SCD patients, in general, experience VOCs due to the stickiness of the sickled red blood cells, which can ultimately perturb blood flow. Cochlear labyrinthine blood vessels are susceptible to labyrinthine hemorrhage and labyrinthitis ossificans and may be caused by VOCs but remains to lack incidence support in the clinic (113,114). Any further molecular studies also remain to be investigated.

Our study broadly explores the potential role of adenosine signaling in SCD and many other plausible causes can be explored in SNHL onset in SCD patients. Other SCD pathologic changes, such as infection and chronic hemolytic anemia, are other branches of study that can be explored in sensorineural hearing loss which adenosine signaling has been associated with in other SCD studies (26,101). Another consideration in studying SNHL in SCD is how its etiology may differ among SCD patients with varying  $\beta$ -globin chain abnormality (HbSS, HbSC, HbS/ $\beta$ -thalassemia). Current methodologies, audiology screenings on SCD patients in different age groups, are still limited, and therapeutic options for hearing loss have yet to be discovered. Therefore, it is imperative to further investigate and explore correlations between SCD, SNHL, and adenosine.



#### 4.4 Future Directions

##### 1) What is the cellular and metabolic basis underlying the natural progression of elevated adenosine-induced HL in *Ada*<sup>-/-</sup> mice?

Our metabolomics profiling, pharmacological tools, and cellular and genetics techniques provide substantial data on our *Ada*<sup>-/-</sup> HL model. HL is often attributed to hair cell and neuronal cell losses in the cochlea; however, our cochleogram and immunofluorescence staining of SGN bodies analyses did not present significant hair cell and SGN loss, respectively, in STOP-treatment *Ada*<sup>-/-</sup> mice. Instead, we found increasing demyelination as adenosine accumulates post PEG-ADA treatment. Conservation of hair cells was also validated via DPOAE analysis, where we found mild differences in DPOAE thresholds between PEG-ADA treated and stop-treatment *Ada*<sup>-/-</sup> mice. Additionally, our preliminary data show elevated adenosine increase cochlear succinate levels, indicating a disruption of the TCA cycle via succinate dehydrogenase (SDH). SDH has been found to be involved in multiple disease conditions (115–118), including ototoxicity and aging cochlea (119,120). SDH is also a part of the mitochondrial electron transport chain (ETC) that contributes to ATP production. Indeed, we also found an accumulation of cochlear long-chain acylcarnitines (LCA) in *Ada*<sup>-/-</sup> mice with elevated adenosine and as previously mentioned, a disruption in mitochondrial function has been shown to disrupt axon degeneration and neuropathy. However, a deeper molecular understanding in this HL model is still missing.

- i) Cochlear Schwann Cell profiling – The limitations of our finding lie on the fact that pharmacological therapies were applied on a systemic level while investigating a complex multi-cellular sensory organ. It would be interesting to investigate whether demyelination is caused by a perturbation in TCA cycle metabolism in Schwann cells. While metabolomic profiling is a sophisticated way to delineate molecular pathways,

our results reflect metabolism in the whole cochlear system under different adenosine levels. Metabolic profiling of isolated Schwann cell from PEG-ADA treated and STOP-treatment *Ada*<sup>-/-</sup> mice would be most ideal to see how sustained adenosine levels play a role in fatty acid metabolism in Schwann Cell. Alternatively, establishing and observing Schwann cell cultures under increasing adenosine levels would be interesting. Previous studies have shown that adenosine promotes differentiation and myelination in the CNS (65), however ATP does the opposite in the PNS (65). This finding supports our hypothesis of the detrimental cyclic behavior of sustained elevated adenosine, where ATP is continuously released extracellularly under stressful environments, such as hypoxia and acoustic overstimulation, consequently increasing adenosine levels via increased CD73 expression and function. To our knowledge, adenosine's direct affect on Schwann cell differentiation or myelination remains to be investigated. Therefore, determining whether elevated adenosine can directly increase MPZ expression and palmitoylcarnitines would be imperative.

- ii) TCA Cycle and Acylcarnitine Metabolism – While specifying the cell type responsible for a sustained-adenosine neuropathy that leads to sensorineural hearing loss is important, the goal is to always delineate a mechanism that can contribute to a molecular-based therapy. As previously mentioned, accumulation of long-chain acylcarnitines disrupts overall ATP generation and can potentially contribute to membrane potential equilibrium through changes in membrane fluidity (96–98). It would be interesting to see if sustained adenosine levels indeed disrupt fatty acid metabolism by testing for decreased CPT2 activity or expression levels, and how it correlates with overall ATP levels. Other acylcarnitine metabolism enzyme functions should also be considered, such as CPT1, since it is responsible for the transesterification of coA for carnitine. However, CPT1 is not known to be expressed

in mitochondria of neurons in the central nervous system (90,93). It would also be interesting to see if changing adenosine levels affects SDH expression and function and determine whether this is the cause of a perturbation in TCA cycle leading to accumulation of succinate.

- iii) Specific inner-ear approach – To mimic elevated adenosine levels outside of a rare genetic disorder that is *Ada*-deficiency, introduction of high adenosine levels in wild-type C57BL/6J mice using 2'-Deoxycoformycin (DCF) to block ADA can reveal how chronic elevated levels of adenosine underlie HL. To determine whether sustained adenosine levels truly affect inner ear physiology, 2'-Deoxycoformycin (DCF)-soaked gelatin sponge (Gelfoam) application in the round window membrane can directly block ADA in C57BL/6J inner ear. This will allow us to monitor if we can recapitulate elevated cochlear adenosine pathology on a metabolic, cellular, and physiological levels.
- iv) Direct CPT2 rescue therapy - Using the same hydrogel technique, directly increasing *Cpt2* expression in the inner ear via virus vector-mediated gene therapy in both untreated *Ada*<sup>-/-</sup> mice and DCF-treated C57BL/6J mice can reveal whether chronic adenosine-mediated sensorineural hearing loss disrupts fatty acid metabolism or not. Alternatively, a direct increase of *Cpt2* expression and function in the inner ear via bezafibrate therapy in both untreated *Ada*<sup>-/-</sup> mice and DCF-treated C57BL/6J mice could be used to test changes in hearing sensitivity. Bezafibrate is an FDA-approved drug used to increase CPT2 expression and function, however, whether CPT2-deficient patients have sensorineural hearing loss remains to be evaluated.
- v) PEG-ADA rescue therapy – We have shown that PEG-ADA resumption can reverse hearing loss after a 2-week PEG-ADA withdrawal for adenosine accumulation. While we showed that this could improve hearing sensitivity, axon integrity, and MPZ

compaction, we have yet to show that it affects myelin integration. We also did not show whether metabolic profiling, palmitoylcarnitine levels in particular, was reversed to normal levels after PEG-ADA resumption; therefore, CPT2 expression or function should also be determined. Further EM analysis on these cochleae to see whether myelin compaction is back normal would also be imperative.

- vi) Adenosine-mediated hearing loss in SCD and aging models – Although we determined that these models, indeed, have hearing loss that parallel with clinical findings, we have yet to determine whether they have elevated cochlear adenosine. HPLC analysis in different age groups (young, middle-aged, and aged) of the aging model are needed to test whether presbycusis is correlated with increasing adenosine levels over time. Although systemic adenosine was found in SCD patients and mouse models, cochlear adenosine is yet to be determined compared to control models. Further inner ear cellular experiments, such as cochleograms and EM, would be pertinent to determine whether adenosine-mediated demyelination is a pathway applicable to all types of sensorineural hearing loss incidences. Additionally, therapeutic models aforementioned would also be an exciting scientific venture. PEG-ADA and bezafibrate are FDA-approved drugs that might have minimal side-effects that can be used to see if loss of hearing sensitivity can be reversed or prevented through a reasonable regimen application.
- vii) Other alternative strategies – Consideration of loss of other cell types (endothelial, stria cells, etc) and testing for stria vascularis and blood-labyrinth barrier integrity via Evan's blue staining is imperative (56,121–123). Overall, if these models do not represent the relationship of HL and adenosine accumulation, one can invest in noise-induced HL mice models where noise-exposed rodents have shown to have elevated ATP and have been posited to have elevated adenosine (3,4,9,124). This HL model

can be used to investigate whether lowering adenosine levels with PEG-ADA therapy can ameliorate HL in noise-exposed rodents.

2) What is ADORA2B's role in the cellular and metabolic disturbance in HL in *Ada*<sup>-/-</sup> mice?

Our RT-PCR profiling confirmed *Adora2b* to be expressed the most in stop-treatment *Ada*<sup>-/-</sup> mice compared to WT and PEG-ADA treated *Ada*<sup>-/-</sup> mice. We found that *Ada*<sup>-/-</sup> mice with PEG-ADA withdrawal, treated with ADORA2B antagonist (PSB1115), displayed a significant hearing improvement compared with stop-treatment mice. On a genetic level, *Adora2b*-deficient *Ada*<sup>-/-</sup> mice (*Ada*<sup>-/-</sup>/*Adora2b*<sup>-/-</sup>) have improved hearing compared to PEG-ADA treated and untreated *Ada*<sup>-/-</sup> mice. Overall, we have shown that ADORA2B signaling ablation under elevated and sustained adenosine conditions can ameliorate SNHL in *Ada*<sup>-/-</sup> mice. We augmented this finding by extending how ADORA2B signaling can affect presbycusis in aging and SCD mouse models, further validating the receptors role in SNHL. Opportunities to explore ADORA2B signaling in chronic cochlear adenosine levels can be achieved by applying techniques mentioned in the previous section. However, much is to be investigated downstream of ADORA2B in other models.

- i) ADORA2B and Adenosine levels – Although we have shown that blocking or genetically deleting ADORA2B is beneficial in ameliorating hearing loss under chronic levels of adenosine, adenosine HPLC analyses and metabolomic profiling were not performed in these models. To date, there are no evidences that ADORA2B signaling affects adenosine levels, however, it is an imperative piece of information to delineate whether ADOR2B is activating pathologic downstream mechanisms or simply lowering adenosine levels. Metabolomic profiling in models that we have used will also shed light into whether acylcarnitines are

decreased under these circumstances that lead to better myelination and hearing loss.

- ii) ADORA2B signaling in SCD and aging models - ADORA2B is known to be elevated in chronic disease states, particularly in sustained adenosine levels (26–32). Moreover, ADORA2B has the least affinity to adenosine and is, therefore, dependent on sustained accumulation of extracellular adenosine for activation. ADORA2B has been shown to be expressed in rodent cochlea, however, increased cochlear *Adora2b* expression is yet to be determined models we have used. A simple RT-PCR or western blot of whole cochlea could determine *Adora2b* expression in SCD and aged WT mice; however, specific *Adora2b* expression changes from isolated Schwann cells from these models would be most ideal. Alternatively, a simple co-immunofluorescent staining of any Schwann cell marker (MPZ, myelin basic protein, etc) and ADORA2B antibody in cochlea sections would be ideal. Unfortunately, to this day, adenosine signaling experts have yet to find a good ADORA2B antibody.
- iii) PKA signaling – Our lab previously found that elevated adenosine activates ADORA2B and induces PKA phosphorylation, followed by proteasomal degradation of a protein necessary for cellular homeostasis (103). Additionally, ADORA2B receptors couple to adenylyl cyclase via G-protein (*G $\alpha$ s*) stimulation and increase intracellular cAMP (125). Protein kinase A (PKA) is the first identified downstream target of cAMP (125). It would be interesting to investigate whether cochlear PKA expression and phosphorylation is induced under elevated adenosine levels and inhibited or diminished when ADORA2B is ablated. A simple way to address this is to perform immunofluorescent staining on sectioned cochlea with PKA-substrate antibodies in *Adora<sup>-/-</sup>* mice. Untreated *Adora<sup>-/-</sup>* mice

should have elevated PKA-substrate expression post PEG-ADA withdrawal. PKA-substrate expression, then, would be expected to diminish in *Ada*<sup>-/-</sup>/*Adora2b*<sup>-/-</sup> and PSB111-treated *Ada*<sup>-/-</sup> mice. To determine whether PKA signaling induces the protein degradation pathway, specifically targeting CPT2, immunoprecipitation (IP) of ubiquitinated proteins and PKA substrates followed by western blot analysis of CPT2 can be performed in either whole cochlea or isolated Schwann cells in various of models mentioned above. CPT2 western blot expression should decrease in sustained adenosine conditions.

- iv) Schwann cell-specific *Adora2b* deletion – In order to specify ADORA2B's role in chronic adenosine-mediated HL, experiments can be performed in Schwann cell deletion of *Adora2b* in *Adora2b*-floxed mouse treated with 2'-Deoxycoformycin (DCF) via Gelfoam-soaked adenovirus vector carrying Cre-*Mpz* gene. The use of Gelfoam is a safer way to locally deliver drugs into the inner ear, as opposed to injection of drugs into the cochlea via the round window membrane.
- v) Other alternative strategies – To further validate ADORA2B-mediated HL pathway, a Gelfoam-soaked ADORA2B agonist, BAY 60-6583, in the inner ear of C57BL/6J mice would be expected to have the same cochlear pathologies and HL. Alternatively, a regimented Gelfoam-soaked PSB1115 in aging inner ear would be an interesting experiment to see whether ADORA2B inhibition can prevent presbycusis. Additional investigation of receptor function and expression of other adenosine receptors, such as ADORA1, which is known to be neuroprotective, would also be interesting (9,11).

## BIBLIOGRAPHY

1. WHO. Multi-country Assessment of National Capacity to Provide Hearing Care. 2013;1–49. Available from:  
[http://www.who.int/pbd/publications/WHOReportHearingCare\\_Englishweb.pdf?ua=1](http://www.who.int/pbd/publications/WHOReportHearingCare_Englishweb.pdf?ua=1)
2. Arlinger S. Negative consequences of uncorrected hearing loss—a review. *Int J Audiol* [Internet]. 2003;42(sup2):17–20. Available from:  
<http://www.tandfonline.com/doi/full/10.3109/14992020309074639>
3. Vlajkovic SM, Housley GD, Muñoz DJB, Robson SC, Sévigny J, Wang CJH, Thorne PR. Noise exposure induces up-regulation of ecto-nucleoside triphosphate diphosphohydrolases 1 and 2 in rat cochlea. *Neuroscience*. 2004;126(3):763–73.
4. Ramkumar V, Whitworth CA, Pingle SC, Hughes LF, Rybak LP. Noise induces A1 adenosine receptor expression in the chinchilla cochlea. *Hear Res*. 2004;188(1–2):47–56.
5. Ito K, Dulon D. Purinergic signaling in cochleovestibular hair cells and afferent neurons. *Purinergic Signal*. 2010;6(2):201–9.
6. Köles L, Szepesy J, Berekméri E, Zelles T. Purinergic Signaling and Cochlear Injury-Targeting the Immune System? *Int J Mol Sci*. 2019;20(12):125–50.
7. Whitmore K V., Gaspar HB. Adenosine deaminase deficiency - more than just an immunodeficiency. *Front Immunol*. 2016;7(AUG).
8. Vlajkovic SM, Chang H, Paek SY, Chi HHT, Sreebhavan S, Telang RS, Tingle M,



- Housley GD, Thorne PR. Adenosine Amine Congener as a Cochlear Rescue Agent. *Biomed Res Int.* 2014;2014.
9. Vlajkovic SM, Housley GD, Thorne PR. Adenosine and the auditory system. *Curr Neuropharmacol.* 2009;(3):246–56.
  10. Eltzschig HK, Carmeliet P. Hypoxia and inflammation. *New England Journal of Medicine.* 2011.
  11. Vlajkovic SM, Abi S, Wang CJH, Housley GD, Thorne PR. Differential distribution of adenosine receptors in rat cochlea. *Cell Tissue Res.* 2007;328(3):461–71.
  12. Seidman MD. Effects of dietary restriction and antioxidants on presbycusis. *Laryngoscope.* 2000;
  13. Seidman MD, Khan MJ, Tang WX, Quirk WS. Influence of lecithin on mitochondrial DNA and age-related hearing loss. *Otolaryngol - Head Neck Surg.* 2002;
  14. Dai P, Yang W, Jiang S, Gu R, Yuan H, Han D, Guo W, Cao J. Correlation of cochlear blood supply with mitochondrial DNA common deletion in presbycusis. *Acta Otolaryngol.* 2004;
  15. Housley GD, Morton-Jones R, Vlajkovic SM, Telang RS, Paramanathanasivam V, Tadros SF, Wong ACY, Froud KE, Cederholm JME, Sivakumaran Y, Snguanwongchai P, Khakh BS, Cockayne DA, Thorne PR, Ryan AF. ATP-gated ion channels mediate adaptation to elevated sound levels. *Proc Natl Acad Sci U S A.* 2013;
  16. Munoz DJB, Kendrick IS, Rassam M, Thorne PR. Vesicular storage of adenosine

- triphosphate in the guinea-pig cochlear lateral wall and concentrations of ATP in the endolymph during sound exposure and hypoxia. *Acta Otolaryngol.* 2001;
17. Sebastião AM, Cunha RA, de Mendonça A, Ribeiro JA. Modification of adenosine modulation of synaptic transmission in the hippocampus of aged rats. *Br J Pharmacol* [Internet]. 2000;131(8):1629–34. Available from:  
<http://doi.wiley.com/10.1038/sj.bjp.0703736>
  18. Castillo CA, Albasanz JL, León D, Jordán J, Pallàs M, Camins A, Martín M. Age-related expression of adenosine receptors in brain from the senescence-accelerated mouse. *Exp Gerontol* [Internet]. 2009;44(6–7):453–61. Available from:  
<http://dx.doi.org/10.1016/j.exger.2009.04.006>
  19. Blundon JA, Roy NC, Teubner BJW, Yu J, Eom T-Y, Sample KJ, Pani A, Smeyne RJ, Han SB, Kerekes RA, Rose DC, Hackett TA, Vuppala PK, Freeman BB, Zakharenko SS. Restoring auditory cortex plasticity in adult mice by restricting thalamic adenosine signaling. *Science* (80- ) [Internet]. 2017;356(6345):1352–6. Available from:  
<http://www.sciencemag.org/lookup/doi/10.1126/science.aaf4612>
  20. Headrick J. Impact of aging on adenosine levels, A(1)/A(2) responses, arrhythmogenesis, and energy metabolism in rat heart. *Am J Physiol Circ Physiol* [Internet]. 1996;270(3):H897–906. Available from:  
[http://apps.webofknowledge.com/full\\_record.do?product=WOS&search\\_mode=GeneralSearch&qid=77&SID=S17EOp2PE9fBPDYGGD5&page=2&doc=18&cacheurlFromRightClick=no](http://apps.webofknowledge.com/full_record.do?product=WOS&search_mode=GeneralSearch&qid=77&SID=S17EOp2PE9fBPDYGGD5&page=2&doc=18&cacheurlFromRightClick=no)
  21. Mackiewicz M, Nikonova E V., Zimmermann JE, Romer MA, Cater J, Galante RJ, Pack

- AI. Age-related changes in adenosine metabolic enzymes in sleep/wake regulatory areas of the brain. *Neurobiol Aging*. 2006;27(2):351–60.
22. Dobson Jr. JG, Fenton RA, Romano FD. Increased myocardial adenosine production and reduction of beta-adrenergic contractile response in aged hearts. *Circ Res* [Internet]. 1990;66(5):1381–90. Available from: <http://www.ncbi.nlm.nih.gov/pubmed/2159390>
  23. Jr JGD, Fenton RA. Adenosine inhibition of beta-adrenergic induced responses in aged hearts. *Am J Physiol*. 1993;265(2 Pt 2):H494-503.
  24. Ethier MF, Hickler RB, Dobson JG. Aging increases adenosine and inosine release by human fibroblast cultures. *Mech Ageing Dev*. 1989;50(2):159–68.
  25. Shin SA, Lyu AR, Jeong SH, Kim TH, Park MJ, Park YH. Acoustic trauma modulates cochlear blood flow and vasoactive factors in a rodent model of noise-induced hearing loss. *Int J Mol Sci*. 2019;
  26. Mi T, Abbasi S, Zhang H, Uray K, Chunn JL, Ling WX, Molina JG, Weisbrodt NW, Kellems RE, Blackburn MR, Xia Y. Excess adenosine in murine penile erectile tissues contributes to priapism via A2B adenosine receptor signaling. *J Clin Invest*. 2008;118(4):1491–501.
  27. Iriyama T, Sun K, Parchim NF, Li J, Zhao C, Song A, Hart LA, Blackwell SC, Sibai BM, Chan LNL, Chan TS, Hicks MJ, Blackburn MR, Kellems RE, Xia Y. Elevated placental adenosine signaling contributes to the pathogenesis of preeclampsia. *Circulation*. 2015;131(8):730–41.
  28. Dai Y, Zhang W, Wen J, Zhang Y, Kellems RE, Xia Y. A2B Adenosine Receptor-

Mediated Induction of IL-6 Promotes CKD. *J Am Soc Nephrol* [Internet].

2011;22(5):890–901. Available from:

<http://www.jasn.org/cgi/doi/10.1681/ASN.2010080890>

29. Zhang W, Zhang Y, Wang W, Dai Y, Ning C, Luo R, Sun K, Glover L, Grenz A, Sun H, Tao L, Zhang W, Colgan SP, Blackburn MR, Eltzschig HK, Kellems RE, Xia Y. Elevated ecto-5'-nucleotidase-mediated increased renal adenosine signaling via a2b adenosine receptor contributes to chronic hypertension. *Circ Res*. 2013;112(11):1466–78.
30. Sun CX, Zhong H, Mohsenin A, Morschl E, Chunn JL, Molina JG, Belardinelli L, Zeng D, Blackburn MR. Role of A2B adenosine receptor signaling in adenosine-dependent pulmonary inflammation and injury. *J Clin Invest*. 2006;116(8):2173–82.
31. Hu X, Adebisi MG, Luo J, Sun K, Le TTT, Zhang Y, Wu H, Zhao S, Karmouty-Quintana H, Liu H, Huang A, Wen YE, Zaika OL, Mamenko M, Pochynyuk OM, Kellems RE, Eltzschig HK, Blackburn MR, Walters ET, Huang D, Hu H, Xia Y. Sustained Elevated Adenosine via ADORA2B Promotes Chronic Pain through Neuro-immune Interaction. *Cell Rep* [Internet]. 2016;16(1):106–19. Available from: <http://dx.doi.org/10.1016/j.celrep.2016.05.080>
32. Zhang Y, Dai Y, Wen J, Zhang W, Grenz A, Sun H, Tao L, Lu G, Alexander DC, Milburn M V, Carter-Dawson L, Lewis DE, Zhang W, Eltzschig HK, Kellems RE, Blackburn MR, Juneja HS, Xia Y. Detrimental effects of adenosine signaling in sickle cell disease. *Nat Med* [Internet]. 2011;17(1):79–86. Available from: <http://www.nature.com/doi/10.1038/nm.2280>
33. Albuquerque W, Gaspar HB. Bilateral sensorineural deafness in adenosine deaminase-

- deficient severe combined immunodeficiency. *J Pediatr*. 2004;144(2):278–80.
34. Tanaka C, Hara T, Suzaki I, Maegaki Y, Takeshita K. Sensorineural deafness in siblings with adenosine deaminase deficiency. *Brain Dev*. 1996;18(4):304–6.
  35. Xu X, Negandhi J, Min W, Tsui M, Post M, Harrison R V., Grunebaum E. Early Enzyme Replacement Therapy Improves Hearing and Immune Defects in Adenosine Deaminase Deficient-Mice. *Front Immunol*. 2019;
  36. Dobie R, Van Hemel S. Hearing Loss: Determining Eligibility for Social Security Benefits. *Hearing Loss: Determining Eligibility for Social Security Benefits*. 2005.
  37. Müller U, Barr-Gillespie PG. New treatment options for hearing loss. *Nat Rev Drug Discov [Internet]*. 2015;14(5):346–65. Available from: <http://www.nature.com/doi/10.1038/nrd4533>
  38. Wang J, Puel J-L. Presbycusis: An Update on Cochlear Mechanisms and Therapies. *J Clin Med*. 2020;
  39. Xipeng L, Ruiyu L, Meng L, Yanzhuo Z, Kaosan G, Liping W. Effects of Diabetes on Hearing and Cochlear Structures. *J Otol*. 2013;
  40. Vlajkovic SM, Guo CX, Telang R, Wong ACY, Paramanathasivam V, Boison D, Housley GD, Thorne PR. Adenosine kinase inhibition in the cochlea delays the onset of age-related hearing loss. *Exp Gerontol*. 2011;
  41. WHO. Global costs of unaddressed hearing loss and cost-effectiveness of interventions: a WHO report. 2017. 1–39 p.

42. Kaur T, Borse V, Sheth S, Sheehan K, Ghosh S, Tupal S, Jajoo S, Mukherjea D, Rybak LP, Ramkumar V. Adenosine A1 Receptor Protects Against Cisplatin Ototoxicity by Suppressing the NOX3/STAT1 Inflammatory Pathway in the Cochlea. *J Neurosci* [Internet]. 2016;36(14):3962–77. Available from: <http://www.jneurosci.org/cgi/doi/10.1523/JNEUROSCI.3111-15.2016>
43. Wong ACY, Guo CX, Gupta R, Housley GD, Thorne PR, Vlajkovic SM. Post exposure administration of A1 adenosine receptor agonists attenuates noise-induced hearing loss. *Hear Res*. 2010;260(1–2):81–8.
44. Whitworth CA, Ramkumar V, Jones B, Tsukasaki N, Rybak LP. Protection against cisplatin ototoxicity by adenosine agonists. *Biochem Pharmacol*. 2004;
45. Vlajkovic SM, Ambepitiya K, Barclay M, Boison D, Housley GD, Thorne PR. Adenosine receptors regulate susceptibility to noise-induced neural injury in the mouse cochlea and hearing loss. *Hear Res* [Internet]. 2017;345:43–51. Available from: <http://dx.doi.org/10.1016/j.heares.2016.12.015>
46. Ford MS, Maggirwar SB, Rybak LP, Whitworth C, Ramkumar V. Expression and function of adenosine receptors in the chinchilla cochlea. *Hear Res*. 1997;105(1–2):130–40.
47. Gao ZG, Van Muijlwijk-Koezen JE, Chen A, Müller CE, Ijzerman AP, Jacobson KA. Allosteric modulation of A3 adenosine receptors by a series of 3-(2-pyridinyl)isoquinoline derivatives. *Mol Pharmacol*. 2001;
48. Fredholm BB, Ijzerman AP, Jacobson KA, Klotz KN, Linden J. International Union of

Pharmacology. XXV. Nomenclature and classification of adenosine receptors.

Pharmacological Reviews. 2001.

49. Wang J, Van De Water TR, Bonny C, De Ribaupierre F, Puel JL, Zine A. A peptide inhibitor of c-Jun N-terminal kinase protects against both aminoglycoside and acoustic trauma-induced auditory hair cell death and hearing loss. *J Neurosci*. 2003;
50. Blackburn MR, Aldrich M, Volmer JB, Chen W, Zhong H, Kelly S, Hershfield MS, Datta SK, Kellems RE. The use of enzyme therapy to regulate the metabolic and phenotypic consequences of adenosine deaminase deficiency in mice. Differential impact on pulmonary and immunologic abnormalities. *J Biol Chem*. 2000;
51. Chunn JL, Young HWJ, Banerjee SK, Colasurdo GN, Blackburn MR. Adenosine-Dependent Airway Inflammation and Hyperresponsiveness in Partially Adenosine Deaminase-Deficient Mice. *J Immunol*. 2001;
52. Chunn JL, Mohsenin A, Young HWJ, Lee CG, Elias JA, Kellems RE, Blackburn MR. Partially adenosine deaminase-deficient mice develop pulmonary fibrosis in association with adenosine elevations. *Am J Physiol - Lung Cell Mol Physiol*. 2006;
53. Chunn JL, Molina JG, Mi T, Xia Y, Kellems RE, Blackburn MR. Adenosine-Dependent Pulmonary Fibrosis in Adenosine Deaminase-Deficient Mice. *J Immunol*. 2005;
54. Ding D, McFadden SL, Salvi RJ. Cochlear hair cell densities and inner-ear staining techniques. In: *Handbook of Mouse Auditory Research: From Behavior to Molecular Biology*. 2001.
55. Johnson KR, Tian C, Gagnon LH, Jiang H, Ding D, Salvi R. Effects of Cdh23 single

- nucleotide substitutions on age-related hearing loss in C57BL/6 and 129S1/Sv mice and comparisons with congenic strains. *Sci Rep.* 2017;
56. Cai T, Seymour ML, Zhang H, Pereira FA, Groves AK. Conditional Deletion of *Atoh1* Reveals Distinct Critical Periods for Survival and Function of Hair Cells in the Organ of Corti. *J Neurosci* [Internet]. 2013;33(24):10110–22. Available from: <http://www.jneurosci.org/cgi/doi/10.1523/JNEUROSCI.5606-12.2013>
  57. Blackburn MR, Datta SK, Kellems RE. Adenosine deaminase-deficient mice generated using a two-stage genetic engineering strategy exhibit a combined immunodeficiency. *J Biol Chem.* 1998;273(9):5093–100.
  58. Müller M, Von Hünerbein K, Hoidis S, Smolders JWT. A physiological place-frequency map of the cochlea in the CBA/J mouse. *Hear Res.* 2005;
  59. Reed JC, Green DR. Apoptosis: Physiology and pathology. *Apoptosis: Physiology and Pathology.* 2011.
  60. Stevens B, Porta S, Haak LL, Gallo V, Fields RD. Adenosine: A neuron-glia transmitter promoting myelination in the CNS in response to action potentials. *Neuron.* 2002;36(5):855–68.
  61. Kamil K, Yazid MD, Idrus RBH, Das S, Kumar J. Peripheral Demyelinating Diseases: From Biology to Translational Medicine. *Front Neurol.* 2019;10(March):1–12.
  62. Shen HY, Huang N, Reemmer J, Xiao L. Adenosine actions on oligodendroglia and myelination in autism spectrum disorder. *Front Cell Neurosci.* 2018;12(December):1–12.



63. Wrabetz L, Feltri ML, Quattrini A, Imperiale D, Previtali S, D'Antonio M, Martini R, Yin X, Trapp BD, Zhou L, Chiu SY, Messing A. P0 glycoprotein overexpression causes congenital hypomyelination of peripheral nerves. *J Cell Biol.* 2000;
64. Verdú E, Ceballos D, Vilches JJ, Navarro X. Influence of aging on peripheral nerve function and regeneration. *Journal of the Peripheral Nervous System.* 2000.
65. Stevens B, Porta S, Haak LL, Gallo V, Fields RD. Adenosine: A neuron-glia transmitter promoting myelination in the CNS in response to action potentials. *Neuron.* 2002;
66. Fratta P, Ornaghi F, Dati G, Zambroni D, Saveri P, Belin S, D'Adamo P, Shy M, Quattrini A, Laura Feltri M, Wrabetz L. A nonsense mutation in myelin protein zero causes congenital hypomyelination neuropathy through altered P0 membrane targeting and gain of abnormal function. *Hum Mol Genet.* 2019;
67. Wang J, Zhang B, Jiang H, Zhang L, Liu D, Xiao X, Ma H, Luo X, Bojrab D, Hu Z. Myelination of the postnatal mouse cochlear nerve at the peripheral-central nervous system transitional zone. *Front Pediatr.* 2013;1(DEC):5–8.
68. Quarles RH, Macklin WB, Morell P. Myelin Formation, Structure and Biochemistry. *Basic Neurochem Mol Cell Med Asp.* 2006;
69. Stassart RM, Möbius W, Nave KA, Edgar JM. The Axon-Myelin unit in development and degenerative disease. *Frontiers in Neuroscience.* 2018.
70. Kobsar I, Berghoff M, Samsam M, Wessig C, Mäurer M, Toyka K V., Martini R. Preserved myelin integrity and reduced axonopathy in connexin32-deficient mice lacking the recombination activating gene-1. *Brain.* 2003;

71. Berghoff M, Samsam M, Müller M, Kobsar I, Toyka K V., Kiefer R, Mäurer M, Martini R. Neuroprotective effect of the immune system in a mouse model of severe dysmyelinating hereditary neuropathy: Enhanced axonal degeneration following disruption of the RAG-1 gene. *Mol Cell Neurosci.* 2005;
72. Maeda MH, Mitsui J, Soong BW, Takahashi Y, Ishiura H, Hayashi S, Shirota Y, Ichikawa Y, Matsumoto H, Arai M, Okamoto T, Miyama S, Shimizu J, Inazawa J, Goto J, Tsuji S. Increased gene dosage of myelin protein zero causes Charcot-Marie-Tooth disease. *Ann Neurol.* 2012;
73. Kamil K, Yazid MD, Idrus RBH, Das S, Kumar J. Peripheral Demyelinating Diseases: From Biology to Translational Medicine. *Front Neurol.* 2019;
74. Kobayashi M, Inoue K, Warabi E, Minami T, Kodama T. A simple method of isolating mouse aortic endothelial cells. *J Atheroscler Thromb.* 2005;12(3):138–42.
75. Liu H, Zhang Y, Wu H, D'Alessandro A, Yegutkin GG, Song A, Sun K, Li J, Cheng NY, Huang A, Wen YE, Weng TT, Luo F, Nemkov T, Sun H, Kellems RE, Karmouty-Quintana H, Hansen KC, Zhao B, Subudhi AW, Jameson-Van Houten S, Julian CG, Lovering AT, Eltzschig HK, Blackburn MR, Roach RC, Xia Y. Beneficial role of erythrocyte adenosine A2B receptor-mediated AMP-activated protein kinase activation in high-altitude hypoxia. *Circulation.* 2016;134(5):405–21.
76. Liu H, Xia Y. Beneficial and detrimental role of adenosine signaling in diseases and therapy. *Journal of Applied Physiology.* 2015.
77. Wan G, Corfas G. Transient auditory nerve demyelination as a new mechanism for

- hidden hearing loss. *Nat Commun.* 2017;
78. Da Silva JT, Dos Santos FM, Giardini AC, De Oliveira Martins D, De Oliveira ME, Ciena AP, Gutierrez VP, Watanabe IS, De Britto LRG, Chacur M. Neural mobilization promotes nerve regeneration by nerve growth factor and myelin protein zero increased after sciatic nerve injury. *Growth Factors.* 2015;
  79. Hunter KP, Willott JF. Aging and the auditory brainstem response in mice with severe or minimal presbycusis. *Hear Res.* 1987;30(2–3):207–18.
  80. Mikaelian DO. Development and degeneration of hearing in the C57/b16 mouse: Relation of electrophysiologic responses from the round window and cochlear nucleus to cochlear anatomy and behavioral responses. *Laryngoscope.* 1979;
  81. Gratton MA, Schmiedt RA, Schulte BA. Age-related decreases in endocochlear potential are associated with vascular abnormalities in the stria vascularis. *Hear Res.* 1996;
  82. Center SR. Distortion product otoacoustic emissions in the C57BL/6J mouse model of age-related hearing loss. *Hear Res.* 1997;112:216–34.
  83. Perez P, Bao J. Why do hair cells and spiral ganglion neurons in the cochlea die during aging? *Aging and Disease.* 2011.
  84. Long P, Wan G, Roberts MT, Corfas G. Myelin development, plasticity, and pathology in the auditory system. *Developmental Neurobiology.* 2018.
  85. Melcangi RC, Magnaghi V, Cavarretta I, Martini L, Piva F. Age-induced decrease of glycoprotein Po and myelin basic protein gene expression in the rat sciatic nerve. *Repair*

- by steroid derivatives. *Neuroscience*. 1998;
86. Melcangi RC, Magnaghi V, Martini L. Aging in peripheral nerves: Regulation of myelin protein genes by steroid hormones. *Progress in Neurobiology*. 2000.
  87. Rangaraju S, Hankins D, Madorsky I, Madorsky E, Lee WH, Carter CS, Leeuwenburgh C, Notterpek L. Molecular architecture of myelinated peripheral nerves is supported by calorie restriction with aging. *Aging Cell*. 2009;
  88. Tritsch NX, Rodríguez-Contreras A, Crins TTH, Wang HC, Borst JGG, Bergles DE. Calcium action potentials in hair cells pattern auditory neuron activity before hearing onset. *Nat Neurosci*. 2010;
  89. Kim KX, Payne S, Yang-Hood A, Li SZ, Davis B, Carlquist J, Ghaffari B V., Gantz JA, Kallogjeri D, Fitzpatrick JAJ, Ohlemiller KK, Hirose K, Rutherford MA. Vesicular glutamatergic transmission in noise-induced loss and repair of cochlear ribbon synapses. *J Neurosci*. 2019;39(23):4434–47.
  90. Schooneman MG, Vaz FM, Houten SM, Soeters MR. Acylcarnitines: Reflecting or inflicting insulin resistance? *Diabetes*. 2013;62(1):1–8.
  91. Holloway GP, Bezaire V, Heigenhauser GJF, Tandon NN, Glatz JFC, Luiken JJFP, Bonen A, Spriet LL. Mitochondrial long chain fatty acid oxidation, fatty acid translocase/CD36 content and carnitine palmitoyltransferase I activity in human skeletal muscle during aerobic exercise. *J Physiol*. 2006;
  92. Violante S, IJlst L, van Lenthe H, de Almeida IT, Wanders RJ, Ventura F V. Carnitine palmitoyltransferase 2: New insights on the substrate specificity and implications for

- acylcarnitine profiling. *Biochim Biophys Acta - Mol Basis Dis.* 2010;1802(9):728–32.
93. Jones LL, McDonald DA, Borum PR. Acylcarnitines: Role in brain. Vol. 49, *Progress in Lipid Research.* 2010. p. 61–75.
  94. Lee J, Ellis JM, Wolfgang MJ. Adipose fatty acid oxidation is required for thermogenesis and potentiates oxidative stress-induced inflammation. *Cell Rep.* 2015;10(2):266–79.
  95. Viader A, Sasaki Y, Kim S, Strickland A, Workman CS, Yang K, Gross RW, Milbrandt J. Aberrant schwann cell lipid metabolism linked to mitochondrial deficits leads to axon degeneration and neuropathy. *Neuron.* 2013;
  96. McCoin CS, Knotts TA, Adams SH. Acylcarnitines-old actors auditioning for new roles in metabolic physiology. *Nature Reviews Endocrinology.* 2015.
  97. Bruder ED, Raff H. Cardiac and plasma lipid profiles in response to acute hypoxia in neonatal and young adult rats. *Lipids Health Dis.* 2010;
  98. Wu H, Bogdanov M, Zhang Y, Sun K, Zhao S, Song A, Luo R, Parchim NF, Liu H, Huang A, Adebisi MG, Jin J, Alexander DC, Milburn M V., Idowu M, Juneja HS, Kellems RE, Dowhan W, Xia Y. Hypoxia-mediated impaired erythrocyte Lands' Cycle is pathogenic for sickle cell disease. *Sci Rep.* 2016;
  99. Adebisi MG, Manalo JM, Xia Y. Metabolomic and molecular insights into sickle cell disease and innovative therapies. *Blood Adv.* 2019;3(8):1347–55.
  100. Zhang Y, Berka V, Song A, Sun K, Wang W, Zhang W, Ning C, Li C, Zhang Q, Bogdanov M, Alexander DC, Milburn M V., Ahmed MH, Lin H, Idowu M, Zhang J,

- Kato GJ, Abdulmalik OY, Zhang W, Dowhan W, Kellems RE, Zhang P, Jin J, Safo M, Tsai AL, Juneja HS, Xia Y. Elevated sphingosine-1-phosphate promotes sickling and sickle cell disease progression. *J Clin Invest*. 2014;124(6):2750–61.
101. Sun K, Zhang Y, Bogdanov M V., Wu H, Song A, Li J, Dowhan W, Idowu M, Juneja HS, Molina JG, Blackburn MR, Kellems RE, Xia Y. Elevated adenosine signaling via adenosine A2B receptor induces normal and sickle erythrocyte sphingosine kinase 1 activity. *Blood*. 2015;125(10):1643–52.
102. Koupenova M, Ravid K. Adenosine, Adenosine Receptors and Their Role in Glucose Homeostasis and Lipid Metabolism. *J Cell Physiol*. 2013;
103. Song A, Zhang Y, Han L, Yegutkin GG, Liu H, Sun K, D'Alessandro A, Li J, Karmouty-Quintana H, Iriyama T, Weng T, Zhao S, Wang W, Wu H, Nemkov T, Subudhi AW, Jameson-Van Houten S, Julian CG, Lovering AT, Hansen KC, Zhang H, Bogdanov M, Dowhan W, Jin J, Kellems RE, Eltzschig HK, Blackburn M, Roach RC, Xia Y. Erythrocytes retain hypoxic adenosine response for faster acclimatization upon re-ascent. *Nat Commun*. 2017;8.
104. Xu W, Shy M, Kamholz J, Elferink L, Xu G, Lilien J, Balsamo J. Mutations in the cytoplasmic domain of P0 reveal a role for PKC-mediated phosphorylation in adhesion and myelination. *J Cell Biol*. 2001;
105. Gaboreanu AM, Hrstka R, Xu W, Shy M, Kamholz J, Lilien J, Balsamo J. Myelin protein zero/P0 phosphorylation and function require an adaptor protein linking it to RACK1 and PKC $\alpha$ . *J Cell Biol*. 2007;

106. Burch-Sims GP, Matlock VR. Hearing loss and auditory function in sickle cell disease. *J Commun Disord*. 2005;38(4 SPEC. ISS.):321–9.
107. Desai P, Dejoie-Brewer M, Ballas SK. Deafness and Sickle Cell Disease: Three Case Reports and Review of the Literature. *J Clin Med Res [Internet]*. 2015;7(3):189–92. Available from:  
<http://www.ncbi.nlm.nih.gov/pmc/articles/PMC4285067/> <http://www.jocmr.org/index.php/JOCMR/article/view/2028>
108. Mgbor N, Emodi I. Sensorineural hearing loss in Nigerian children with sickle cell disease. *Int J Pediatr Otorhinolaryngol*. 2004;68(11):1413–6.
109. Okbi MH Al, Alkindi S, Al Abri RK, Mathew J, Nagwa AA, Pathare A V. Sensorineural hearing loss in sickle cell disease-A prospective study from Oman. *Laryngoscope*. 2011;121(2):392–6.
110. da Silva LPA, Nova CV, Lucena R. Sickle cell anemia and hearing loss among children and youngsters: Literature review. *Braz J Otorhinolaryngol [Internet]*. 2012;78(1):126–31. Available from: <http://dx.doi.org/10.1590/S1808-86942012000100020>
111. Zhang Y, Dai Y, Wen J, Zhang W, Grenz A, Sun H, Tao L, Lu G, Alexander DC, Milburn M V, Carter-Dawson L, Lewis DE, Zhang W, Eltzschig HK, Kellems RE, Blackburn MR, Juneja HS, Xia Y. Detrimental effects of adenosine signaling in sickle cell disease. *Nat Med [Internet]*. 2011;17(1):79–86. Available from:  
<http://www.nature.com/doi/10.1038/nm.2280>
112. Kiser ZM, Clark KA, Sumner JL, Vercellotti GM, Nelson MD. Association between

- Sensorineural Hearing Loss and Homozygous Sickle Cell Anemia: A Meta-Analysis. *Blood*. 2019;
113. Saito N, Nadgir RN, Flower EN, Sakai O. Clinical and radiologic manifestations of sickle cell disease in the head and neck. *Radiographics*. 2010;
114. Saito N, Watanabe M, Liao J, Flower EN, Nadgir RN, Steinberg MH, Sakai O. Clinical and radiologic findings of inner ear involvement in sickle cell disease. *Am J Neuroradiol*. 2011;
115. Mills E, O'Neill LAJ. Succinate: A metabolic signal in inflammation. *Trends Cell Biol* [Internet]. 2014;24(5):313–20. Available from: <http://dx.doi.org/10.1016/j.tcb.2013.11.008>
116. King A, Selak MA, Gottlieb E. Succinate dehydrogenase and fumarate hydratase: linking mitochondrial dysfunction and cancer. *Oncogene* [Internet]. 2006;25(34):4675–82. Available from: <http://www.nature.com/doifinder/10.1038/sj.onc.1209594>
117. Bardella C, Pollard PJ, Tomlinson I. SDH mutations in cancer. Vol. 1807, *Biochimica et Biophysica Acta - Bioenergetics*. 2011. p. 1432–43.
118. Tannahill GM, Curtis AM, Adamik J, Palsson-McDermott EM, McGettrick AF, Goel G, Frezza C, Bernard NJ, Kelly B, Foley NH, Zheng L, Gardet A, Tong Z, Jany SS, Corr SC, Haneklaus M, Caffrey BE, Pierce K, Walmsley S, Beasley FC, Cummins E, Nizet V, Whyte M, Taylor CT, Lin H, Masters SL, Gottlieb E, Kelly VP, Clish C, Auron PE, Xavier RJ, O'Neill LAJ. Succinate is an inflammatory signal that induces IL-1 $\beta$  through HIF-1 $\alpha$ . *Nature* [Internet]. 2013;496(7444):238–42. Available from:



<http://www.nature.com/doi/10.1038/nature11986>

119. McFadden, S., Ding, D., Salvi, R. H. Anatomical, metabolic and genetic aspects of age-related hearing loss in mice. *Audiology*. 2001;40(6):313–21.
120. Jensen-Smith HC, Hallworth R, Nichols MG. Gentamicin rapidly inhibits mitochondrial metabolism in high-frequency cochlear outer hair cells. *PLoS One*. 2012;7(6).
121. Cai Q, Du X, Zhou B, Cai C, Kermany MH, Zhang C, Yoo T. Effects of simvastatin on plasma lipoproteins and hearing loss in apolipoprotein e gene-deficient mice. *ORL*. 2009;71(5):244–50.
122. Zhang W, Dai M, Fridberger A, Hassan A, DeGagne J, Neng L, Zhang F, He W, Ren T, Trune D, Auer M, Shi X. Perivascular-resident macrophage-like melanocytes in the inner ear are essential for the integrity of the intrastrial fluid-blood barrier. *Proc Natl Acad Sci* [Internet]. 2012;109(26):10388–93. Available from: <http://www.pnas.org/cgi/doi/10.1073/pnas.1205210109>
123. Tang LS. COUP-TFI controls Notch regulation of hair cell and support cell differentiation. *Development* [Internet]. 2006;133(18):3683–93. Available from: <http://dev.biologists.org/cgi/doi/10.1242/dev.02536>
124. Axelsson A, Dengerink H. The effects of noise on histological measures of the cochlear vasculature and red blood cells: A review. *Hear Res*. 1987;31(2):183–91.
125. Godinho RO, Duarte T, Pacini ESA. New perspectives in signaling mediated by receptors coupled to stimulatory G protein: The emerging significance of cAMP efflux and extracellular cAMP-adenosine pathway. Vol. 6, *Frontiers in Pharmacology*. 2015.

## VITA

Jeanne Marie Dominique P. Manalo was born in Quezon City, Rizal, Philippines, daughter of Alexander C. Manalo and Ma. Leah Caridad P. Manalo. After completing her work at Hastings High School, Houston, Texas in 2011, she entered the University of St. Thomas in Houston, Texas. She received the degree of Bachelor of Science with a major in Biology from UST in May, 2015. For the next year, she worked as a research assistant and lab manager in the Department of Neuroscience at Baylor College of Medicine. In August of 2016, she entered The University of Texas MD Anderson Cancer Center UTHHealth Graduate School of Biomedical Sciences.

Permanent address:

11602 Main Cedar Dr.

Houston, TX 77025